PARP INHIBITOR: ABROGATION OF CHROMOSOMAL RADIAL-INDUCED MITOTIC CELL DEATH AND INDUCTION OF MULTIPOLAR DIVISION VIA LOSS OF CENTROSOME INTEGRITY

By

Nichole M. Owen

A DISSERTATION

Presented to the Department of Molecular and Medical Genetics
and the Oregon Health & Science University
School of Medicine
In partial fulfillment of
the requirements for the degree of

Doctor of Philosophy

June 2015

TABLE OF CONTENTS:

Abbreviations iv

Acknowledgements v

Dedication vi

Technical Acknowledgements vii

Abstract 1

Introduction 2-11

Manuscript I: *Bloom Syndrome Radials are Predominantly Non-homologous and are Suppressed by Phosphorylated BLM*

- Abstract 14-15
- Introduction 16-19
- Methods 20-23
- Results 24-32
- Discussion 33-36

Manuscript II: *Chromosomal Radials Form in Response to Double Strand Breaks and Trigger PARP-dependent Mitotic Cell Death*

- Abstract 39-40
- Introduction 41-44
- Methods 45-49
- Results 50-68
- Discussion 69-73

Manuscript III: *Multipolar Division without Centrosome Amplification or De-clustering in PARP Inhibitor-treated Cells*

- Abstract 76-77
- Introduction 78-80
- Methods 81-87
- Results 88-116
- Discussion 117-120

Conclusion 121-128

References 129-145

FIGURES:

Introduction None

Manuscript I: *Bloom Syndrome Radials are Predominantly Non-homologous and are Suppressed by Phosphorylated BLM*

Figure 1 25
Figure 2 27
Figure 3 31
Figure 4 32
Figure 5 35

Manuscript II: *Chromosomal Radials Form in Response to Double Strand Breaks and Trigger PARP-dependent Mitotic Cell Death*

Figure 1 51-52
Figure 2 54
Figure 3 56
Figure 4 58
Figure 5 60-61
Figure 6 63-64
Figure S1 66-67
Figure 7 73

Manuscript III: *Multipolar Division without Centrosome Amplification or De-clustering in PARP Inhibitor-treated Cells*

Figure 1 90-92
Figure 2 95
Figure 3 98,100
Figure S1 99
Figure 4 103-105
Figure S2 107
Figure 5 109-110
Figure 6 113-114
Figure S3 115-116

Conclusion None

TABLES:

Introduction

Manuscript I: *Bloom Syndrome Radials are Predominantly Non-homologous and are Suppressed by Phosphorylated BLM*

Table 1 25

Table 2 29

Table 3 29

Manuscript II: *Chromosomal Radials Form in Response to Double Strand Breaks and Trigger PARP-dependent Mitotic Cell Death*

Manuscript III: *Multipolar Division without Centrosome Amplification or De-clustering in PARP Inhibitor-treated Cells*

Conclusion

ABBREVIATIONS:

FA	Fanconi anemia
BS	Bloom syndrome
AML	Acute myeloid leukemia
PARP	Poly(ADP-ribose) polymerase
MPD	Multipolar division
DSB	Double strand break
SSB	Single strand break
SCE	Sister chromatid exchange
ICL	Interstrand crosslink
MMC	Mitomycin C
DEB	Diepoxybutane

Acknowledgements

I would like to take this opportunity to thank my advisor, Dr. Susan Olson for her help and support while in graduate school, and for allowing me to grow as an independent researcher. I would also like to thank the members of my committee—Dr. Amanda McCullough, Dr. Mike Liskay, and Dr. Robb Moses—for their invaluable guidance during my graduate career and particularly for reining me in when I wanted to explore a hundred different directions. This acknowledgement would not be complete without saying a special thank you to Dr. Moses for flying in from Houston for all of my committee meetings and requirements. I would also like to thank the members of the Knight Diagnostic Laboratory who became my extended lab family during my time at OHSU, and kept me company during the weekend and when I was the only one in lab. Lastly, I would like to thank my fellow MMG graduate students who kept me sane during the ups and downs of graduate school. This dissertation would not have been possible without the unwavering support of everyone recognized above.

Dedication

I would like to dedicate this dissertation to the memory of my father, Geryl Owen. I would not be here today if he had not nurtured the curiosity and inquisitiveness of my childhood, and raised me to be the strong and independent person I am today. I got my thirst for knowledge from him, and I know he would have been proud.

Technical Acknowledgements

I would like to thank everyone that helped to make this dissertation possible. Details pertaining to data collection that was not done personally are as follows. In Manuscript I, the paper published was a joint paper pertaining to radial formation in Bloom syndrome cells. The data presented in Figures 3 and 4 were collected by Dr. James Hejna as part of the laboratory of Dr. Robb E. Moses, and the remaining data were my own. Asia Mitchell in the laboratory of Dr. Paul Spellman assisted with the Monte Carlo simulations. The Western blots (2) in Manuscript III were performed by Ellie Juarez in the laboratory of Dr. Amanda McCullough.

Abstract

Fanconi anemia (FA) and Bloom syndrome (BS) are disorders defined by the genome instability that leads to chromosomal abnormalities known as radials. This instability is thought to be a large factor contributing to increased predisposition to cancer seen in these patients. However, the exquisite sensitivity of these cells to most DNA damaging agents limits the available chemotherapeutics that can be tolerated. Thus it is imperative that new chemotherapeutic agents be identified, and that new drugs are studied thoroughly to determine if they are safe specifically for these patients. The information presented here is a collection of manuscripts pertaining to chromosomal radials in FA and BS, and the possibility of using PARP inhibitor as a chemotherapeutic agent in patients who have these disorders. These data identified BS radials as anomalous chromosome structures, identical to FA radials, thus allowing for the continued study of the disorders in parallel. Secondly, the minimal lesion responsible for radial formation was identified as a double strand break and the fate of radial containing cells shown to be elimination via PARP-dependent mitotic cell death. Lastly, PARP inhibitor was studied in detail as it has been identified as a possible chemotherapeutic option for FA patients. While there were specific effects of PARP inhibitor unique to FA and BS cells, a detailed analysis was performed to better understand the general mechanism of action. Most importantly, PARP inhibitor was able to induce multipolar division and chromosome instability in non-cancerous and HR-

proficient cells suggesting that the cytotoxic effects of PARP inhibitor are more universal than initially realized.

Introduction

Overview

Fanconi anemia (FA) and Bloom syndrome (BS) are two genome instability disorders that have been studied completely separately for nearly 5 decades despite similar cellular phenotypes that have emerged over the years. However, they share many characteristics in common including the focus of this dissertation—increased cancer predisposition due to chromosomal abnormalities called radials. The focus of the data presented here is to gain a clearer understanding of the causes and consequences of radial formation in FA and BS cells, and thoroughly investigate a chemotherapeutic agent that has been suggested as a possible treatment option for FA patients.

Clinical Presentation

FA is an autosomal and X-linked recessive genome instability disorder characterized by radial ray defects, absent thumbs, skin hyperpigmentation, short stature, progressive bone marrow failure, and an increased predisposition to cancer [1]. Specifically, FA patients are highly susceptible to developing myelodysplastic syndrome and acute myeloid leukemia at a young age, followed by solid tumors of the head, neck, esophagus and genitourinary tract later in life [1]. There is currently limited treatment for FA and efforts have concentrated on

addressing the severe bone marrow failure that is responsible for much of the mortality associated with the disorder. While bone marrow transplant is effective at ameliorating both the bone marrow failure and eventual progression to acute myeloid leukemia (AML), patients remain at risk for developing solid tumors for which chemotherapeutic options are limited.

Bloom Syndrome (BS) is an autosomal recessive instability syndrome that possesses many phenotypic similarities to FA. BS patients have severe growth retardation, reduced fertility and are at 150-300-fold increased risk for developing cancer [2]. AML is one of the most common cancers in BS patients, but they are also prone to developing many other forms of cancer including lymphomas and solid tumors of the gastrointestinal tract, genitourinary tract, larynx, and skin. Also similar to FA, hematological cancers in BS patients tend to develop earlier in life, while solid tumors develop later. This parallels the general development of BS neoplasia where cancers develop early and frequently, with patients often presenting with multiple primary tumors. Other clinical manifestations such as bone marrow failure and café-au-lait spots can occur, but are not as common as in FA patients. BS patients have an additional immunological phenotype that is unique among genome instability disorders, manifesting as increased susceptibility to pneumonia and gastrointestinal infections, chronic lung disease, and type II diabetes.

Roles of BLM and FA proteins in DNA repair

FA and BS are two distinct disorders with different etiologies, yet in accordance with phenotypic similarities, the respective dysregulated DNA repair pathways are highly intertwined. The FA pathway is composed of 18 known proteins which work in concert with other proteins from the nucleotide excision repair, translesion synthesis, and homologous recombination (HR) pathways to orchestrate the repair of complex lesions including interstrand crosslinks (ICLs) and DNA-protein crosslinks. The pathway can be grouped into three stages: core complex assembly, mono-ubiquitination of FANCD2 and FANCI, and recruitment of downstream HR factors. Initially, lesions such as ICLs are recognized at structures resembling stalled replication forks by a complex of FANCM and FA-associated proteins FAAP24, MHF1 and MHF2 [3,4]. Once activated by FANCM, the core complex comprised of FANCA/B/C/E/F/G and the E3 ligase FANCL assembles, acting to mono-ubiquitinate both FANCD2 and FANCI in the heterodimerized ID2 complex [5-7]. The ID2 complex then recruits repair proteins FANCD1 (BRCA2), FANCJ (BRIP), FANCN (PALB2), FANCO (RAD51C), FANCP (SLX4) and FANCQ (XPF). These proteins are coopted from the canonical HR pathway and are responsible for HR-mediated repair after lesion processing.

BLM protein is a 3'→5' RecQ helicase that has roles in many cellular processes including HR for DNA repair in somatic cells, the suppression of sister chromatid exchange, resolution of ultrafine bridges during mitosis, and in meiosis where it functions as an anti-recombinase [8-15]. Specifically relating to DNA

repair, BLM function is intricately intertwined with the FA pathway in both core complex-dependent and core complex-independent ways. BLM physically interacts with the FA helicase FANCJ, the FA sensor FANCM, and members of the FA pathway are found in the BRAFT supercomplex (BLM, RPA, TOP3A, and associated proteins) [16-18]. Additionally, a functional FA pathway is required for phosphorylation of BLM, suggesting BLM is dysregulated in FA cells [19,20].

Underscoring the necessity of the FA pathway is that clinically, 95% of patients with FA have mutations in the core complex genes, with the most common being *FANCA*, *FANCC* and *FANCG* [4]. This is most likely due to the absolute necessity of the downstream repair proteins for cell viability. The few patients who do harbor mutations in the ID2 complex or recruited repair factors generally have more severe cases of FA, suggesting that biallelic full loss of function mutations are not compatible with life, thus patients are likely to harbor at least one hypomorphic mutant allele [21,22]. BS is caused solely by mutations in *BLM*, and mouse studies have determined complete knockouts to be embryonically lethal suggesting that patients with BS may rely on at least one hypomorphic mutation as well [23,24].

FA and BS patients exhibit similar chromosome instability, which is most likely the result of extensive crosstalk now recognized between the two pathways. Chromosomal radial formation is present in both FA and BS cells, occurring spontaneously and in response to clastogens [25-28]. The first manuscript presented in this dissertation focuses on identifying BS radials as structurally identical to FA radials, thus likely to evolve from the same DNA repair

defect. The similarity of FA and BS radials had been disputed since radials were shown to form spontaneously in the cells of BS patients, and had precluded the study of BS radials alongside FA radials [25,26]. Now that FA and BS radials were determined to be identical, the cells could be studied in parallel for further experiments relating to chromosomal radial formation. It has been widely debated what the causative DNA lesion is that leads to radial formation and it is currently unknown what the consequences are of radials as they proceed through mitosis. Thus, five decades after the discovery of radials, we are still left with two very important questions: where do they come from and where do they go? The answer to both of these questions is detailed in the second manuscript presented as part of this dissertation.

Limited Chemotherapeutic Options

Currently, one of the most critical situations facing FA and BS cancer patients is the shortage of chemotherapeutic agents that they can tolerate. The goal of chemotherapy is to selectively target cancer cells. In many cases this is done by targeting disrupted DNA repair capabilities and chromosome instability that are common developments as cancers dysregulate the cell cycle and accumulate mutations. In doing so, DNA repair-deficient tumor cells are selectively killed while repair proficient normal tissue is less affected. However, patients with genome instability disorders are unable to tolerate many of these therapies due to constitutional DNA repair deficiency, rather than acquired DNA repair deficiency exclusive to cancer cells. Thus many of these therapies can be

toxic and even deadly to FA and BS patients. Given the high incidence of cancer in these patients, the need for chemotherapeutics that can be tolerated is critical.

One compound that has been gaining traction as a chemotherapeutic agent is PARP inhibitor. Initially recognized for its potent and specific killing of BRCA2-deficient cancer cells, this class of inhibitors targets the multifunctional protein Poly(ADP-ribose) Polymerase 1 (PARP1) [29,30]. PARP1 has many roles within the cell including posttranslational modification of proteins by poly(ADP-ribosyl)-lation, gene transcription regulation, direction of cell death pathways, and is essential for the control of various signaling pathways including ERK–mediated angiogenesis, the NF-κβ-mediated inflammatory response, and sex hormone signaling [31]. However, the role that is most well-characterized is the role that PARP1 plays in single strand break repair. PARP1, and its binding partner XRCC1, are the sensors of unrepaired single strand breaks. Thus, when PARP1 is inhibited, single strand breaks accumulate. Eventually, prolonged unrepaired single strand breaks become double strand breaks (DSBs) at collapsed replication forks as cells attempt DNA synthesis. Given the inhibition of DNA repair, PARP inhibitors have also been used in combination therapy to sensitize tumor cells to radiotherapy, broadening their therapeutic use [32,33].

Due to the ability to specifically target HR-deficient tumors mutated in *BRCA2*, PARP inhibitors have been suggested as possible chemotherapeutic agents for sporadic tumors deficient in other HR proteins—specifically FA and BS [34,35]. Sporadic tumors can acquire deficiencies in both the FA pathway and *BLM*, providing an even broader group of tumors that could be susceptible to

PARP inhibitor treatment. Whether through mutation, promoter methylation or unascribed downregulation, dysregulation of the FA pathway is common in a variety of cancers including AML and sporadic head and neck squamous cell carcinoma [36]. These are the two common cancers in patients with FA indicating there is likely a unique feature of these tumors that depends on dysregulation of the FA pathway to develop. Additionally, dysregulation has been seen in breast cancer and ovarian cancer which is unsurprising considering the close ties between BRCA loss, breast and ovarian cancer, and the FA pathway [37]. BLM is dysregulated in both breast cancer and sporadic gastric carcinomas [38,39]. It should also be noted that in cancers that have dysregulation of the FA pathway, two of the most common FA proteins to be affected are FANCJ and FANCM which are the two that directly interact with BLM [16,17,40]. A fairly new approach is the possible use of PARP inhibitor to treat patients with FA or BS that have developed cancer, particularly given the limited chemotherapeutic options. A large part of the research presented here focuses on understanding the effects of PARP inhibitor on non-neoplastic FA and BS cells to begin gauging the efficacy of PARP inhibitor as a recommended chemotherapeutic agent. This dissertation focuses on the possible genome instability induced and the cell death pathways that are corrupted under conditions of PARP inhibition.

Expanding Cellular Consequences of PARP Inhibitor Treatment

Though the role in DNA repair is by far the most studied function of PARP1, there are additional effects of inhibiting PARP that are just beginning to

be understood. All PARP inhibitors catalytically inhibit PARP1, but many vary in having additional PARP-mediated effects within the cell. For instance, the trapping of PARP-DNA complexes at sites of DNA damage varies depending on the inhibitor used. Furthermore, these complexes are considered to be particularly cytotoxic to cells [41]. Of more interest is an effect that is not directly related to DNA repair which is the ability of some PARP inhibitors to induce aberrant mitosis and multipolar division (MPD). Because chemotherapeutic agents often target the highly proliferative nature of cancer cells, the ability to induce catastrophic mitosis independent of the DNA repair capability of the tumor would broaden the therapeutic options for PARP inhibitors. In instances of amplified centrosomes, such as those in solid tumors, centrosomes cluster at two spindle poles forming a pseudo-bipolar spindle in an attempt to avoid gross chromosome instability [42,43]. Thus centrosome de-clustering agents such as PARP inhibitor force cells to undergo MPD [43]. However, *PARP1* knockout cells undergo spontaneous centrosome amplification and MPD suggesting the relationship between PARP1, mitotic fidelity, and centrosome homeostasis is complex [44]. PJ34 is a unique PARP inhibitor shown to induce centrosome de-clustering, multinucleation, and cell death via mitotic catastrophe [43,45,46]. However, it has been reported that normal cells without amplified centrosomes are unaffected by PJ34 treatment [45].

The third manuscript of this dissertation focuses on the MPD induced by PJ34 and whether it is exacerbated in FA or BS cells that have inherent genome instability. FA and HR proteins localize to centrosomes and cells that are

deficient in HR have been shown to be susceptible to fragmented centrosomes and mitotic catastrophe. Thus, we hypothesized that they may be more susceptible to MPD induction by PARP inhibitor [47-50]. MPD is usually due to deregulation of the centrosome duplication cycle leading to amplified centrosomes. However, MPD can occur without centrosome amplification due to loss of centrosome integrity. This kind of MPD is usually associated with premature entry into mitosis with unrepaired DNA or as a result of replication stress, suggesting that this lesser known form of MPD may be induced in FA or BS cells treated with PARP inhibitor [51,52].

Tying it all Together

The following are a collection of published and prepared manuscripts that address some of the gaps in knowledge related to genome instability in FA and BS cells, as detailed above. *While traditionally considered two separate DNA repair abnormalities, I hypothesized that BS and FA radials were indeed the same abnormal chromosome structures* and identifying them as such would allow for BS and FA cells to be considered equally when researching radial formation. Additionally, Manuscript I identifies two key phosphorylation sites that are essential for the function of BLM in inhibiting radial formation, but are dispensable for the suppression of sister chromatid exchange. These key sites are unable to be phosphorylated in FA cells, suggesting BLM dysregulation may be a key factor to radial formation in FA cells. Manuscript II attempts to reconcile the competing arguments currently in the literature regarding the DNA lesion responsible for radial formation. ICLs, DNA-protein crosslinks and reactive

oxygen species have all been implicated in radial formation—thus I theorized that any lesion that was processed through a transient DSB, or was caused DSBs if not repaired properly, could cause radials. *I hypothesized that inducing DSBs via the inhibition of SSB repair would be sufficient to cause radial formation, without the need for initial complex lesions such as ICLs*. Once radials are formed they can be observed at a specific metaphase, but there is no visible evidence of them resolving such as structural chromosome abnormalities. Thus, *I hypothesized that radial-containing cells were dying during mitosis due to the inherent mitotic instability of chromosomal radials.* Both of these hypotheses were proven true as DSBs alone were sufficient to cause radial formation and radial-containing cells died specifically at metaphase via a PARP-dependent mechanism requiring hyperfragmentation. While working with PARP inhibitor, it became evident that there were additional cellular effects of PARP inhibitor treatment relating to the induction of MPD. *I hypothesized that FA and BS cells would be more susceptible to MPD due to the inherent chromosome instability and predisposition to mitotic catastrophe.* The answer to this hypothesis is complex, and will be discussed in more detail in the manuscript, but the essence is that while the MPD rates are similar, FA and BS cells undergo more mitotic catastrophe while wild-type cells complete more divisions. Additionally, *I hypothesized that the mechanism of MPD would be via centrosome amplification since loss of PARP1 induces supernumerary centrosomes.* However, this hypothesis was proven wrong (for the most part) as the predominant method of MPD was via loss of centrosome integrity. Together, these manuscripts provide

answers to some of the outstanding questions relating to genome instability in FA and BS cells, and provide new mechanistic information on a chemotherapeutic agent that should be considered carefully before being used in FA or BS patients.

Manuscript I overview: This manuscript uses detailed cytogenetic techniques to determine that BS radials are the same chromosomal abnormalities as FA radials, and thus can be studied in parallel. For the prevention of radial formation, BLM is determined to require phosphorylation of T99 and T122 which is dispensable for BLM's role in the suppression of sister chromatid exchange. FA cells are unable to phosphorylate BLM at these sites, raising the possibility that radial formation in FA cells may be due to the inability to properly modify BLM.

Bloom Syndrome Radials are Predominantly Non-homologous and are Suppressed by Phosphorylated BLM

Nichole Owen[1*], James Hejna[2*], Scott Rennie[1], Asia Mitchell[1], Amy Hanlon Newell[1], Navid Ziaie[1], Robb E. Moses[3], and Susan B. Olson[1]

1. Department of Molecular and Medical Genetics

Oregon Health & Science University,

3181 SW Sam Jackson Park, Portland, OR 97239

Telephone: 503-494-8336

2. Graduate School of Biostudies, Kyoto University, Sakyo-ku, Kyoto 606-8501 Japan

3. Department of Molecular and Cellular Biology, Baylor College of Medicine

Houston, TX 77030

*Equally contributing authors

Corresponding author email: olsonsu@ohsu.edu

Published:

Cytogenet Genome Res 144: 255-263, 2015

Abstract

Biallelic mutations in *BLM* cause Bloom syndrome (BS), a genome instability disorder characterized by growth retardation, sun sensitivity and a predisposition to cancer. As evidence of decreased genome stability, BS cells demonstrate not

only elevated levels of spontaneous sister chromatid exchanges (SCE), but also exhibit chromosomal radial formation. The molecular nature and mechanism of radial formation is not known, but they have been thought to be DNA recombination intermediates between homologs that failed to resolve. However, we find that radials in BS cells occur over 95% between non-homologous chromosomes, and occur non-randomly throughout the genome. BLM must be phosphorylated at T99 and T122 for certain cell cycle checkpoints, but it is not known whether these modifications are necessary to suppress radial formation. We find that exogenous *BLM* constructs preventing phosphorylation at T99 and T122 are not able to suppress radial formation in BS cells, but are able to inhibit SCE formation. These findings indicate that BLM functions in two distinct pathways requiring different modifications. In one pathway, for which the phosphorylation marks appear dispensable, BLM functions to suppress SCE formation. In a second pathway, T99 and T122 phosphorylation are essential for suppression of chromosomal radial formation, either formed spontaneously or following interstrand crosslink damage.

Introduction

The highly conserved human BLM tumor suppressor protein is a RecQ helicase that functions to maintain genome stability [53-56]. Biallelic mutations in *BLM* cause Bloom syndrome, which is characterized by short stature, sun-sensitive skin lesions primarily affecting the face, and predisposition to a wide spectrum of cancers. BLM is a multifunctional protein with distinct roles in somatic and germ cells where it is essential for regulating homologous recombination (HR) for DNA repair and during meiosis, where it localizes to programmed double strand breaks (DSB) to promote holliday junction resolution [10-13,57,58]. BLM regulates recombination by acting to ensure dissolution of crossover intermediates, promoting primarily non-crossover resolution [14,56]. Thus, BS cells manifest genomic instability as increased spontaneous and damage-induced sister chromatid exchanges (SCE) [25,59,60]. SCE formation appears to reflect instances of HR-dependent DSB repair [61]. Normally, double holliday junction intermediates are resolved via two pathways: BLM/TOP3A-mediated dissolution, which results in non-crossovers, or by HR resolvases, which result in crossovers. In the absence of BLM, repair is skewed towards the crossover pathway of resolution, which can be observed as SCEs at mitosis [61-63]. More recently, BLM has been localized to ultrafine DNA bridges during anaphase, along with ERCC6L and members of the Fanconi anemia (FA) pathway, where it is proposed to have a role in bridge resolution, ensuring faithful chromosome segregation [8,64-66].

BS cells manifest chromosomal radial formation following DNA damage, a sign of genome instability most commonly associated with defects in the FA pathway [25,26,67]. FA [reviewed in [68,69]], is a recessive disorder resulting from a defect in any of sixteen or more proteins acting to maintain genome stability during replication and during interstrand crosslink (ICL) damage repair [70,71]. BLM participates in the FA pathway, interacting specifically with the FA helicase, FANCJ [16]. Additionally, several members of the FA core complex associate with BLM in the BRAFT supercomplex (BLM, RPA, TOP3A, and associated proteins), as defined by co-immunoprecipitation [17,18,70]. The BLM-TOP3A complex, a conserved association, acts epistatically with the FA pathway during ICL repair and is necessary for SCE suppression [67]. The BLM-FA interaction appears to be required for phosphorylation of BLM [19,20]. Phosphorylation of BLM at T99 and T122 is required for normal checkpoint response to stalled replication forks, and BS cells arrest in G2/M if phosphorylation does not occur following replication stress [72]. Thus, the functions of BLM and the FA pathway proteins are intricately intertwined, and are required for maintaining genome stability.

Although spontaneous chromosomal radials are a feature of both BS and FA cells, most research has focused on FA radials since they are the basis of diagnostic testing for the disorder [26,27,73]. Both BS and FA cells show increased radials after exposure to ICL-inducing agents, such as mitomycin C (MMC) or diepoxybutane (DEB). Though spontaneous radials are unique to BS and FA cells, induced radials are not and can be found after ICL damage in cells

depleted of proteins that function in DNA repair or maintenance of genome stability, including BRCA1 or BRCA2, non-homologous end joining (NHEJ) proteins Ku70 (now known as XRCC6) and LIG4, and HR proteins RAD51 and RAD52 [74]. However, unlike BS cells, FA cells generally do not exhibit elevated spontaneous SCEs [67,75]. Studies characterizing BS radials have previously classified them as homologous, or occurring between homologous chromosomes [25,26]. However, radials are non-homologous in FA cells and occur between various chromosome combinations [28]. Thus, despite their similarity, BS and FA-derived radials have been documented as different types of chromosome abnormalities and have been thought to arise from different DNA repair defects.

The observation that BS cells show increased SCE and radial formation, while FA cells show only elevated radials, suggests a segregation of BLM activities with one function acting to suppress SCE formation and another to inhibit radial formation. BLM constructs mutated at T99 and T122 to preclude phosphorylation are reported to correct SCE formation to normal levels [72]. Since BS cells lack functional BLM protein and FA cells are unable to phosphorylate BLM [20], yet both manifest radials, we questioned whether phosphorylated BLM is required to suppress radial formation after ICL damage.

We find that spontaneous and ICL-induced radials in BS cells are over 95% non-homologous, appearing to be the same as in FA cells. To determine if phosphorylated BLM is required to suppress radial formation, we used an engineered mutant BLM that cannot be phosphorylated due to substitutions of alanines for native threonines at T99 and T122. We found that such constructs

suppress SCEs in BS cells, but fail to suppress radial formation after ICL damage. In fact, exogenous, un-phosphorylatable BLM appears to have a dominant negative effect, increasing spontaneous and clastogen-induced radial formation in normal fibroblasts. These data suggest that BLM functions in two distinct pathways for maintenance of genome stability: one pathway suppresses radial formation and requires the phosphorylation of T99 and T122; the other pathway suppresses SCE formation, independent of those modifications.

Methods

Cell culture and reagents:

Primary BS fibroblasts (GM01492) (Coriell) were cultured in α-MEM (Gibco) supplemented with 20% FBS (Gibco), 4 mM L-glutamine, and 50 µg/ml gentamicin. Cells were grown at 37^0 C with 5% CO_2 and maintained at subconfluency. Transformed fibroblasts were cultured in α-MEM medium (Mediatech) supplemented with 10% fetal bovine serum (Hyclone). Immortalized fibroblast cell lines GM00639 (wild-type), and GM08505 (BS), were obtained from the NIGMS Human Genetic Cell Repository (Coriell). The functionally complemented control for GM08505 was obtained by transfection with a pMMP vector containing the full-length coding sequence for *BLM*.

G-banding studies:

The GM01492 primary fibroblasts were characterized for the karyotype, as well as for chromosome involvement in radial formation, both spontaneous and clastogen-induced. The treated cells were exposed to 200 ng/ml diepoxybutane (DEB) or 20 ng/ml mitomycin C (MMC) diluted in Hank's balanced salt solution for 48 hr at 37^0 C with 5% CO_2 prior to harvest. Colcemid (0.05 µg/ml) was added overnight to arrest cells at metaphase. Cells were trypsinized, pelleted, and incubated in a hypotonic solution (0.075 M KCl, 5% FBS) for 10 min prior to being fixed with 3:1 methanol:acetic acid. Cells were fixed to slides and baked at 95^0 C for 20 min. After cooling, each slide was trypsinized for 45 sec followed by Wright's stain for 1 min 20 sec, rinsed with diH_2O and dried. Radials were

imaged using bright field microscopy and analyzed using Cytovision software (Applied Imaging, San Jose, CA). Chromosome breakpoints were identified according to the ISCN [76].

Chromosome stability:

For SCE analysis, cells were allowed to go through two rounds of replication in 25 μg/ml BrdU, 24 hr post-transfection. Clastogen-induced SCEs were elicited by a 4-hr pulse of 20 ng/ml MMC 20 hr prior to harvest. Cells were harvested following a 3 hr exposure to 0.05 μg/ml colcemid (Gibco), treated with a 1:3 solution of 5% fetal calf serum:0.075 M KCl, and fixed in 3:1 methanol:acetic acid. Cells were then dropped onto slides and stained for 5 min in 0.01% Acridine Orange. Following staining, slides were rinsed with di$H_2$0 and treated with Sorenson Buffer (pH 6.8) (1:1 volume of 0.06 M Na_2HPO_4 and 0.06 M KH_2PO_4). After treatment, slides were placed on a UV transilluminator (UVP model TM-36) for 12 minutes, and then visualized using a FITC filter. Twenty to 25 metaphases from each culture were scored for chromosome counts and numbers of SCEs. The SCE rate was calculated as the number of SCEs per chromosome.

For chromosome breakage studies, $5x10^4$ cells were seeded in T25 flasks, and were treated 24 hr later with 10-20 ng/ml MMC, depending on the cell line and its sensitivity. Following a 48 hr incubation with MMC, cells were harvested as described [77]. Slides were stained with Wright's stain and 50 metaphases

from each culture were scored for radial formation. The results are presented as the percentage of total cells containing at least one radial.

Constructs:

FLAG-tagged full-length *BLM* coding sequence in a pMMPpuro retroviral vector was digested with ClaI and SphI (NEB) to produce a 3.5 kb pMMP-*BLM* junction fragment containing the T99 and T122 phosphorylation sites (Fig. 3a). The 3.5 kb ClaI-SphI fragment was ligated into ClaI-SphI digested pBR322 vector and minipreps were sequence-verified. Miniprep DNA was used as the template for site directed mutagenesis (Stratagene). Individual mutant candidate minipreps were sequence-verified. Mutations were then shuttled back into the full-length pMMP-*BLM* construct via the ClaI-SphI sites. Final midipreps were sequenced prior to transfection of human cells.

Transfection:

Cell lines were transfected with pMMP-*BLM* constructs using Lipofectamine 2000 (Invitrogen) or TransIT-293 (Mirus) in 6-well plates as directed by the manufacturer. The red fluorescent plasmid pDs-Red2-C1 (ClonTech) was used in a parallel transfection to monitor transfection efficiency. After 24 hr cells were re-plated in 100 mm or 150 mm plates, based on transfection efficiency, and placed under 0.1-0.4 µg/ml puromycin (Sigma) selection. After 10 days of growth colonies were selected, expanded, and expression was confirmed by immunoblotting.

Immunoblotting:

Cells grown in T-75 flasks were washed with PBS, trypsinized, pelleted, and frozen at -80° C. Whole cell extracts were prepared as previously described [77]. 50 μg whole cell extract per lane was run on a 7.5% acrylamide gel and transferred to a nitrocellulose membrane (Osmonics). Membranes were blocked overnight in TBST (TBS plus 0.1% Tween) plus 5% dry milk. Membranes were probed with anti-BLM rabbit polyclonal antibody (Abcam) at a 1:1000 dilution in TBST with 5% dry milk. For β-tubulin blots, membranes were probed with a rabbit polyclonal antibody (H-235, Santa Cruz) at a 1:3000 dilution in TBST. All antibodies were visualized with HRP-conjugated secondary antibodies and enhanced chemiluminescence.

Statistics:

Hot and cold chromosomes, and hot bands, were identified using a Monte Carlo simulation. Multiple iterations were run (300, 500, 1000, and 2500) to compute z-scores for each sample, and then converted to a p-value. P-values below 0.05 were considered “hot” and above 0.95 considered “cold”. For chromosome bands, “hot-spots” were considered those with an observed frequency two standard deviations from the mean (95% confidence interval).

Results

Radials in BS cells are non-homologous

The GM01492 BS primary fibroblast cell line was karyotyped and found to be 46,XY (data not shown). Analysis of rare spontaneous chromosome radials showed them to occur primarily between non-homologous chromosomes (Table 1). To increase the number of radial formations available for characterization, the cells were treated with two different clastogens, DEB or MMC. Representative radials are shown with an example of intact chromosomes juxtaposed in order to orient the chromosomes within a radial (**Figure 1a**). Again, radials occurred predominantly between non-homologous chromosomes. Homologous radials, such as in **Figure 1b,** occurring between two homologs of chromosome 8 at breakpoints 8q13, were rare. Radials can also occur between homologous chromosomes, but at non-homologous positions, such as between sites on the short and long arms of chromosome 6 (data not shown). These radials were also uncommon, but were observed in the present study. Despite occurring between homologous chromosomes, these radials do not occur at regions of gross homology—rather, they are akin to non-homologous radials that chanced to form at a non-homologous region on the other homolog present in each cell. Results of radial formation are summarized in **Table 1**. Spontaneous (n=42), DEB-induced (n=101), and MMC-induced (n=101) radials all primarily (>95%) formed between non-homologous chromosomes.

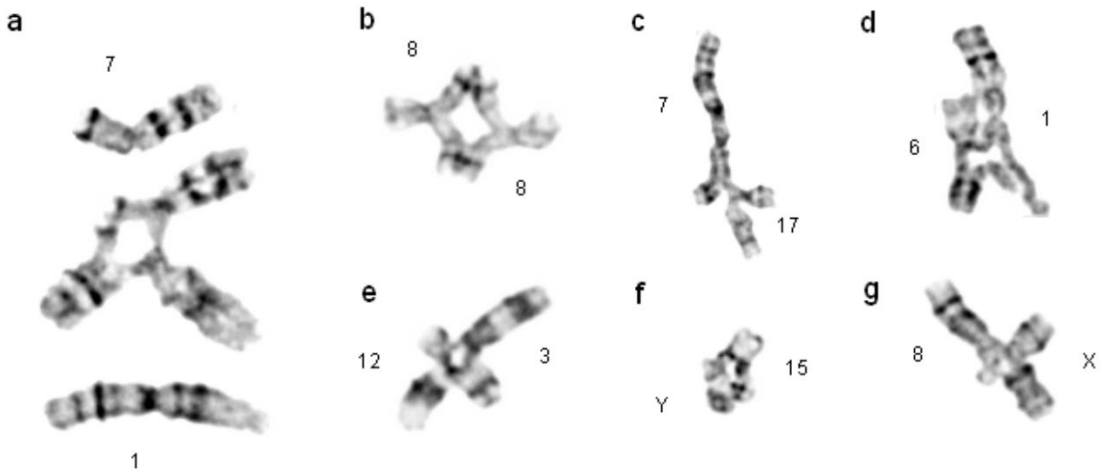

Figure 1. Radials occurring in Bloom Syndrome cells are non-homologous. (a) Intact chromosomes are superimposed alongside a radial occurring between two non-homologous chromosomes to orient individual chromosomes within a radial. (b) A homologous radial and (c-g) representative non-homologous radials isolated from clastogen-treated BS cells.

Table 1: Summary of radials observed in the present study occurring between various chromosome configurations

	Non-homologous chromosomes	Non-homologous sites on homologous chromosomes	Homologous Chromosomes
Spontaneous	95.2%	2.4%	2.4%
DEB	96%	2%	2%
MMC	93%	3%	4%

Breakpoint hotspots are independent of chromosome size

Radials seen in FA cells are not formed with a uniform distribution along the chromosomes but are concentrated in hotspots [28]. We evaluated whether the radials seen in BS cells showed similar clustering. We started by plotting the radials observed in a Circos plot (**Figure 2**), which allowed for the visualization of every chromosome pair within a radial including the specific chromosome bands that were broken. "Hot" and "cold" chromosomes for radial formation could be visualized, as well as the overall non-homologous nature of the radials. For a more detailed analysis of the clustering, a Monte Carlo simulation was done to determine if observed chromosome radial frequencies suggested hot and cold spots. The Monte Carlo simulation randomizes choice based on a discrete distribution. We performed 300, 500, 1,000, and 2,500 iterations. The discrete distribution was defined to be chromosome size, with the assumption that radial frequencies were proportionate to chromosome size. For each sample (observed count and those generated from Monte Carlo simulation), z-scores were computed then converted to a p-value. **Table 2** summarizes the results for chromosomes that were determined to contain hot or cold spots for 1,000 iterations of the Monte Carlo simulation.

Chromosomes 2, 5, 6, and 14 were determined to have low radial formation and were designated as "cold", while chromosomes 11, 17, 19, 20, and 22 were determined to have high radial formation and were designated as "hot". Chromosome 19 was the only chromosome to be "hot" when exposed to both MMC and DEB as a DNA damaging agent. Conversely, chromosome 2 was

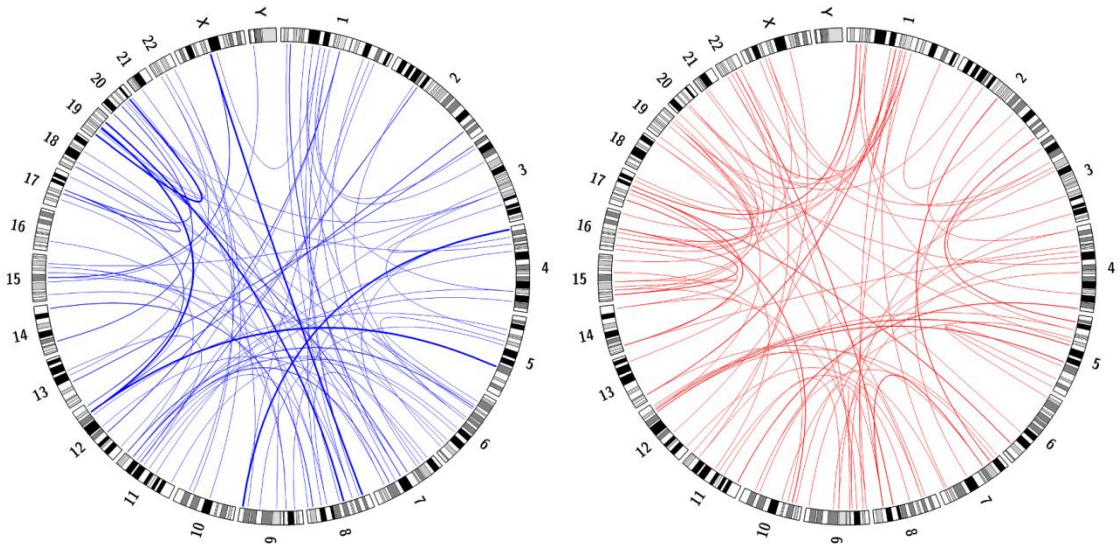

Figure 2. Circos plots depicting radial breakpoints and chromosome partners for radials isolated from DEB (blue) or MMC (red)–treated BS cells. Ideogram depictions of chromosomes are arranged p-arm to q-arm. Blue and red lines connect the breakpoint in the first chromosome to the breakpoint in the partner chromosome for each radial analyzed. The line thickness is quantitative, with the thin lines indicating one observation, medium lines two, and thick lines three.

“cold” when exposed to either damaging agent. This can be visualized by the densely clustered lines at chromosome 19, and the lack of chromosome 2 involvement given its size, shown in **Figure 2**.

To determine hot spots by chromosome band, we assumed a uniform distribution across the genome and set a threshold of observed radial frequency to be greater than two standard deviations from the mean, representing >95% confidence interval. **Table 3** summarizes these results. Chromosome 22 was the only “hot” chromosome to not contain any “hot” bands. Chromosome 14 was determined to be “cold” for radial formation, yet band 14q16 was determined to be a “hot” band. Chromosome 1 had three “hot” bands, but was not determined to be a “hot” chromosome overall. The remaining “hot” bands occurred alone in unique chromosomes. Our results indicate that there are hotspots for radial formation, but the occurrence of hotspots is independent of the chromosome average. Seven of the twelve hot bands coincided with recognized fragile sites indicating a possible link between fragile site stability and radial formation [78].

Table 2: Summary of Monte Carlo simulation (1,000 iterations) to determine hot and cold spots for chromosome radial formation.

Chromosome	ICL agent	# Obs. Radials	P-value	Comment
2	MMC	6	0.996384862	Cold
2	DEB	6	0.996264578	Cold
5	DEB	5	0.984008375	Cold
6	MMC	5	0.978934717	Cold
14	DEB	2	0.978817400	Cold
11	DEB	16	0.011362183	Hot
17	MMC	10	0.024462551	Hot
19	DEB	9	0.005868607	Hot
19	MMC	11	0.000203494	Hot
20	DEB	8	0.036558558	Hot
22	MMC	8	0.006393191	Hot

Table 3. Summary of radial hot-spots by chromosome band.

Observed Radials				Hot Spot		
Bands	DEB	MMC	Total	DEB	MMC	Total
1p13	2	4	6		YES	YES
1p12	2	6	8		YES	YES
1q21	4	4	5		YES	YES
8q24.1	1	4	5		YES	YES
14p11.2	0	5	5		YES	YES
19q13.3	2	6	8		YES	YES
20q11.2	1	4	5		YES	YES
1q12	4	2	6	YES		YES
4p16	4	2	6	YES		YES
11q23	6	2	8	YES		YES
12q24.1	5	2	7	YES		YES
17q21	3	3	6			YES

BLM T99A/T122A suppresses SCEs, but not radials

In order for BLM to act in DNA replication recovery, it must be phosphorylated at specific sites—T99 and T122 [72]. To determine whether phosphorylation of BLM is also required to suppress chromosomal radial formation after ICL damage, a *BLM* construct was made encoding BLM with amino acids T99 and T122 converted to alanine, preventing phosphorylation of those sites (BLM-T99A/T122A) (**Figure 3a**). Expression from the modified *BLM* constructs was monitored using anti-BLM or anti-FLAG detection by immunoblotting to verify expression and size (**Figure 3b**). BS cells transfected with wild-type *BLM* (*BLM*-WT) showed a decrease in SCEs as expected (**Figure 3c**). BS cells transfected with *BLM*-T99A/T122A suppressed SCE formation both with and without ICL damage as well, as previously reported [72]. This result indicates that BLM protein is required for regulation of SCE formation, but phosphorylation of these two sites is not needed. Similarly, BS cells transfected with *BLM*-WT had a significant decrease in radials following MMC treatment (**Figure 3d**). However, BS cells transfected with the BLM-T99A/T122A construct failed to suppress chromosome radial formation following ICL damage. This indicates that T99 and T122 phosphorylation are required for BLM to perform its function in preventing radial formation, but not for it to suppress SCEs.

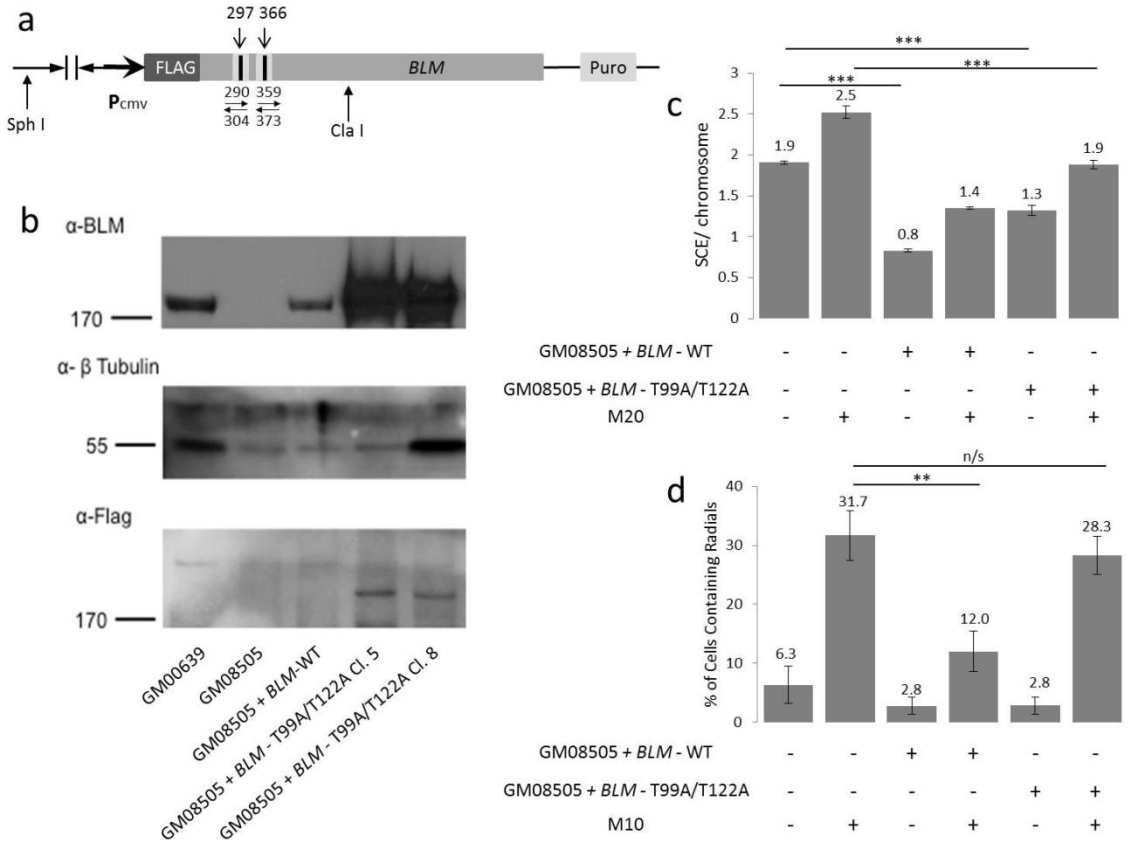

Figure 3. *BLM* Construct and Expression. (a) *BLM* Construct. The numbers above the linear construct refer to nucleotide position of targeted sites. The numbers below with opposing arrows indicate PCR primers used for mutagenesis. (b) Immunoblots of representative clones expressing *BLM* constructs with anti-BLM or anti-FLAG antibody, as indicated. Tubulin was used as a loading control. GM00639 are wild-type cells, GM08505 are BS cells, and lanes 3 through 5 contain GM08505 cells transfected with various constructs. *BLM*-WT encodes full length BLM protein and *BLM* - T99A/T122A encodes BLM protein with two threonine→alanine mutations at key phosphorylation sites. (c) SCE formation in BS cells, cells expressing *BLM*-WT construct, and cells expressing the *BLM* - T99A/T122A construct. Data represent 25 or more metaphase analyses from each of four independent clones. 'M20' is treatment with 20 ng/ml MMC. (d) Radial formation in cells from part "c". M10 is a dose of 10 ng/ml of MMC. The error bars in "c" and "d" represent standard error. **p<0.01; ***p<0.001; n/s is "not significant".

BLM T99A/T122A acts as a dominant negative

Normal transformed human fibroblasts (GM00639) were transfected with *BLM*-T99A/T122A in an effort to determine whether dysfunctional BLM protein interfered with functional BLM. Without ICL damage, the rate of spontaneous radial formation increased with the addition of *BLM*-T99A/T122A (**Figure 4**). Additionally, an increase (approximately 65%) in radial formation was observed with ICL damage. Thus, expression of a BLM that cannot be phosphorylated appears to hinder the function of normal phosphorylated BLM present in the cells, suggesting a possible dominant negative effect on suppression of radial formation.

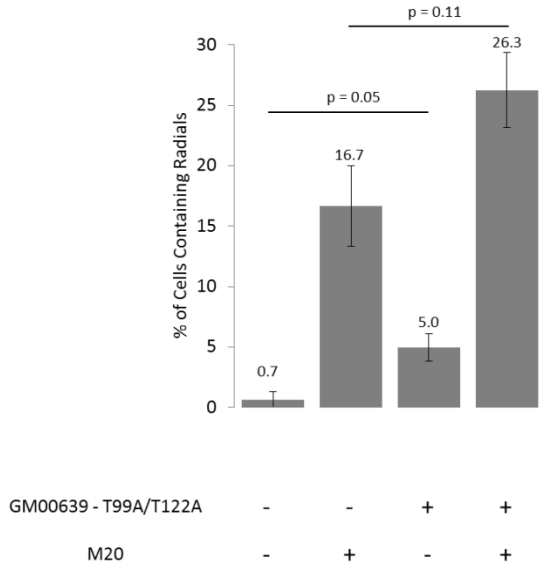

Figure 4. Radial formation in normal transformed human fibroblasts (GM00639) expressing the *BLM* - T99A/T122A construct. Data are the average of combined results from eight trials (duplicates of four independent T99A/T122A clones). 'M20' represents treatment with 20 ng/ml MMC. The error bars represent standard error.

Discussion

Radials in both BS and FA cells form preferentially between non-homologous chromosomes. This is contrary to previous reports that had classified BS radials as occurring between primarily homologous chromosomes. Previous studies utilized a solid staining method, such as Giemsa or Wright's stain, which does not allow specific identification of the chromosomes involved. The homologous interpretation was largely based on symmetry, which we now appreciate can also be the presentation for non-homologous radials. For example, the radial formation between chromosomes 1 and 7 in Figure 1a would appear to be symmetrical and, without identification by G-banding, assumed to involve homologous chromosomes.

The chromosome pairing with respect to radial formation provides valuable information about the underlying repair defect that causes them. Homologous radials were thought to result from a failure to resolve recombination intermediates, and thus represented a defect in homologous recombination. However, non-homologous radials suggest that a non-homologous end-joining pathway—either canonical or alternative—is more likely responsible for radial formation in both BS and FA cells. The physical similarity between both spontaneous and induced radials in BS and FA cells indicates that they most likely arise from a shared DNA repair defect. Similar to FA radials, BS radials also exhibit "hot" and "cold" chromosomes and bands, suggesting preferential spots in the genome for radial formation. The origin of these "hotspots" requires further investigation, but may reflect differences in chromatin

compaction or preference of clastogens to target GC-rich regions [79]. Either of these situations may explain the trend of gene-rich chromosomes being "hotspots" for radial formation. For instance, chromosomes 1 and 19 are similar in size to 2 and 18, respectively. However, chromosomes 2 and 18 are both gene-poor and "colder" for radial formation, while chromosomes 1 and 19 are "hotter" and much more gene-rich. It is also possible that specific fragile sites play a role in radial formation. Interestingly, some of the bands that are considered "hot" are also documented chromosome fragile sites [78]. BLM has been localized to ultrafine bridges that form between chromosome fragile sites, especially after replication stress, and is required for their resolution [80]. In addition, the FA pathway has been shown to be involved in maintaining fragile site stability and localize to these sites regardless of whether they are broken at metaphase [80,81]. Given this, fragile site instability may have an unexplored role in radial formation.

The findings presented show that phosphorylation of BLM at T99 and T122 acts as a molecular switch inhibiting chromosomal radial formation, but that these marks are dispensable for the suppression of SCEs, separating the regulation of these two events. Thus, BLM acts in different modes to limit these two kinds of genomic instability (**Figure 5**). When phosphorylated, BLM prevents radial formation and is known to interact with FA pathway elements. Suppression of SCEs does not require BLM phosphorylation and evidence is lacking to support interaction with the core FA pathway.

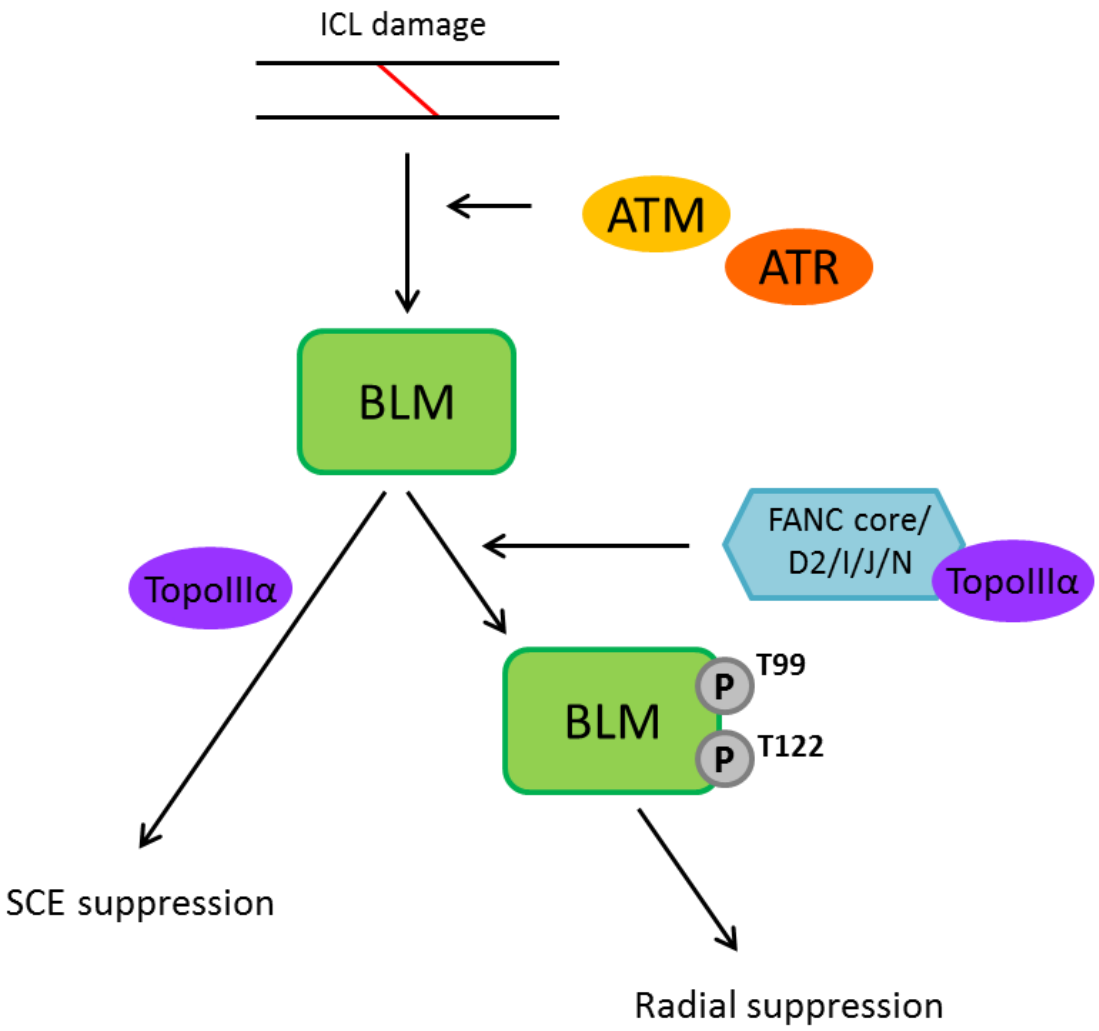

Figure 5. Schematic displaying the segregated actions of BLM. The proposed scheme depicts the separate roles BLM plays in suppression of excess SCE and radial formation, each differentially dependent on the phosphorylation status of BLM.

Blocking phosphorylation of BLM at T99 and T122 has a dominant negative effect on radial suppression that is compatible with models suggesting that BLM acts in a complex with FA proteins, TOP3A, RPA and other proteins functioning in response to ICL formation. Overexpression of an non-phosphorylatable BLM may hinder complex formation, which is likely dependent on those phosphorylation marks, and thus compromises the ability of cells to prevent radial formation.

These results raise the question as to whether the radials characteristically seen in FA cells are the result of defective BLM phosphorylation. If FA cells are unable to phosphorylate BLM protein as reported [20], then radials could ultimately be the result of impaired BLM protein function. This defect would not hinder the ability of BLM to suppress SCEs in FA cells—as we have shown this process to be independent of BLM phosphorylation—but only affect the ability to suppress radials. If this is in fact so, then the interaction of BLM and FA in a single epistatic pathway to process ICLs might reflect a requirement for FA protein function to promote ATM or ATR activation of BLM protein via phosphorylation. The structural similarities observed between FA and BS radials—as both occurring between non-homologous chromosomes—also supports a single pathway of radial formation dependent on both FA and BLM protein function.

Acknowledgements

The authors thank C. Lopez and M. Dai for helpful technical contributions. We thank Dr. Stephen Moore for useful discussions. This work was supported by NHLBI grant PO1HL048546 and NIH training grant 5T32HL007781.

Manuscript II overview: Despite radial induction by complex lesions such as ICLs and DNA-protein crosslinks, the minimum essential lesion for radial formation is a DSB, suggesting any DNA lesion that is processed via a DSB can induce radials. Once radials are formed, they undergo PARP-dependent mitotic cell death that includes hyper-fragmentation of chromosomes. PARP inhibitor not only induces radial formation, but it prevents radials from undergoing the normal mechanism of cell death, suggesting that PARP inhibitor may not be an advisable chemotherapeutic agent for FA or BS patients.

Chromosomal Radials Form in Response to Double Strand Breaks and Trigger PARP-dependent Mitotic Cell Death

Nichole Owen[1], Eleonora Juarez[1], Elena Zherebitskaya[1], Joanna Wolffe[1], Robb E. Moses[2], and Susan B. Olson[1]

1. Department of Molecular and Medical Genetics

Oregon Health & Science University,

3181 SW Sam Jackson Park, Portland, OR 97239

Telephone: 503-494-8336

2. Department of Molecular and Cellular Biology, Baylor College of Medicine

Houston, TX 77030

Corresponding author email: olsonsu@ohsu.edu

Abstract

Fanconi anemia (FA) and Bloom syndrome (BS) are two genome instability disorders that carry an increased risk of developing cancer due to deficiencies in DNA repair that result in unique chromosome abnormalities known as radials. Radials have been attributed to a wide variety of DNA damaging agents in the past—most classically ICL-inducing agents, but it is not well understood how such a variety of lesions can lead to radial formation, and what happens to radials once they are formed. Here, we show that double strand

breaks (DSBs) are the minimum essential lesions necessary to form radials, providing a model whereby any DNA damaging agent that contains a DSB intermediate can be responsible for both spontaneous and induced radial formation. Radial formation triggers PARP-dependent cell death at metaphase, appearing as over-stretched and hyper-fragmented chromosomes. This cell death is abrogated by PARP inhibitor treatment—which itself elicits radials in FA and BS cells—raising concerns for PARP inhibitor as a possible chemotherapeutic agent in FA or BS-derived tumors.

Introduction

Fanconi anemia (FA) is a genome instability disorder characterized by growth delay, developmental abnormalities, progressive bone marrow failure, and an increased risk of developing cancer [69]. Specifically, patients with FA are predisposed to develop acute myeloid leukemia and squamous cell carcinoma of the head, neck, esophagus and gynecologic tract [82]. Recessive mutations in any of the 18 genes that comprise the core FA/BRCA DNA repair pathway lead to FA, while biallelic mutations in FA-associated proteins lead to separate, but similar genome instability disorders such as Bloom syndrome (BS). BS is an extremely rare disorder with less than 300 known cases that results from pathogenic mutations in the *BLM* gene [24]. BLM is a 3'-5' helicase which has been shown to participate in integral steps associated with recombination, replication, DNA repair, and faithful chromosome segregation at mitosis [8,9]. In BS, much like in FA, severe pre- and post-natal growth delay and a predisposition to develop numerous neoplasia are characteristic, though there are differences in the organ systems affected [58]. In general, patients with genome instability disorders are hundreds to thousands of times more likely to develop cancer, yet they cannot be treated currently with most approved chemotherapeutic agents due to the inherent DNA repair deficiency in their cells. A better understanding of the innate chromosome instability in these disorders, and the cellular consequences of irreparable DNA damage, is needed to be able to further understand the pathophysiology of these disorders and develop effective treatments.

Underlying the shared cancer predisposition in FA and BS is inherent chromosome instability due to what is thought to be aberrant DNA repair of DNA interstrand crosslinks (ICLs), a particularly toxic form of DNA damage [83,84]. DNA ICLs are characterized by physical linkage of parallel strands of DNA and have been shown to be induced by both exogenous and endogenous agents, such as cellular metabolites from the breakdown of lipids and alcohol [85]. ICL repair requires the orchestration of multiple DNA repair pathways, under the direction of the FA/BRCA pathway, in order to excise and bypass the lesion, before finally repairing the resulting double strand break (DSB) via homologous recombination [86]. In the absence of an intact FA/BRCA pathway, FA and BS cells form aberrant chromosome structures called radials whose etiology is not well understood despite their clinical use in diagnosing FA [26,27,73,87]. A recent publication in our lab suggests that radials in FA and BS cells are structurally identical chromosome abnormalities and result from a shared DNA repair defect [28,88]. Now, our focus has shifted to identifying the common origin of radials in both these disorders, and understanding the cellular ramifications of their induction.

Traditionally, BS and FA have been considered solely ICL disorders due to their exquisite sensitivity to ICL-inducing agents, but recent evidence suggests a wider spectrum of mutagens may be responsible for radial formation. Aldehyde involvement in DNA damage and radial formation has been suggested from observations showing that concomitant loss of *Fancd2* and *Aldh2*, a gene essential for aldehyde catabolism, led to worsening bone marrow failure and

sporadic leukemia in FA mouse models [89,90]. In addition, it has been shown that FA cells are hypersensitive to plasma levels of formaldehyde and acetaldehyde, and formaldehyde has been shown to stimulate FANCD2 mono-ubiquitination, the seminal step in the FA pathway [91,92]. Likewise, BS cells have been shown to form chromosomal radials after acute formaldehyde treatment [9]. Reactive aldehydes like formaldehyde mainly cause DNA-protein crosslinks suggesting FA and BS may be more than ICL disorders [93,94]. The identification of multiple DNA lesions that could lead to radial formation suggested that the common origin of radials may in fact be an intermediate structure that arises during the process of DNA damage repair rather than the initial lesion. Both ICLs and DNA-protein crosslinks form a double strand break (DSB) as a repair intermediate [95,96]. *We hypothesized that DSBs were the underlying cause sufficient to induce radial formation regardless of the original DNA lesion that preceded it.* This implies that any DNA damage capable of transiently becoming a DSB could lead to radial formation, and perturbations to any of many cellular detoxification processes could exacerbate the FA phenotype, as observed with the simultaneous loss of *Fancd2* and aldehyde catabolism [89].

In order to make simple transient DSBs, we utilized PARP inhibitor which has been shown not to directly induce any DNA damage, but rather blocks the repair of nascent PARP1-dependent single strand breaks (SSBs) [30,97]. The nascent unrepaired single strand breaks then enter S-phase and become DSBs during replication at collapsed replication forks [98]. This process mimics—on a

larger scale—the natural evolution of endogenous DSBs where it is estimated that roughly 1% of single strand breaks, arising from AP sites, topoisomerase-induced breaks and reactive oxygen species, are converted to DSBs [99]. By assessing this process in FA and BS cells, we can identify whether transient DSBs, no matter the source, are sufficient to induce radials. Further, our hypothesis that a plethora of endogenous agents can contribute to radial formation in FA and BS cells provided they are processed through a transient DSB may explain conflicting results in the field over the endogenous source of radial formation.

The fate of both the chromosomes involved in radials and the cells containing them is currently unknown. Radials are mitotically unstable structures that compromise chromosome integrity and eventually the fitness of the cell. *Thus we hypothesized that radials would either resolve prior to anaphase or trigger cell death*. Here, we determined that radials are not resolved into structural chromosome abnormalities, but rather trigger a crucial hyper-fragmented metaphase and PARP1-dependent mitotic cell death. This process is essential for clearing radial-containing cells directly at the metaphase in which radials appear, suppressing further instability at the expense of increased cell death.

Materials and Methods

Cell Culture and Reagents:

Transformed fibroblasts GM00639 (Wild-type), GM08505 (BS) and GM06914 (FA) were obtained from the NIGMS Human Genetic Cell Repository and maintained as subconfluent cultures in a humidified incubator at 37° C w/ 5% CO_2. Cell lines were cultured in α-MEM (Gibco) supplemented with 10% FBS (GeneTex), 4 mM GlutamaX (Gibco) and 50 µg/ml gentamicin (Gibco). Primary FA fibroblasts (PD220) were a gift from the OHSU Fanconi anemia Cell Repository and maintained in α-MEM supplemented with 20% FBS, 4 mM GlutamaX and 50 µg/ml gentamicin.

Chromosomal Breakage Studies:

For the experiment in Figure 1, cells were treated with PARP inhibitor PJ-34 (Enzo Life Sciences; ALX-270-289) for 48 hrs prior to harvest. For the chromosomal breakage experiment in Figure 4, cells were treated for 24 hrs before media was removed, cells were washed with Hanks balanced salt solution (HBSS), and new media was added. Three hr before harvest, colcemid (0.05 µg/ml) was added to arrest cells at metaphase and allow for the visualization of radials and breaks. Cells were trypsinized, pelleted, and resuspended in a hypotonic solution (0.075 M KCl, 5% FBS) for 10 min prior to being fixed with 3:1 methanol:acetic acid. Cells were stained with Wright's stain for 2 min 30 sec and read on a Brightfield Microscope using Cytovision software (Applied Imaging,

San Jose, CA). For each sample, 50 metaphases were scored and each experiment was done in triplicate.

Immunofluorescence:

Cells were seeded on coverslips and grown overnight prior to treatment or harvesting. For 53BP1 time course, 16 μM PARPi was added to all treatment wells at T0 (time 0) and every timepoint thereafter, a treated coverslip and a paired untreated coverslip were harvested. For harvest, coverslips were washed in cold HBSS for 1 minute, and fixed in 4% PFA for 15 minutes. Three (5) minute washes with PBS were followed by permeabilization with PBS-T (PBS + 0.25% Triton-X) for 15 minutes. Cells were blocked in 5% BSA for 1 hr followed by incubation with primary antibody to XRCC1 (Genetex; GTX111712; 1:200) or 53BP1 (BD Transduction; 612522; 1:350), and incubated at room temperature overnight. Following three (5) minute washes with PBS + 0.1% TritonX, the appropriate secondary antibody for each was diluted 1:250 or 1:500 in PBS (Jackson Immunoresearch) and incubated for 45 min at room temperature. FITC-donkey-α-mouse was used for 53BP1 and FITC-donkey-α-rabbit was used for XRCC1. After a final set of washes with PBS + 0.01% TritonX, cells were mounted in Antifade with DAPI to visualize the nucleus. Cells were imaged using a Nikon E800 Fluorescence Microscope with an Applied Imaging Camera, and analyzed using Cytovision Software. For each experiment, foci were counted using Image J. For 53BP1, 100 cells were counted and positive cells were those that had ≥10 foci. For XRCC1, 25 random cells were counted from each

experiment to assess the basal level of XRCC1 foci. Each experiment was performed in triplicate.

Neutral Comet Assay:

Neutral comet assay was performed according to manufacturer's protocol with minor modifications (Trevigen). Briefly, cells were treated with PARPi for 4 or 24 hrs before being harvested. Cells were trypsinized, pelleted, and resuspended in HBSS so that they could be immobilized in LM Agarose on the provided Comet slides before being placed in chilled lysis solution overnight at 4° C. Slides were drained and placed in 1x Neutral Electrophoresis Buffer (NEB) at 4° C for 30 min before undergoing electrophoresis for 35 min at 22 V in 1x NEB at 4° C. Slides were placed in DNA precipitation solution for 30 min at room temperature, then 70% ethanol for 30 minutes at room temperature. Slides were dried for 15 min prior to being stained with SYBR Green. Cells were imaged using a fluorescence microscope (described above) and analyzed using CometScore software. For each experiment, 100 individual comets were scored and each experiment was done in triplicate. To ensure the assay worked each time, a positive control was done by treating cells with 75 μM H_2O_2 for 20 min, and running the sample in parallel with the PARPi-treated and untreated samples.

Colony Forming Assay:

Each cell line was plated according to their respective growth kinetics (500-1000 cells for GM00639, 1200-3600 for GM06914, and 2000-8000 for

GM08505). Cells were seeded and allowed to attach for 24 hrs before being treated with 0-32 μM PARPi for 24 hrs. Media was then removed and cells were washed with HBSS before new growth media was added. Cells were allowed to grow until colonies were of appropriate size to count (10 days for GM00639, 12 days for GM06914, and 15 days for GM08505). Colonies were visualized by staining with methylene blue. These assays were performed in triplicate.

G-Banding for Structural Chromosome Abnormalities:

PD220 primary FA-A fibroblasts were treated for 4 hrs with 25 ng/ml mitomycin C (Sigma) diluted in HBSS, then washed with HBSS, given fresh media and allowed to recover. At time zero and every 24 hrs (24, 48, and 72 hrs), a recovery sample, along with an untreated PD220 control sample, was harvested to analyze the accumulation of structural chromosome abnormalities over time following ICL induction. Cells were harvested and slides made as described in chromosomal breakage methodology, except colcemid was added for 6 hrs prior to harvest. Slides were then baked at 95°C for 20 min, cooled, trypsinized for 45 sec and stained with Wright's stain. Cells were imaged using Brightfield microscopy and analyzed using Cytovision software. Chromosome abnormalities were characterized according to the ISCN (2012).

Metaphase fragmentation studies:

Cells were treated as indicated with PARPi (32 μM), MMC (varies), or PARPi + MMC, and then collected at the indicated time points. MMC doses were selected based on each cell line's sensitivity to the clastogen, using a treatment

dose that would consistently induce 30-60% radial formation. Cells were collected using a mitotic shake off, pelleted for 2 min 30 sec and resuspended in HBSS. Cells were attached to slides using 3:1 methanol:acetic acid dropped onto beads of cell suspension pipetted onto glass slides. Slides were stained with Wright's stain for 2 min 30 sec and imaged with a Brightfield Microscope (described above). Paired radial studies took two flasks of the same cell line, treated them with the same dose of MMC, and collected them at the same time, one for chromosomal breakage analysis (described above) and one for metaphase plate analysis, to determine the correlation between the number of cells containing radials and the number of fragmented metaphases. They cannot be studied in the same sample because chromosomal breakage requires disrupting microtubule attachments to analyze each individual chromosome while fragmented metaphase analysis aims to maintain microtubule attachment to observe an intact metaphase plate. For each experiment, 50 metaphases were analyzed for normal metaphase alignment or fragmentation across the metaphase plate and each experiment was performed in triplicate.

Results

PARP inhibitor induces chromosomal radials in FA and BS cells, but not in WT cells, despite equivalent DSB formation

The role of transient DSBs is difficult to study using common DNA damaging agents due to the simultaneous induction of diverse classes of lesions, many of which are repaired using different repair pathways. In order to address the impact of DSBs alone on radial formation, we utilized PARP inhibitor (PARPi), which produces exclusively DSBs by inhibiting the repair of endogenous SSBs by PARP1, leading to persistent SSBs that are converted via replication into DSBs. If radials are the result of DSBs alone, regardless of the initial lesion that preceded them, then FA and BS cells should form radials in response to PARPi. Radials have been reported to take two replication cycles, or roughly 48 hr, to form after DNA damage or perturbation to DNA repair pathways [100]. Treatment of cells with PARPi for 48 hr resulted in a dose-dependent formation of chromosomal radials in FA and BS cells, but not in Wild-type cells (**Figure 1**). PARPi-dependent radial formation was not observed after 24 hr treatment (data not shown) indicating these radials followed similar kinetics to classical radial formation.

Next, we wanted to assess whether radial formation was a quality or a quantity issue—that is, is radial formation a response to a disproportionate amount of DSB damage in FA and BS cells compared to wild-type cells, or is it an inability to deal with equivalent levels of minor DSB damage. Given the

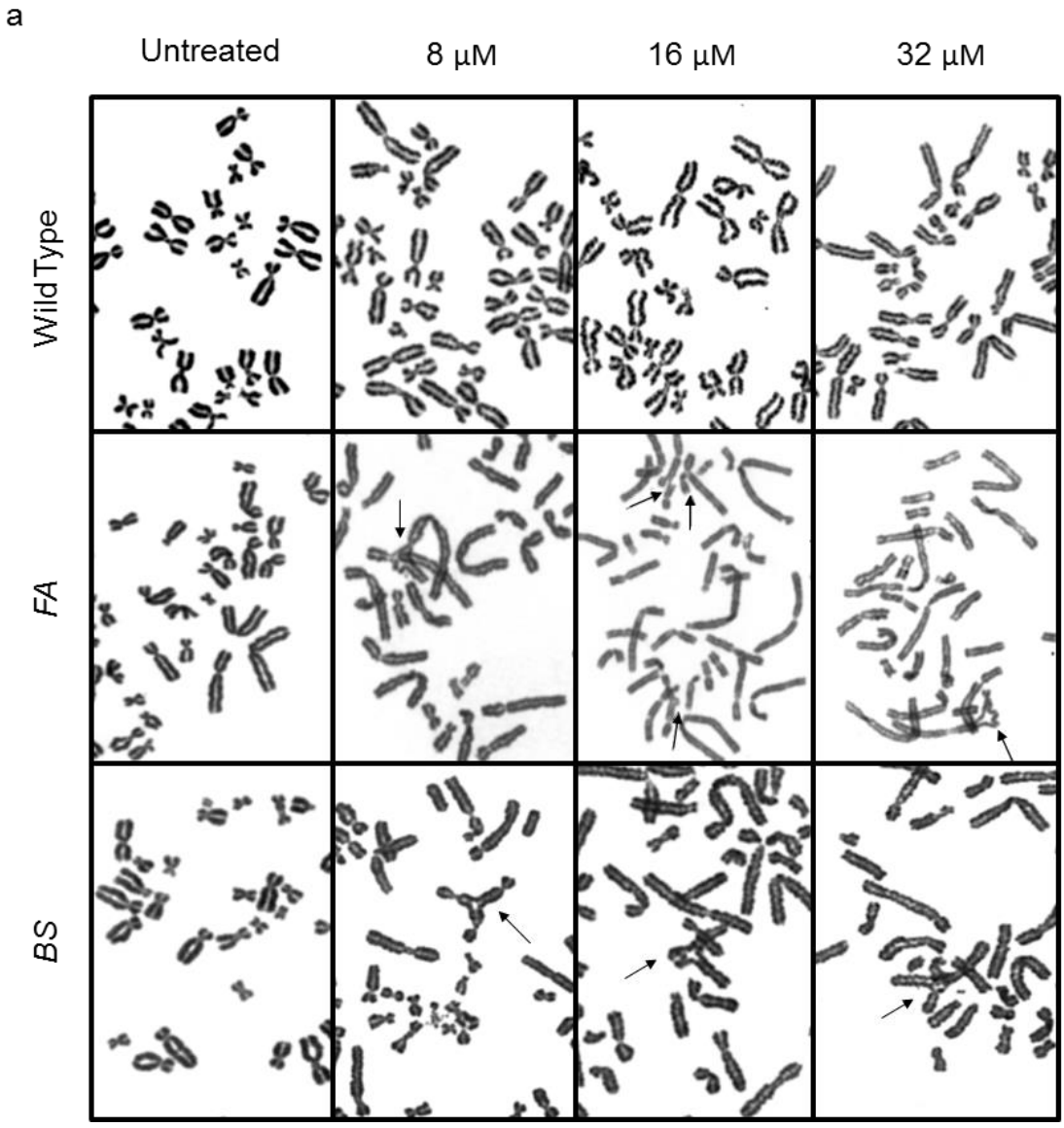

Figure 1: PARP inhibitor induces chromosomal radials in Fanconi anemia and Bloom syndrome fibroblasts. (a) Chromosomal breakage studies were used to assess radial formation in FA, BS, and wild-type cells at metaphase in response to escalating doses of PARPi treatment.

b

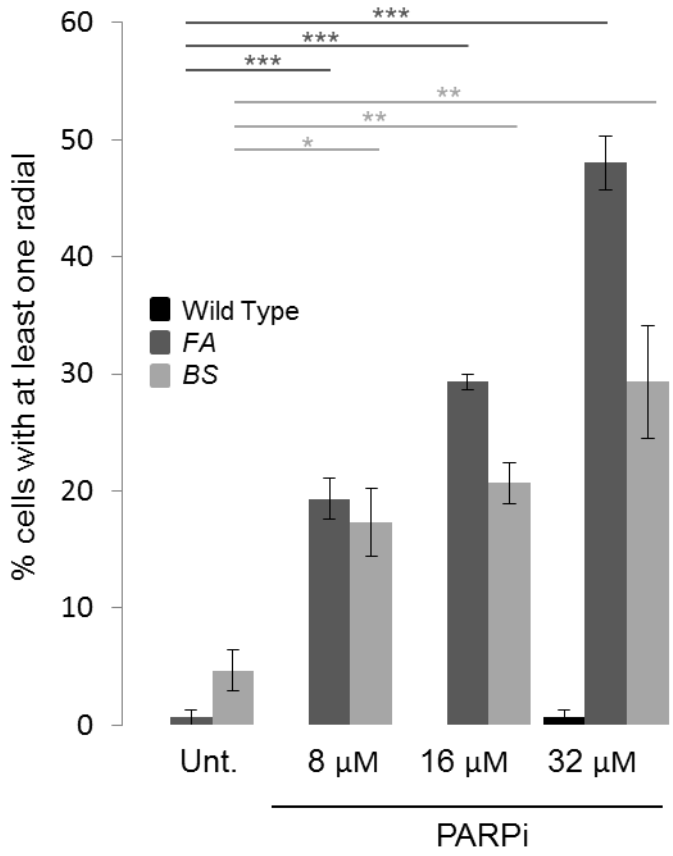

Figure 1: PARP inhibitor induces chromosomal radials in Fanconi anemia and Bloom syndrome fibroblasts. (b) Quantification of radials observed in each cell type showing a dose-dependent induction of radial formation in FA and BS cells. For each study, 50 metaphase cells were analyzed for each indicated treatment dose in each cell line. Each experiment was performed in triplicate and error bars represent standard error. Significance was calculated using two-tailed students t-test.
* = $p<0.05$, ** = $p<0.01$, *** = $p<0.001$

mechanism of action of PARPi, we assessed the levels of spontaneous PARP1-dependent single strand breaks and induced DSBs to gauge the relative damage induced by PARPi treatment in each cell type. Others have shown that analysis of endogenous PARP1-dependent single strand breaks can be assessed by using XRCC1 as a surrogate marker, since XRCC1 forms discrete foci at PARP1 positive SSB during PARP1-dependent SSB repair [97]. We found that the levels of endogenous XRCC1 foci were not significantly different across the three cell types (**Figures 2a, 2b**), indicating similar levels of spontaneous SSB lesions that can be repaired by PARP1, and thus are susceptible to PARPi treatment. To assess whether treatment with PARPi results in a similar conversion of endogenous SSB lesions to DBSs in the three cell lines tested, we performed a neutral comet assay. The neutral comet assay measures only DSB damage and not SSBs, so it is a measure of the SSBs that have been converted to DSBs by PARPi. We found that PARPi-induced DSBs were not significantly different between mutant and wild-type cells after 4 or 24 hr treatments (**Figures 2c, 2d**) suggesting that the number of SSBs converted to DSBs is not discernably different in any of the cells lines. FA cells do have noticeably elevated spontaneous DSBs, as has been previously recognized using fluorescent DSB markers [101,102]. Given that treatment with PARPi exclusively resulted in radial formation in FA and BS cells, and that the levels of endogenous SSBs and PARPi-treatment induced DSBs were not significantly different across these cells types, these results indicate that FA and BS cells are not only exquisitely sensitive to DSB damage, but also form radials directly as a result of DSB

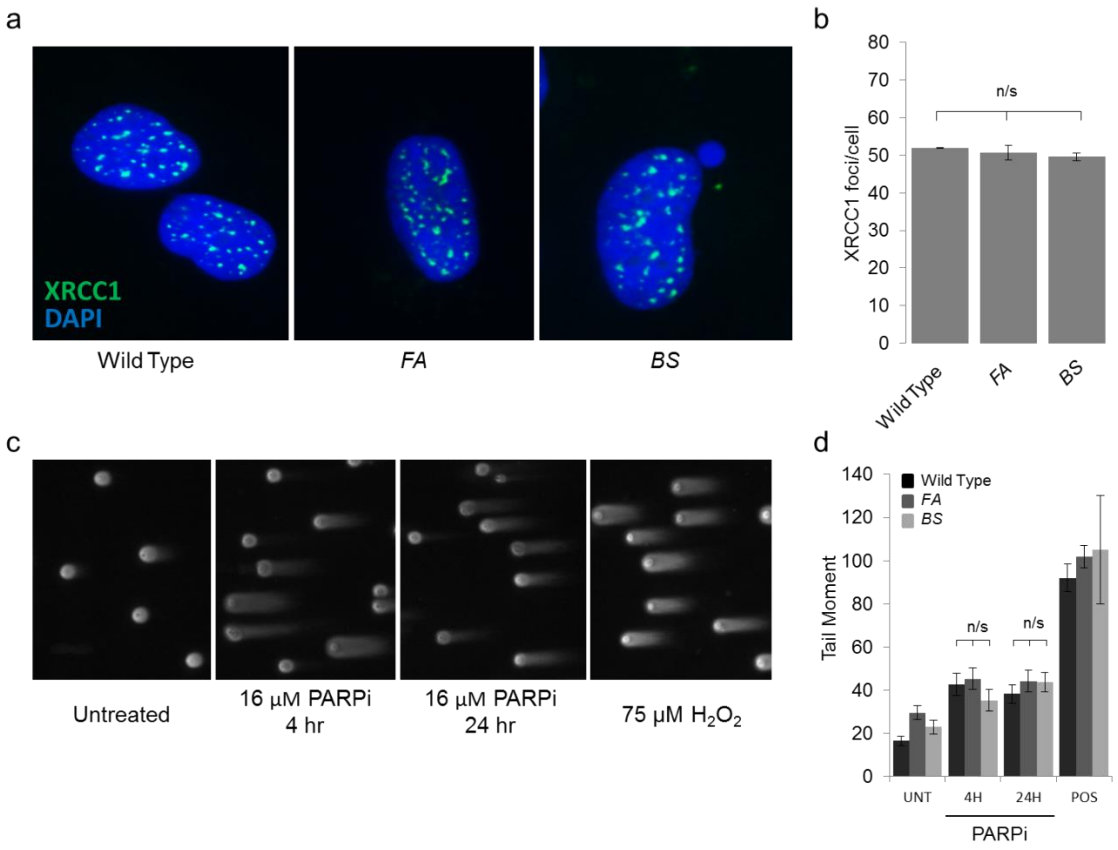

Figure 2: Endogenous PARP1-dependent single strand breaks and PARPi-induced double strand breaks are identical across FA, BS, and wild-type cells. (a) PARPi works by inhibiting the repair of PARP1-dependent single strand breaks which can be identified using an antibody to XRCC1, the binding partner of PARP1 during PARP1-dependent single strand break repair. Representative images of each cell type are shown with XRCC1 foci in green and nuclear stain DAPI in blue. (b) Quantification of the experiment in (a) showing no significant difference between the endogenous XRCC1 foci in FA, BS and wild-type cells. For each, the foci in 75 cells were counted in three independent experiments. (c) Neutral comet assay measures only DSBs (not SSBs) and was used to assess the total induction of DSBs by PARPi. Representative images from wild-type cells are shown along with the positive control (75 μM H_2O_2) run with each experiment. (d) Quantification of the damage observed in the experiments in (c) expressed as the average tail moment. For each, 300 random comets were scored from 3 independent experiments. For all experiments, error bars reflect standard error and significance was calculated using two-tailed students t-test. n/s = not significant.

formation. It is also evident that radials do not appear to be the result of an inordinate amount of DNA damage amassing in FA and BS cells, but rather the inability of those cells to repair damage comparable to what is observed in wild-type cells.

FA and BS cells display aberrant DSB repair kinetics

In light of the exclusivity of radial formation in *FA and BS* cells in response to PARPi-induced DSBs, we hypothesized that radial formation was a result of persistent unrepaired DSBs. Repair delay in response to DNA damage has been observed before in FA cells in response to gamma irradiation, and in BS cells in response to formaldehyde treatment [9,101]. Therefore, to assess the repair kinetics of PARPi-induced DSBs, we analyzed the formation and resolution of 53BP1 foci, a widely-used marker of DSBs. The percentage of cells positive for 53BP1 was analyzed at both early (1-4 hr) and late (24-72 hr) time points during continuous PARPi treatment (**Figure 3**). For all cell types, 53BP1 positive cells accumulated and eventually peaked at 4 hr, indicating that PARPi treatment does not result in a gross delay in initial accumulation of 53BP1 foci and DSB formation. However, both FA and BS cells failed to resolve their 53BP1 foci even after 72 hr, while wild-type cells returned to basal levels by 24 hr. Similar results were observed with an earlier DSB marker, γH2A.X (data not shown). This, combined with the data from the neutral comet assay, indicates that delayed repair kinetics leading to the persistence of DSBs may be the key contributor to radial formation, and that the quantity of DSBs induced may be of less importance.

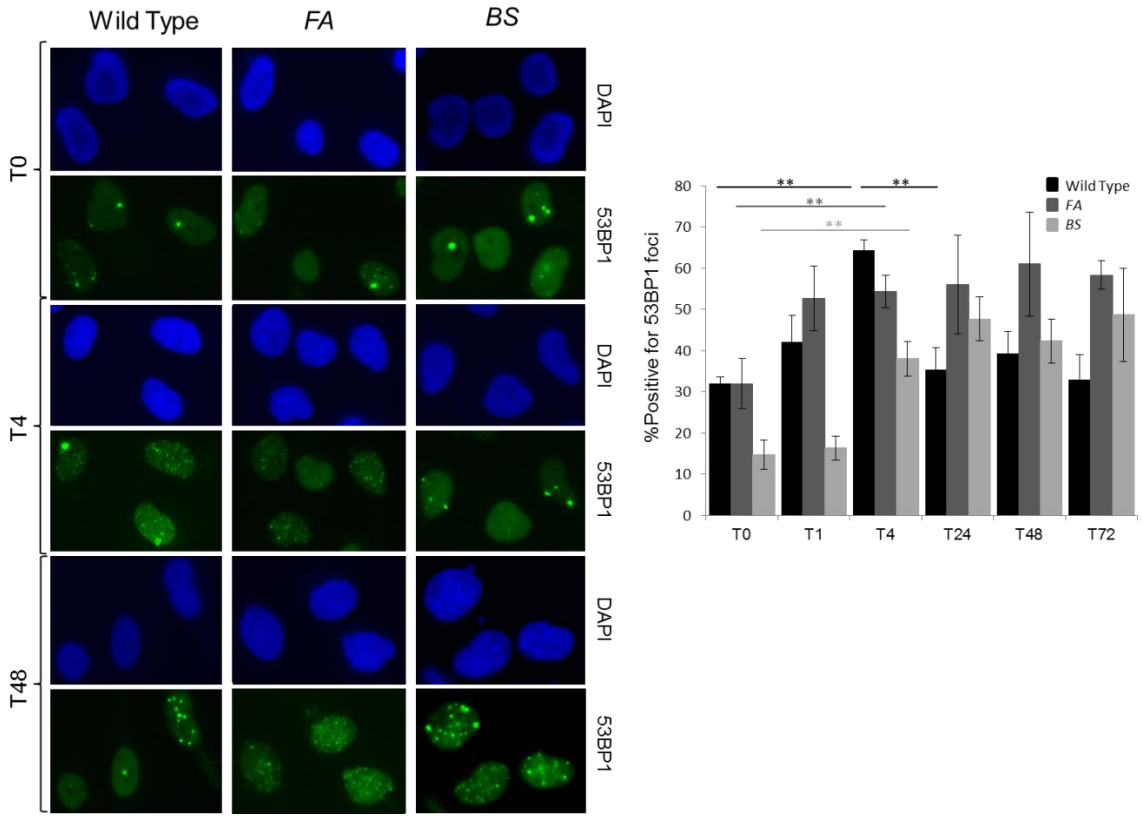

Figure 3: FA and BS cells display aberrant DSB repair kinetics. (a) Representative images from a time course measuring induction and resolution of DSBs after PARPi treatment. T0 = time of treatment, T4 = 4 hr post treatment, T48 = 48 hr post treatment. (b) Quantification of the experiments in (a) including short term (1-4 hr) and long term (24-72 hr) time points. The percentage of cells positive for 53BP1 foci are charted over time with cells containing ≥10 foci called positive. For each, 300 cells were scored from 3 independent experiments. For all experiments, error bars reflect standard error and significance was calculated using two-tailed students t-test. ** = $p<0.01$

DNA damage directly caused by acute PARP inhibitor treatment results in chromosomal radial formation and induced cellular death

Given PARP1's role as both a DNA repair protein and a post-translational modifier, we investigated whether the cellular effects observed were either 1) due directly to an accumulation of DNA damage or 2) as a result of continued catalytic inhibition of PARP1, which is responsible for poly(ADP)-ribosylation of multiple proteins important for cell function [103]. Cells were treated with PARPi for 24 hr to allow DSBs to accumulate during replication before being washed and given new growth media. After a 24 hr recovery without PARPi, radial formation was again assessed and both FA and BS cells showed a dose-dependent formation of chromosomal radials reminiscent of that observed with continuous PARPi treatment (**Figures 4a and 1**). Furthermore, survival assessed via colony forming assay following acute rather than continuous PARPi treatment revealed a dose-dependent increase in cell death in accordance with chromosome radial formation (**Figure 4b**). Altogether, these results indicate DNA DSBs accrued during PARPi treatment are the primary cause of radial formation, and not continued catalytic inhibition of PARP.

Chromosomal radials induce PARP1-mediated cell death during mitosis

Given the structural architecture of a chromosomal radial—two or more chromosomes associated with each other—it is expected that mitosis could not proceed without consequence. Therefore, we initially investigated whether chromosome radials would result in specific structural chromosome

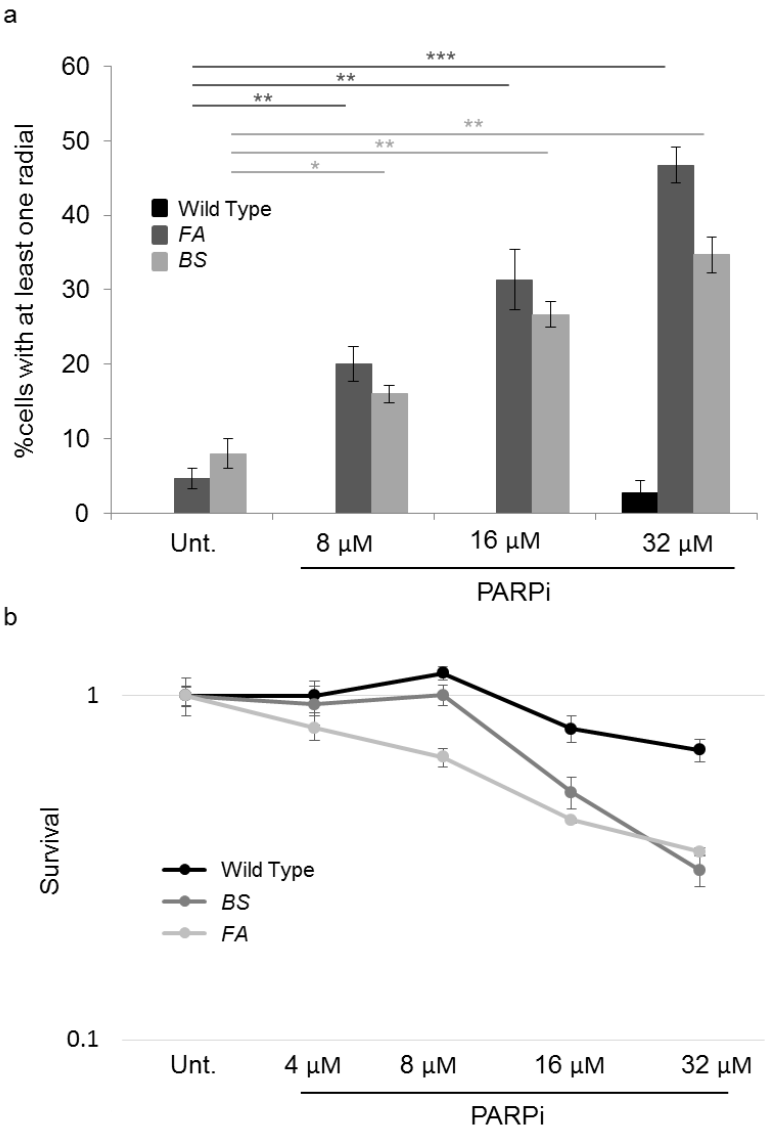

Figure 4: Radial formation and cell death occur as a direct result of accumulated DSB damage. (a) Acute PARPi treatment followed by 24 hr of recovery in normal media is able to cause radial formation indicating accrued DSB damage is responsible for radial formation, not continued catalytic inhibition of PARP1 by PARPi. For each study, 50 metaphase cells were analyzed for each indicated treatment dose in each cell line. Each experiment was performed in triplicate and error bars represent standard error. Significance was calculated using two-tailed students t-test. * = $p<0.05$, ** = $p<0.01$, *** = $p<0.001$ (b) Survival curves as a result of colony forming assays indicating increased sensitivity of FA and BS cells to PARPi. The amount of cell death is directly related to the induction of radials in FA and BS cells.

abnormalities, such as the translocations that occur in *Brca2*$^{-/-}$ cells following MMC-induced chromosomal radial formation [104]. MMC directly induces ICLs and is used to induce radials in the clinical diagnosis of Fanconi anemia [105]. As radials form roughly 48 hr, or two replication cycles, after MMC exposure, we devised the scheme in Figure 5a to assess any and all chromosomal abnormalities (including translocations) that were the direct result of radial formation in primary FA cells (PD220). An acute treatment with MMC to induce DNA damage was followed by periods of recovery in normal growth media. Every 24 hr, or roughly one replication cycle, a recovery flask and an untreated flask were harvested to collect metaphase cells and look for any chromosome abnormalities (**Figure 5a**). Given that radials do not appear until 48 hr, we would expect no, or limited, amounts of chromosomal abnormalities resulting from radial formation until at least 48 hr, and for any significant chromosomal abnormalities directly resulting from radial formation to not be present until 72 hr, or roughly one replication cycle after radial formation. MMC treatment induced a minimal increase in structural chromosomal abnormalities but no specific type was observed at an increased frequency (**Figures 5b-d**). If radials were specifically resolving into translocations, then we would expect a disproportionately high number of translocations at the metaphase following radial formation. On the contrary, the metaphases collected after radial formation had few overall abnormalities and they were of no particular type. Thus, it appeared that radials either resolved without a gross cytogenetic footprint, or more likely—that the cells containing any radials died.

a

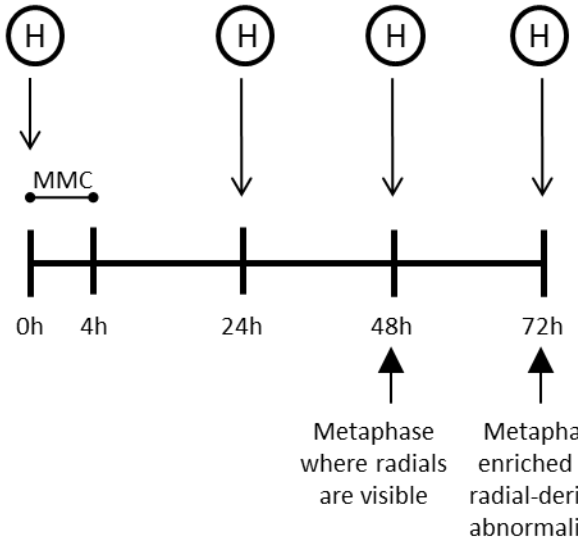

b

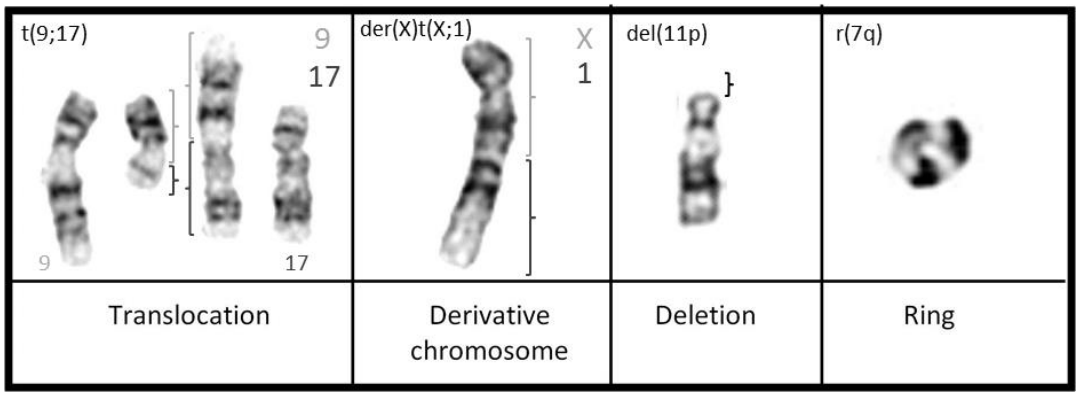

Figure 5: Radials do not result in specific structural chromosome abnormalities. (a) Treatment schematic for the present experiment to observe chromosome abnormalities that would be the result of radial formation. A pulse of MMC to induce radials was followed by harvests of paired treated (radial induced) and untreated cells every 24 hr, or one replication cycle. Radials normally appear at 48 hr so the expectation is for radial-induced chromosome abnormalities to be visible and concentrated at the subsequent metaphase (72 hr). (b) A selection of the different types of structural chromosome abnormalities observed in the current study.

c

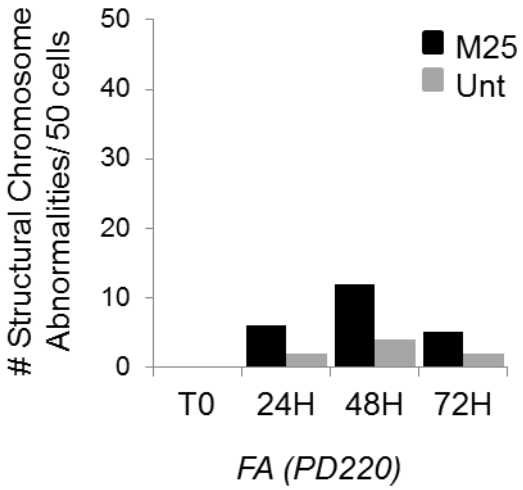

d

Structural Abnormality	T0	U24	T24	U48	T48	U72	T72
Deletion	0	1	2	3	6	0	0
Derivative Chromosome	0	0	2	1	1	1	2
Translocation	0	0	0	0	0	1	2
Ring chromosome	0	0	1	0	1	0	1
Inversion	0	1	0	0	1	0	0
Marker chromosome	0	0	1	0	3	0	0

Figure 5: Radials do not result in specific structural chromosome abnormalities. (c) Quantification of the total number of structural chromosome abnormalities observed after treatment with 25 ng/ml MMC (M25). (d) Detailed description of all of the abnormalities observed in each sample. U = untreated, T = treated with MMC.

To investigate whether the lack of chromosomal abnormalities following radial formation was in fact due to radial-induced cell death, we analyzed radial-containing cells as they proceeded through the cell cycle, beginning with the remainder of mitosis. First, we wanted to assess the ability of cells to align along the metaphase plate by allowing them to proceed through metaphase without the use of colcemid to arrest them. We observed that concurrent with the induction of radials was the appearance of fragmented metaphases, where chromosomes appear to be pulled and highly fragmented across the metaphase plate, with chromosome fragments aggregating at the spindle poles and lagging along the cell periphery (**Figures 6a-b and S1a**). The percentage of metaphase-stage cells undergoing this fragmented metaphase correlates almost exactly with the percentage of radial-containing cells observed in a paired metaphase study (**Figure 6c**). These fragmented metaphases were also observed spontaneously in FA and BS cells at levels similar to the rates of spontaneous radial formation (**Figure 6b**). Importantly, highly fragmented metaphases were observed in wild-type cells at the same rate as radial formation in response to high-dose MMC treatment (**Figure 6b**), indicating this is a normal cellular response to radial formation and not a genome instability-specific response to radial formation.

We have shown that PARPi induces chromosomal radials in FA and BS cells. Therefore, we investigated whether radials induced by PARPi, like those induced by MMC, resulted in fragmented metaphases. Surprisingly, PARPi treated cells did not undergo this fragmentation and PARPi treatment even suppressed the spontaneous fragmented metaphases observed in FA and BS

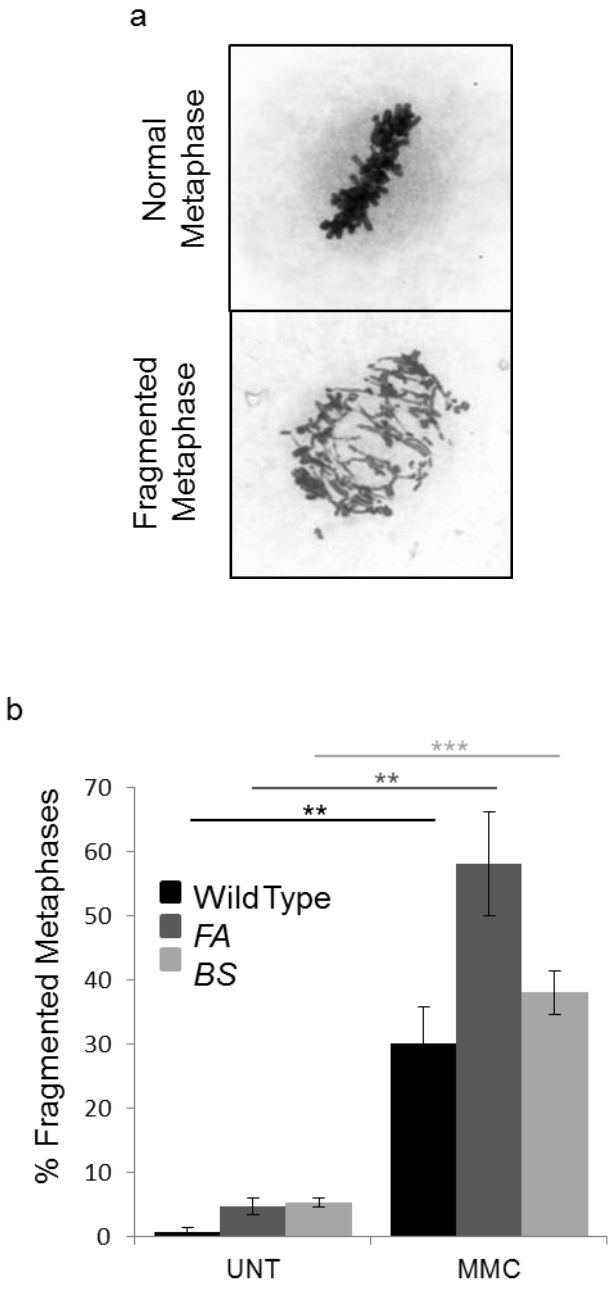

Figure 6: Chromosomal radials induce PARP-mediated cell death during metaphase that appears as hyper-fragmented chromosomes. (a) Examples of a normal metaphase (top) and a fragmented metaphase (bottom). (b) Quantification spontaneous and MMC-induced fragmented metaphases. Each experiment was performed in triplicate and error bars represent standard error. Significance was calculated using two-tailed students t-test. * = $p<0.05$, ** = $p<0.01$, *** = $p<0.001$, n/s = not significant.

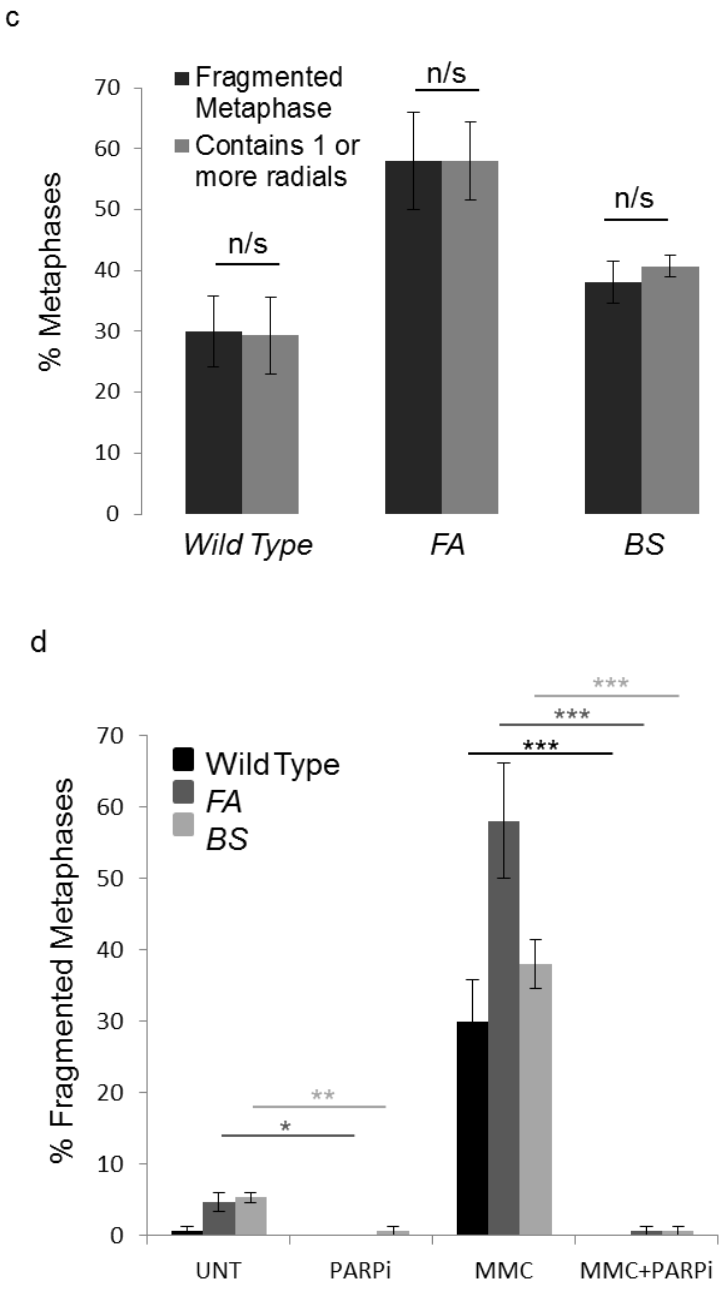

(c) Paired metaphase studies for each cell line treated with MMC showing the percentage of cells containing radials versus the percentage of cells undergoing fragmented metaphase at the same time point (48 hr) when radials occur after DNA damage. (d) The process metaphase hyper-fragmentation is dependent on PARP. PARPi suppresses spontaneous fragmented metaphases and fragmented metaphases induced by MMC. Despite being able to induce radial formation, PARPi treatment does not result in fragmented metaphases. Each experiment was performed in triplicate and error bars represent standard error. Significance was calculated using two-tailed students t-test. * = $p<0.05$, ** = $p<0.01$, *** = $p<0.001$, n/s = not significant.

cells (**Figure 6d**). To clarify the role of PARP in this process, we set out to determine whether PARPi-induced radials were dealt with differently than spontaneous and MMC-induced radials, or if PARP was essential for cellular initiation of fragmented metaphase in response to all radials. In order to tease out the difference, cells were co-treated with MMC and PARPi. If PARPi radials were simply dealt with in a different manner by the cell, then co-treatment would result in the same amount of fragmented metaphases as observed with MMC treatment alone. However, if PARP was necessary to trigger a fragmented metaphase in response to all radial formation, then co-treatment with PARPi would eliminate the fragmented metaphases normally observed with MMC treatment. In accordance with the latter, PARPi completely abolished fragmented metaphases in all cell types when co-treated with MMC (**Figure 6d**). To rule out the possibility that the absence of fragmented metaphases were due to a lack of radial induction with PARPi and MMC combination treatment, radial formation was assessed following co-treatment (**Figure 6d**). We observed that combination treatment with PARPi and MMC was additive with regards to chromosomal radial formation, and therefore could not explain the absence of fragmented metaphases (**Figure S1b**). Mitotic indices were taken following 48 hr of PARPi treatment and the loss of fragmented metaphases could not be explained by a loss in total metaphases either (**Figure S1c**). Further validating our hypothesis was that PARPi-induced DSB damage caused radial-dependent cell death if the acute treatment was removed prior to radial formation (**Figure 4b**). Detailed microscopy of wild-type cells at metaphase that were treated with

a

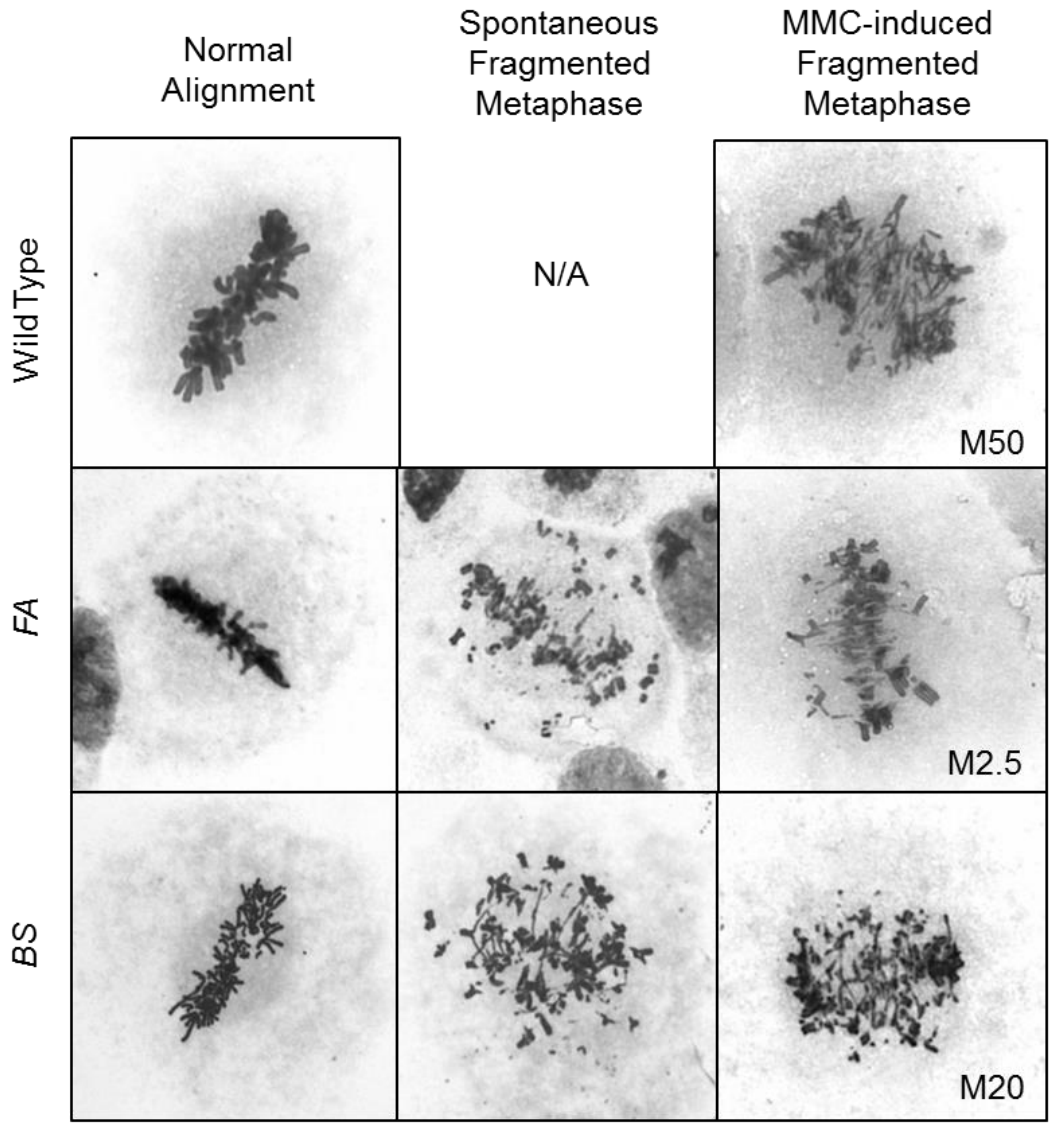

Figure S1: (a) Fragmented metaphases occur spontaneously in FA and BS cells, and in response to MMC-induced DNA damage. M50 = 50 ng/ml MMC treatment.

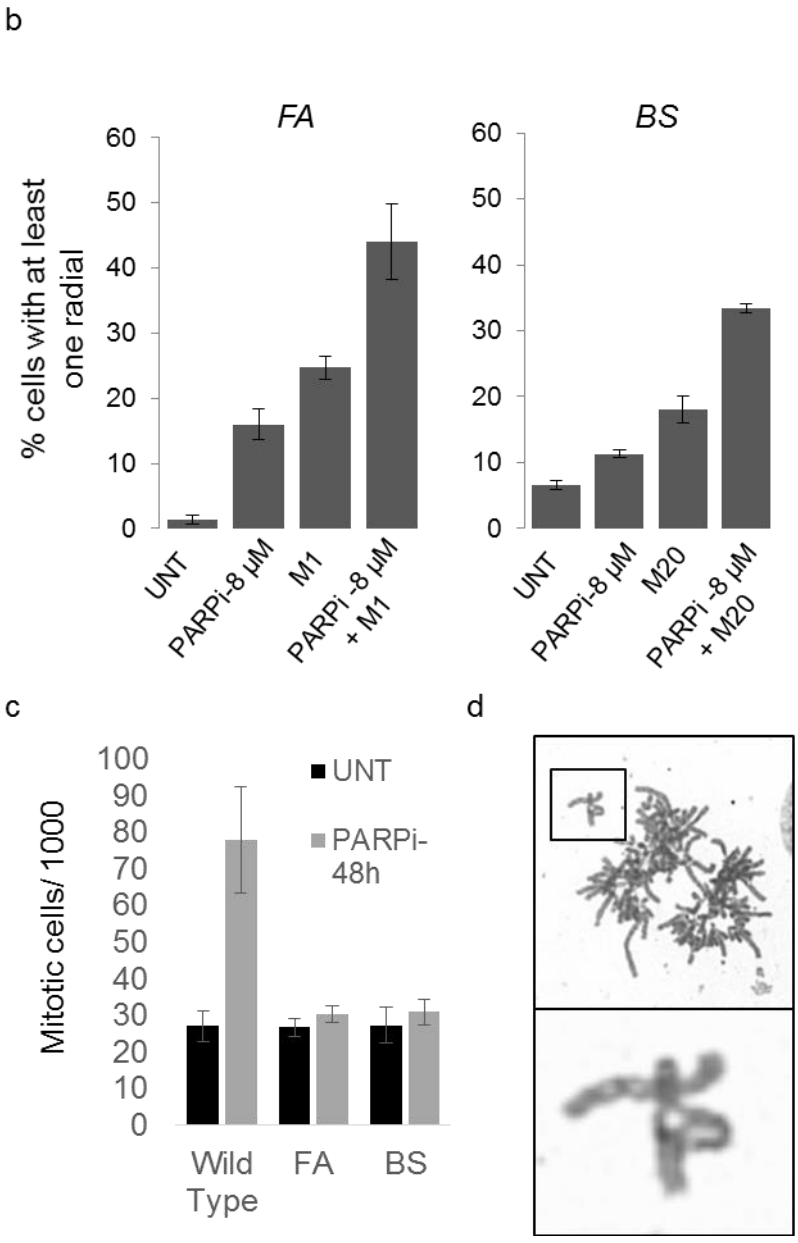

Figure S1: (b) The loss of fragmented metaphases with MMC and PARPi combination treatment is not due to reduced radial formation. (c) The absence of fragmented metaphases in PARPi treated samples is not due to an overall reduction in metaphases. (d) A radial aligning at metaphase and not triggering fragmentation in a cell treated with MMC and PARPi.

both PARPi and MMC allowed for the visualization of a chromosomal radial aligning at metaphase and not inducing a fragmented mitosis (**Figure S1d**). Altogether, these findings indicate that cells regularly dispense with radial-containing cells via a PARP-dependent mitotic cell death that morphologically appears as a severely fragmented metaphase. Moreover, given that the level of chromosome fragmentation observed in fragmented metaphases is much too severe to be accounted for by a single radial observed at metaphase, it is likely that the mechanism of cell death due to radial formation is directly at metaphase and involves hyper-DNA fragmentation in addition to PARP1.

Discussion

Despite years of clinical use for the diagnosis of Fanconi anemia, chromosomal radials have remained enigmatic in the DNA repair field. Historically attributed to a defect in the processing of ICLs, recent evidence points to radial formation as a possible byproduct of other classes of DNA lesions. Recent work has shown FA cells to be exquisitely sensitive to perturbations in aldehyde metabolism, and DNA-protein crosslinks induced by formaldehyde have been shown to induce chromosomal radials in BS cells [9,89]. These somewhat contradictory findings regarding the endogenous lesion responsible for radial formation lead us to address the question as to what DNA lesion is the source of chromosomal radial formation. We hypothesized that the most likely answer was that it was in fact all of the aforementioned DNA lesions that were causing radial formation. DNA ICLs, DNA-protein crosslinks, and unrepaired SSBs all share a common step in their processing—they all converge at a DSB. Whether via direct processing of the initial complex lesion by DNA repair proteins, or through transformation of unrepaired SSBs during S-phase, all of the lesions so far shown to induce radial formation are capable of becoming DSBs [99]. These experiments aimed to ascertain whether the commonality between multiple suspected perpetrating DNA lesions—a transient DSB—is sufficient to cause radial formation, and thus explains the wide-spectrum of mutagens that can cause radial formation.

The mechanism by which PARP inhibitor leads to DSB damage is to impede the repair of PARP1-dependent SSBs. SSBs then become DSBs during

replication, leading to an accumulation of DSBs that must be repaired via alternative methods. Acute PARPi treatment rather than continued inhibition of PARP1 was sufficient to cause chromosomal radial formation in FA and BS cells indicating DSBs alone are able to induce radial formation. Given DSBs can be generated endogenously from a variety of sources, including byproducts of lipid peroxidation and unrepaired ROS damage, multiple DNA lesions could lead to spontaneous chromosomal radial formation. It follows that manufactured perturbations to mechanisms that assist with clearing endogenous DNA-damaging agents from the cell would exacerbate the genome instability phenotype associated with Fanconi anemia and Bloom syndrome, such as the concomitant loss of *Fancd2* and detoxifying *Aldh2* [89]. Furthermore, antioxidants and other therapeutics that detoxify the cell of DNA damaging agents have been shown to be beneficial to FA cells, such as delaying tumor formation in FA animal models [106].

PARPi has been investigated for the last decade for its potent action against BRCA1/2-deficient tumors. In this same vein, PARPi has been assessed as a possible chemotherapeutic option for sporadic tumors deficient in other HR factors including the FA proteins. Recently, the question was raised as to whether FA-derived tumors would benefit from PARPi treatment, given the limited chemotherapeutic options these patients face. This research suggests that PARPi treatment in FA-patients may be detrimental as it both induces chromosomal radials and abrogates the associated mechanism of cell death. Not only are PARPi-derived radials prevented from triggering cell death as long

as PARP1 is inhibited, but PARPi is able to eliminate all radial-induced cell death, including those triggered by other mutagens. This is concerning if PARPi is to be considered as a potential chemotherapeutic agent—especially in combination therapy—for Fanconi anemia and Bloom syndrome patients who are highly predisposed to cancer development. Chromosomal radials are mitotically unstable structures that, if allowed to proceed unimpeded through mitosis, would most likely lead to broken chromosomes or gross chromosomal rearrangements like those observed after radial induction in *Brca2*$^{-/-}$ cells [104]. Cytogenetic changes can lead to further loss of tumor suppressor genes and activation of proto-oncogenes, both hallmarks of cancer progression. In a similar situation, sporadic attenuation of the G2 damage checkpoint has been observed in the peripheral blood of Fanconi anemia patients which abrogates DNA damage-associated cell death and promotes tumorigenesis [107]. Continuing research should focus on understanding the fate of chromosomal radials once they are blocked from undergoing PARP1-dependent mitotic cell death, to better comprehend the liability of PARPi treatment in the context of FA and BS.

The mechanism of cell death employed by wild-type, FA and BS cells in response to radial formation is a PARP1-dependent mitotic cell death occurring at metaphase. While the signaling cascade leading to this specific type of cell death has yet to be elucidated, the process shares features of both parthanatos and caspase-independent mitotic death (CIMD). Parthanatos is PARP1-dependent programmed necrosis that has been shown to occur in response to DNA alkylation and ROS damage [108,109]. PARP1 catalyzes the formation of

PAR polymers that deliver the death signal, prompting the translocation of AIF from the mitochondria into the cytoplasm and initiating chromosome condensation and large-scale DNA fragmentation. CIMD is a form of mitotic death that shares many features with parthanatos. It is a form of programmed cell death similarly caspase-independent and reliant on AIF translocation and DNA fragmentation. Most importantly, it represents a mechanism of cell death immediately at mitosis as a way of suppressing aneuploidy when cells fail to fulfill the spindle assembly checkpoint between metaphase and anaphase [110]. It has not been shown directly whether CIMD is PARP1-dependent, but PARP1 has been localized to centromeres where it has been implicated in spindle assemble checkpoint control, and PARPi is able to down-regulate essential spindle assembly protein BUBR1, providing an intriguing possible mechanism of action [111,112]. If PARPi is able to suppress the SAC through inhibiting PARP1 and down regulating essential SAC proteins, then radial containing cells would not trigger the SAC, but would continue unimpeded through mitosis, as observed in **Figure S1d**, potentially resulting in compromised or broken chromosomes. Further studies are needed to tease apart the specific mechanism of cell death beyond a PARP1-dependent pathway employing large-scale hyper-DNA fragmentation at metaphase, and understand the full effect of PARPi on chromosome stability.

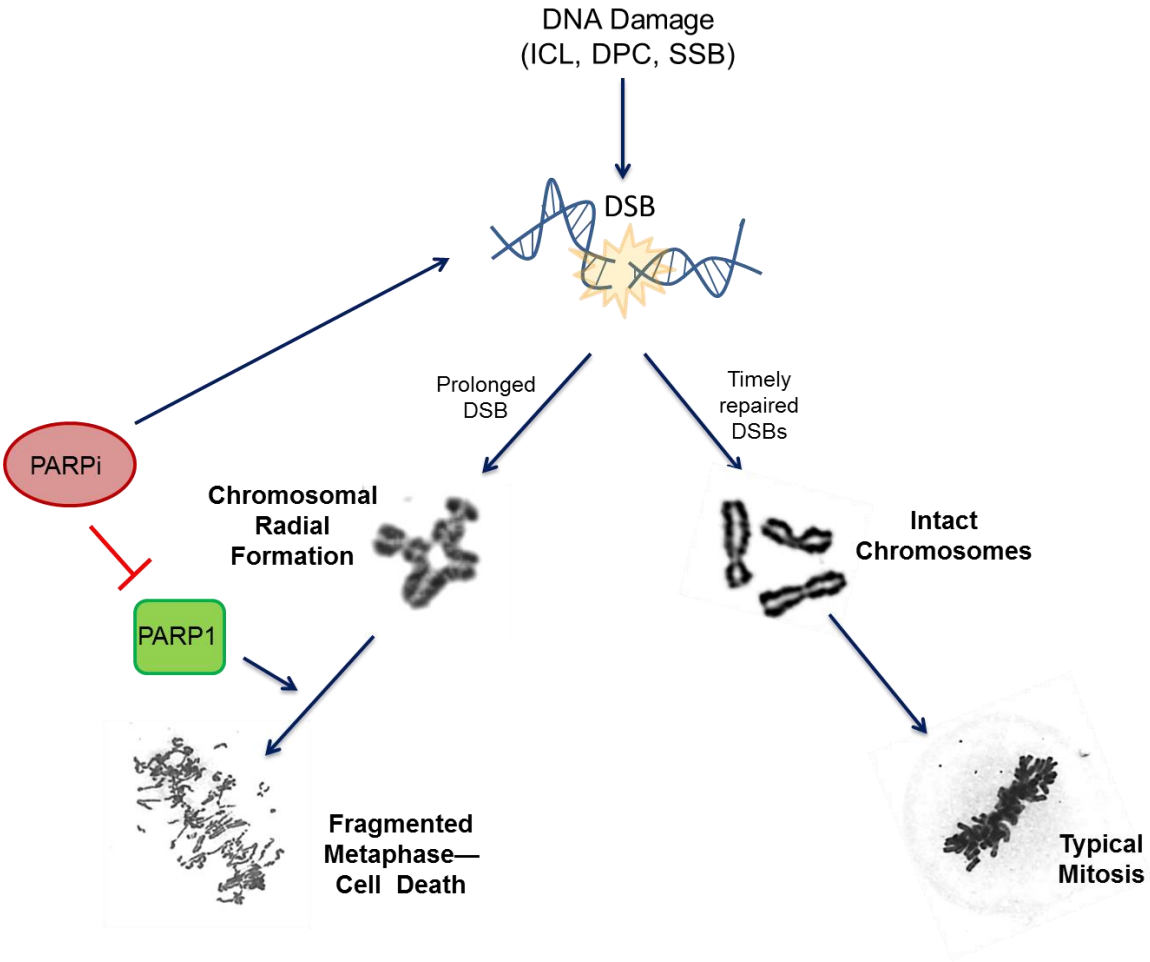

Figure 7: A schematic of PARP-mediated fragmented cell death during metaphase.

Acknowledgements

We would like to thank Dr. Stephen Moore for his helpful discussions. This work was supported by NHLBI grant PO1HL048546 and NIH training grant 5T32HL007781.

Manuscript III: PARP inhibitor PJ34 is able to induce MPD via loss of centrosome integrity rather than through amplification of centrosomes. This finding is contrary to the current understanding of PJ34 which proposes it acts as a centrosome de-clustering agent targeting cancer cells with previously amplified centrosomes. These data raise questions regarding the mechanism of action for PARP inhibitors and suggest that these inhibitors are able to induce chromosome instability in normal cells.

Multipolar Division Without Centrosome Amplification or De-clustering in PARP Inhibitor-treated Cells

Nichole Owen[1], Eleonora Juarez[1], Robb E. Moses[2], and Susan B. Olson[1]

1. Department of Molecular and Medical Genetics

Oregon Health & Science University,

3181 SW Sam Jackson Park, Portland, OR 97239

Telephone: 503-494-8336

2. Department of Molecular and Cellular Biology, Baylor College of Medicine

Houston, TX 77030

Corresponding author email: olsonsu@ohsu.edu

Abstract

PARP inhibitors have primarily been studied for their role in BRCA1/2-combined synthetic lethality, but many have additional effects on cancer cells related to the preservation of a bipolar spindle during mitosis that are not as well understood. Tight control of centrosome number and cohesion is essential for maintaining a bipolar spindle and loss of either can lead to multipolar division and gross chromosome instability. Most of the multipolar division in response to

PARP inhibition has been tied to either the direct induction of centrosome amplification or the de-clustering of endogenously amplified centrosomes, as is common in solid and hematological tumors. Moreover, it has long been thought that normal cells are refractory to PARP inhibition, increasing the therapeutic efficacy of PARP inhibitors. Here, we present evidence for the induction of multipolar division via loss of centrosome integrity rather than whole centrosome amplification. In normal cells and cells prone to chromosome instability, MPD is primarily via loss of centrosome integrity. Only BS-derived cells that have spontaneous supernumerary centrosomes developed amplified centrosomes in response to PARP inhibitor, suggesting that amplification may only happen under certain cellular conditions. Additionally, chromosome instability in response to PARP inhibitor is not limited to cells undergoing multipolar division, which is likely underestimating the toxicity of PARP inhibitors where MPD-induction is often the only readout of toxicity.

Introduction

The discovery of Poly(ADP-ribose) polymerase (PARP) inhibitors as potential treatments for homologous recombination (HR)-deficient cancers promised to be a groundbreaking discovery in targeted chemotherapy. These inhibitors exclusively targeted BRCA1/2-deficient cancer cells with staggering efficiency, spurring an explosion of research aimed at further understanding their mechanism of action, and broadening the scope of potential tumor types that could benefit from treatment [30,34]. Their utility in tumors deficient in HR-associated proteins, such as members of the Fanconi anemia pathway, have been explored, as well as for tumors mutated in PTEN due to shared susceptibility to induced DNA damage [34,112]. However, more extensive research into the details of PARP inhibition has led to the identification of stark differences in cellular responses to various PARP inhibitors, suggesting a need to reexamine the wide-ranging effects of PARP inhibition and identify other possible cellular pathways that are affected by PARP inhibitor treatment.

PJ34 is a potent phenanthrene-derived inhibitor of PARP1 that has been investigated for use as a chemotherapeutic agent in solid tumors and hematologic cancers [43]. Not only does it have the classic DNA damage-inducing and chemosensitizing phenotypes of other PARP inhibitors, but it has the unique ability to eliminate cells with supernumerary centrosomes—a common characteristic of solid tumors and other neoplasia. Cancers favor amplified centrosomes as a way to induce genomic instability and promote tumor progression through the generation of genetically diverse subclones [113].

However, constant multipolar division can eventually compromise cell viability through unfavorable aneuploidies. Thus, in an effort to avoid gross chromosome and mitotic instability, cancer cells with supernumerary centrosomes have developed a mechanism of centrosome clustering to mimic bipolar mitotic division [114,115]. PJ34 has previously been shown to be a centrosome de-clustering agent, negating this important survival mechanism and leading to the death of cells with supernumerary centrosomes via mitotic catastrophe [43]. Mitotic catastrophe is an H2AX-ATM-p53-mediated apoptosis that occurs either directly at mitosis or at the subsequent G1 following multipolar division (MPD) [116,117]. It is a mechanism of cell death specific to the inhibition of PARP1 and related proteins, such as Poly(ADP-ribose) glycohydrolase, that results in multinucleation and eventual cell death. Recent research has also shown that the loss of PARP1 can itself directly cause amplified centrosomes by deregulating the centrosome duplication cycle. Thus, there is a dichotomy to the relationship between PARP1 and centrosome homeostasis that is not fully understood.

These experiments were aimed at gaining a detailed understanding of the mitotic instability and centrosome defects induced by PJ34 treatment, particularly in the context of intrinsic genome instability. Fanconi anemia (FA) and Bloom syndrome (BS) are two instability disorders that are characterized by growth abnormalities and an increased cancer predisposition. At the cellular level, aberrant double strand break repair, a predilection for aneuploidy, and cytokinesis defects result in spontaneous chromosome instability and

multinucleation. The FA proteins have also been localized to the mitotic spindle apparatus and centrosomes where they are thought to be essential for spindle assembly checkpoint signaling, suggesting these cells may be particularly sensitive to centrosome perturbations. BS protein has an unexplored role in spindle assembly checkpoint control as well as through its incorporation into the BTR (BLM-TOP3A-αRMI1-RMI2) complex, which is essential for maintaining mitotic arrest. Here, we find that multinucleation is a universal response to PJ34, but the mechanisms are distinct between different cell types and are not universally dependent on supernumerary centrosomes. *Given the association between PARP1 and amplified centrosomes, and the lack of endogenous supernumerary centrosomes, we hypothesized that MPD due to PARP inhibition was via induction of centrosome amplification.* Surprisingly, this was not the case and we present the first evidence that extensive multipolar division in response to PARP inhibition is not associated with amplified centrosomes, but rather the loss of centrosome integrity.

Methods

Cell Culture and Reagents:

Transformed fibroblasts GM00639 (wild-type), GM08505 (BS) and GM06914 (FA) were obtained from the NIGMS Human Genetic Cell Repository and maintained as subconfluent cultures in a humidified incubator at 37° C w/ 5% CO_2. Cell lines were cultured in α-MEM (Gibco) supplemented with 10% FBS (GeneTex), 4 mM GlutamaX (Gibco) and 50 µg/ml gentamicin (Gibco). Primary FA fibroblasts (PD220) were a gift from the OHSU Fanconi anemia Cell Repository and maintained in α-MEM supplemented with 20% FBS, 4 mM GlutamaX and 50 µg/ml gentamicin. PARP inhibitor PJ-34 (ALX-270-289) was purchased from Enzo Life Sciences and kept as a stock concentration of 1 mM in HBSS at 4º C.

Lagging Chromosome Assay:

Cells were treated with PJ34 for varying times (see Figure 1) and collected via mitotic shake off. Cells were centrifuged at 1000 rpm for 2 min15 sec and resuspended in 40 µl HBSS. Cells were attached to glass slides using 3:1 methanol:acetic acid fixative. Briefly, a drop of fixative was placed on a glass slide to create a thin layer that would repel and hold 5 µl drops of cell suspension. Then, additional fixative was dropped directly on the apex of the cell suspension that beads up while repelling the fixative. Cells were stained with Wright's stain for 2 min 30 sec and imaged with a Brightfield Microscope. Images were taken with Cytovision Software. For each cell line and treatment,

100 metaphase cells were analyzed for the number of lagging chromosomes. Chromosomes were considered to be lagging if there was clear separation and at least one chromosome width between the chromosome and the metaphase plate.

Micronucleus Assay:

Cells were seeded on coverslips, allowed to recover for at least 24 hrs, and treated for the indicated timepoints (see Figure 1) with 16 μM PJ34. Coverslips were harvested by washing in cold HBSS for 1 min before being fixed in 4% PFA for 15 min. Three (5) minute washes with PBS were followed by permeabilization with PBS-T (PBS + 0.25% Triton-X) for 15 min. Cells were stained with Phalloidin to visualize actin and determine cell borders before being mounted with antifade plus DAPI to visualize DNA. Imaging was performed on a Nikon E900 Fluorescence Microscope with an Applied Imaging Camera, and images were captured using Cytovision software. For each cell line and timepoint, 100 cells were scored for the presence and number of micronuclei.

Mitotic Index:

PJ34-treated and untreated cells were harvested via trypsinization, pelleting, and resuspension in a hypotonic solution (0.075 M KCl, 5% FBS) for 10 min prior to being fixed with 3:1 methanol:acetic acid. Cells were stained with Wright's stain for 2 min 30 sec and read on a Brightfield Microscope. 1000 cells were scored for each condition and each replicate as mitotic or non-mitotic.

Western Blot Analyses:

For Western blot analyses, cells were seeded in T-25 flasks and incubated overnight at 37° C prior to a 16 μM PJ-34 treatment. Cells were harvested at indicated time points and disrupted via a lysis buffer (50 mM Tris-HCl, pH 8.0, 0.5% Nonidet P-40, 5 mM EDTA, 150 mM NaCl, 1 mM pepstatin A, and 1 mM PMSF) and sonicated. Aliquots of total cell lysate (35 μg) for detection of P53, p-P53, GAPDH and Cyclin B1 proteins were run on a SDS–PAGE gel, followed by transfer onto PVDF membranes. Membranes where then immunoblotted independently with the following primary antibodies at 4 °C: rabbit polyclonal anti-Cyclin B1 overnight (Cell Signaling D5C10, 1:1,000 dilution), rabbit polyclonal anti-p53 for 3 hrs (GeneTex GTX102965; 1:1,000 dilution), rabbit polyclonal anit-phospho-p53 (Ser15) overnight (Cell Signaling #9284, 1:1,000), and mouse monoclonal anti-GAPDH for 2 hr (Sigma, 1:10,000 dilution). The membranes were then incubated for 1 hr with appropriate secondary antibodies conjugated to horseradish peroxidase, and proteins were detected by the enhanced chemiluminescence detection system (Western Lightning^{TM} Plus-ECL from Perkin Elmer or Clarity Western ECL Substrate from Bio-Rad).

Metaphase Plates and Multipolar Division Studies:

Cells were collected, fixed and stained as described above for the lagging chromosome studies. For metaphase plate studies, 100 plates were analyzed for each condition. The number of cells scored for the MPD studies are designated in Figure 3.

Anaphase Fluorescent in situ Hybridization (FISH):

Slides were initially made as described in the lagging chromosome assay and stained with Wright's stain to mark the location of anaphase cells and determine which ones were undergoing MPD. Then, slides were de-stained using 3:1 methanol:acetic acid, dried, and put in 2xSSC (0.3 M NaCl, 0.03 M $Na_3C_6H_5O_7*2H_2O$, pH7) at 37º C for 30 min. Slides were transferred to 0.01 N HCl with 0.005% pepsin for 13 minutes at 37ºC. Slides were rinsed in 1xPBS for 5 min, post-fixed (1xPBS with 4.73 mM $MgCl_2$ and 0.925% Formaldehyde) for 5 min, and rinsed in 1xPBS for another 5 min. Then slides were run through 70%, 80% and 90% ethanol for 2 min each to dehydrate the slides. The FISH probe cocktail was CEP8 (aqua), CEP17 (green) and CEP18 (orange) diluted in CEP buffer (Vysis). All FISH probes were purchased from Abbott Molecular. Hybridization was performed on a HYBrite (Vysis) running a hybridization program of ramping up to 72º C and holding for 2 min and then ramping down and holding at 37º C. Slides were incubated overnight at 37º C in a humidified chamber and post-washed the following morning: 0.4X SSC w/ 0.3% NP40 heated to 72º C for 2 min and 2X SSC w/ 0.15% NP-40 at room temperature for 30 sec. Slides were mounted in Antifade with DAPI. Imaging was done using a Nikon E800 Fluorescence Microscope with an Applied Imaging Camera, and analyzed using Cytovision Software.

Interphase FISH:

Cells were harvested and affixed to slides as described in the mitotic index methods section. Slides were baked for 5 min at 95º C before being placed in 2X SSC (0.3 M NaCl, 0.03 M $Na_3C_6H_5O_7*2H_2O$, pH7) at 37º C for 30 min. Slides were then run sequentially through dehydrating alcohols (70%, 80% and 90% for 2 minutes each) and dried. Cells were hybridized and mounted as outlined in the Anaphase FISH methodology, but the FISH probe cocktail consisted of CEP6 (green), CEP17 (aqua) and RB1 (Chr. 13) (orange) in LSI buffer (Vysis). The CEP6 probe was purchased from Aquarius and the CEP17 and RB1 probes were purchased from Abbott Molecular.

Centrosome Immunofluorescence:

Cells were seeded on coverslips prior to being treated with PJ34 for 24 hr. Untreated and treated samples were harvested by washing in cold HBSS for 1 minute before being fixed in ice cold methanol for 10 min. Then, permeabilitzation with PBG (PBS + 100 mM glycine) + 0.5% Triton X for 15 min, 3x5 min washes with PBG + 0.1% Triton X, and blocking in Abdil (PBG-0.1%T + 2% BSA + 0.01% NaAzide) for one hr. Coverslips were incubated overnight at 37º C with primary antibody against γ-tubulin diluted 1:300 (GeneTex; GTX629704). Coverslips were rinsed in PBG + 0.1% Triton X 3x5 min, and incubated with secondary antibody diluted 1:300 for 45 min at room temperature. Three more rinses with PBG + 0.1% Triton X were done prior to mounting coverslips with Antifade + DAPI.

Multipolar Spindle Immunofluorescence:

Cells were collected via mitotic shake off in 1X HBSS and pelleted using a microcentrifuge (1000 rpm; 2 min 15 sec). For each, HBSS was aspirated off and the cell pellets were resuspended in Microtubule Stabilizing Buffer plus fixative (MTSB-PFA) (64 µM PIPES, pH 6.8; 0.8 mM MgCl2; 4.8 mM EGTA; 2% PFA; 0.5% Triton-X). After incubating for 10 min in MTSB-PFA, cells were spun onto glass coverslips using a spin bucket centrifuge (1800 rpm for 5 min). Coverslips were permeabilized in PBS + 0.25% Triton X for 15 min and blocked for 1 hr in Abdil (PBG-0.1%T + 2% BSA + 0.01% NaAzide). Primary antibody to γ-tubulin (GeneTex; GTX629704) was diluted 1:300 in Abdil and incubated overnight at 37º C in a humid chamber. Three washes with PBS + 0.1% Triton X (5 mineach) were done before incubating with β-tubulin primary antibody (Genetex; GTX100117) diluted 1:150 in Abdil. Incubation was done at room temperature for 4 hr. Three more washes with PBS + 0.1% Triton X were done prior to incubating for 45 min with appropriate secondary antibodies (Jackson Immunoresearch) diluted 1:300 (FDAM) and 1:200 (RDAR). Coverslips were washed again prior to being mounted in Antifade with DAPI.

Multinucleation Immunofluorescence:

Cells were seeded on coverslips and grown overnight prior to treatment or harvesting. For the multinucleation time course, 16 µM PARPi was added to all treatment wells at T0 (time 0) and every timepoint thereafter, a treated coverslip and a paired untreated coverslip were harvested. For harvest, coverslips were

washed in cold 1X HBSS for 1 min, and fixed in 4% PFA for 15 min. 3x5 min washes with PBS were followed by permeabilization with PBS-T (PBS + 0.25% Triton-X) for 15 min. Cells were blocked in 5% BSA for 1 hr followed by incubation with Far Red direct-conjugated Phalloidin for 20 min to visualize actin and determine cell boundaries. Three more washes and coverslips were mounted in Antifade with DAPI to visualize the nuclei.

Results

PJ34-induced lagging chromosomes result in spindle assembly checkpoint arrest, which is blunted in FA and BS cells

PARP inhibitors have been studied in detail for their clinical application in treating various HR-deficient cancers, especially those with mutations in BRCA1/2. However, knowledge of the multifunctional role of PARP, alongside the search for a broader chemotherapeutic application of PARP inhibitors, has led to the need for further research on the additional cellular implications of inhibiting PARP. PARP inhibitor PJ34 has been previously shown to be an inducer of cell death via mitotic catastrophe, but the exact mechanism of action is unknown since only terminal cellular multinucleation was observed.

Multinucleation is most likely the result of a defect in mitosis, so in order to better understand the mechanism of PJ34-induced cell death, we began with a detailed analysis of metaphase under conditions of PARP inhibition. Mitotic cells from cultures treated with PJ34 were harvested after 24 and 48 hrs of treatment in order to look for PJ34-induced metaphase defects. In untreated cells, metaphases appeared as tightly clustered chromosomes aligned along a single metaphase (**Figure 1a**). PJ34 treatment induced lagging chromosomes at metaphase in all cell types, but to different degrees (**Figure 1a and 1b**). There were more lagging chromosomes observed in treated FA cells than in wild-type cells, despite similar low levels of lagging chromosomes present in untreated

cultures. Counterintuitively, BS cells had higher endogenous lagging chromosomes, but had significantly fewer PJ34-induced lagging chromosomes.

Given the considerable increase in lagging chromosomes, we wanted to know whether they resolved during metaphase or persisted further in the cell cycle. In accordance with the metaphase data, an increase in lagging chromosomes was observed for all cell types at anaphase (data not shown). Unresolved lagging chromosomes during mitosis can become micronuclei when the nuclear envelope reforms during telophase with lagging chromosomes separated from the primary nucleus (**Figure 1c**). To test this, interphase cells were observed after treatment with PJ34 and a progressive increase in micronuclei was observed, especially starting around 24 hr (after at least one round of mitosis) (**Figure 1d**). Micronuclei can also be the result of damaged DNA being expelled from the nucleus, but the timing of the micronuclei—not appearing until 24 hr after treatment suggests they are more likely lagging chromosomes after undergoing mitosis in the presence of PARP inhibitor. Likewise, in manuscript II we showed equal levels of induced DNA damage in these three cell types, yet BS cells have more micronuclei than FA or wild-type cells indicating a substantial portion of these micronuclei are likely lagging chromosomes and cannot be accounted for by DNA damage levels alone. These data suggest that multipolar division and multinucleation are not necessary for PARP-inhibitor to induce chromosome instability. Thus there is the potential to grossly underestimate the amount of instability generated by PARP1

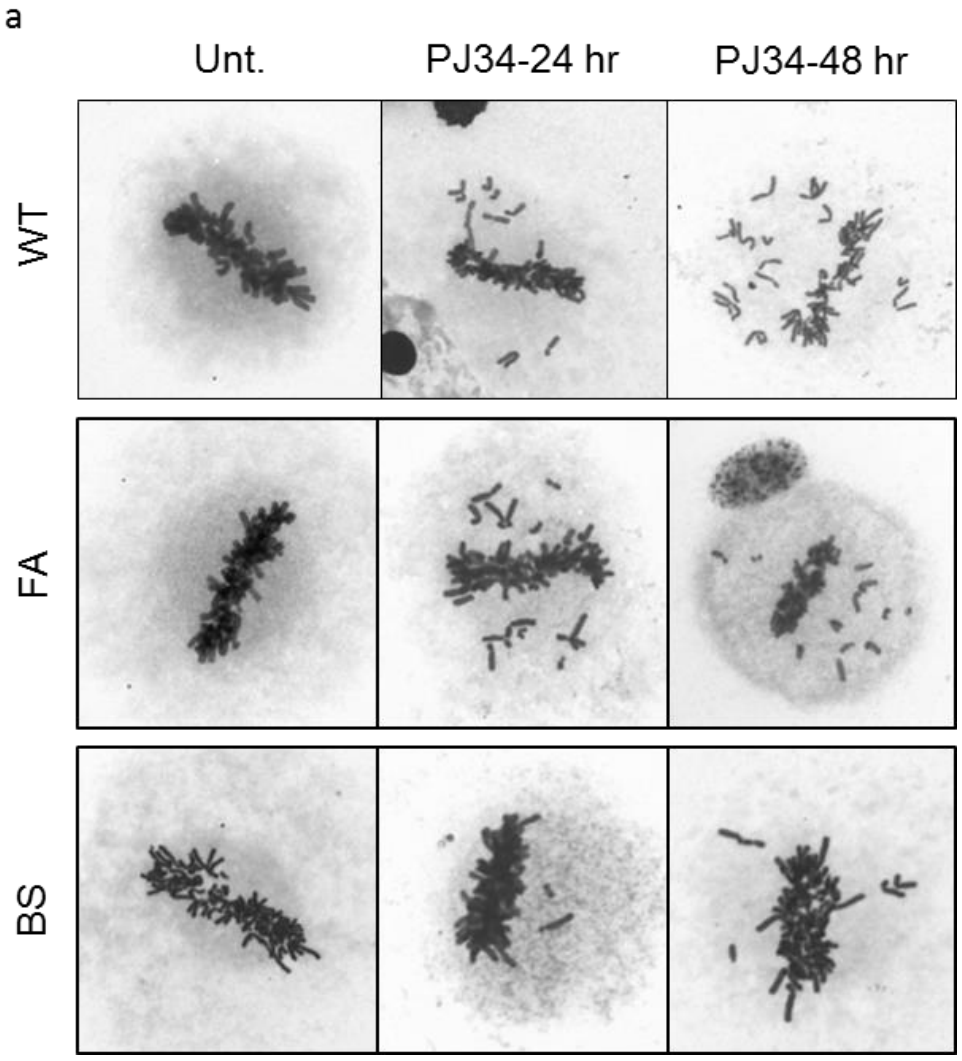

Figure 1: PARP inhibitor treatment induces lagging chromosomes. (a) Representative images of lagging chromosomes at metaphase in wild-type (WT), Fanconi anemia (FA), and Bloom syndrome (BS) fibroblasts. Metaphase plates from untreated (left) and treated (16 μM PJ34) samples are shown.

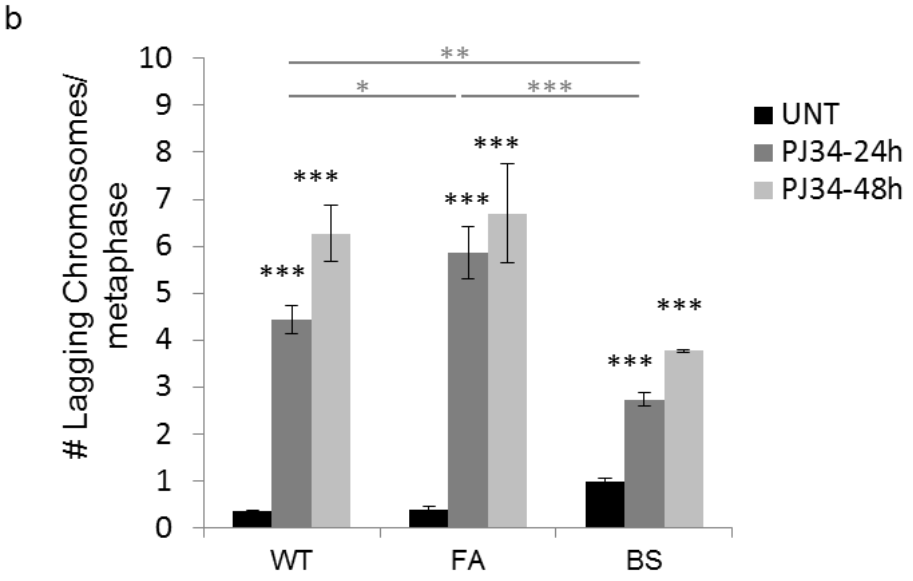

Figure 1: PARP inhibitor treatment induces lagging chromosomes. (b) Quantification of the lagging chromosomes represented in (a). For each condition, 300 metaphases from 3 independent experiments were scored for the number of lagging chromosomes. Chromosomes were deemed lagging if there was clear separation from the primary metaphase plate of at least one chromosome width. Significance was calculated using two-tailed students t-test. * = $p<0.05$, ** = $p<0.01$, *** = $p<0.001$

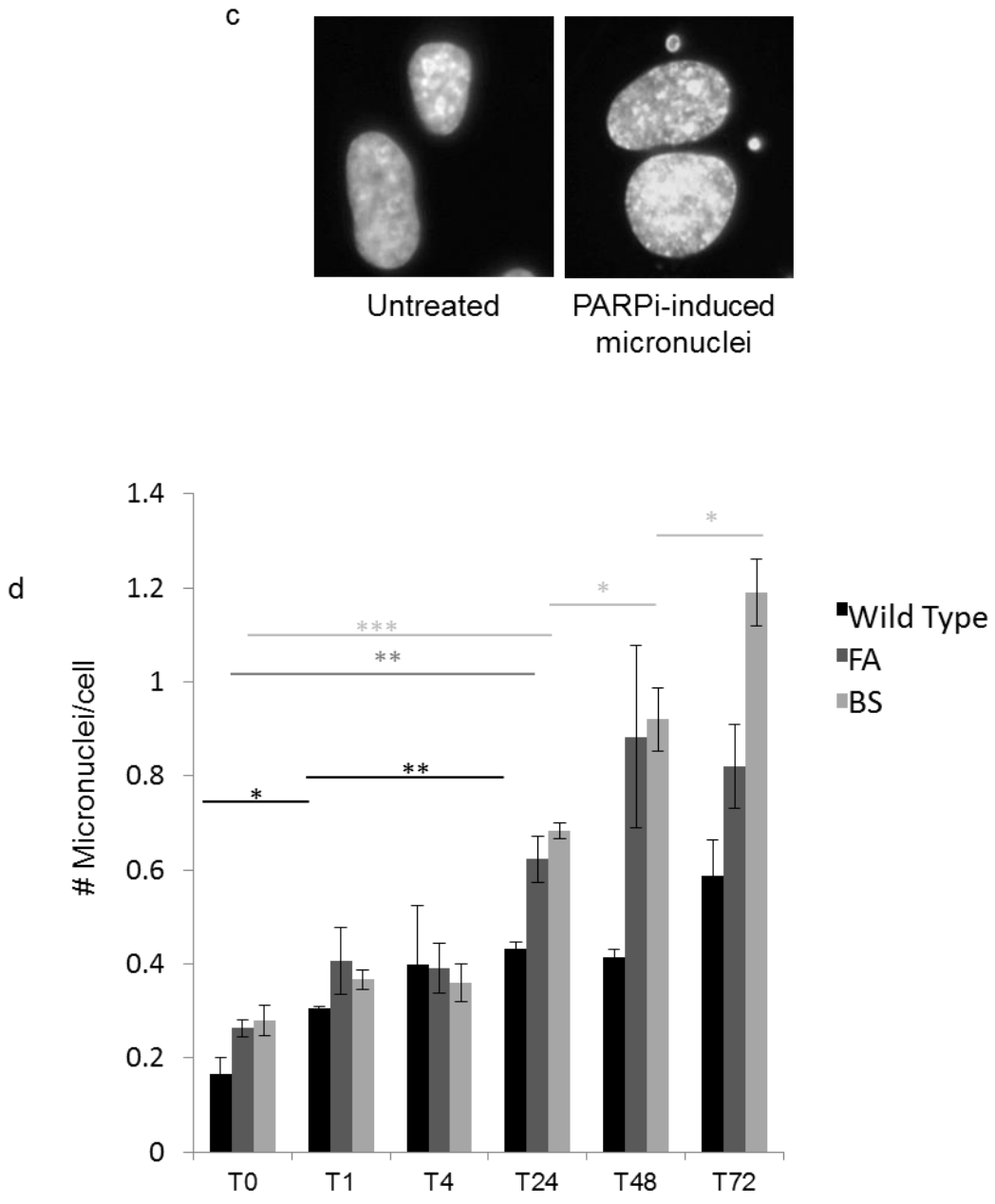

Figure 1: PARP inhibitor treatment induces lagging chromosomes. (c) Representative images of PJ34-induced micronuclei. (d) Quantification of micronuclei represented in (c) as an induction over time. Measurements were taken between one hr (T1) and 72 hr (T72). For each, 300 cells from 3 independent experiments were scored for the number of micronuclei present. Results presented as micronuclei per cell. Significance was calculated using two-tailed students t-test. * = $p<0.05$, ** = $p<0.01$, *** = $p<0.001$

inhibition when only taking into account the induction of catastrophic mitosis.

BS cells accumulated the most micronuclei which is counterintuitive given they had the least number of lagging chromosomes. We hypothesized that the inconsistency between the number of lagging chromosomes at metaphase and the number of observed micronuclei in BS cells may be due to a spindle assembly checkpoint (SAC) defect causing cells to transition to anaphase before full chromosome alignment was achieved. In order to determine if incompletely aligned metaphases were hitting the SAC, mitotic indexes were taken following PJ34 treatment. In a mitotic index, the ratio of metaphases to all other cell stages is determined to calculate any possible enrichment or loss of metaphase-stage cells. If cells were arresting at the SAC, they would be stalling at the metaphase-anaphase transition and this would be reflected as an increase in the mitotic index. Wild-type cells showed a robust arrest at the SAC in response to the observed lagging chromosomes with a 6-fold increase in the number of metaphase cells at 24 hrs (**Figure 2a**). FA cells had a blunted SAC arrest, only doubling the number of metaphases at 24 hr, despite having more lagging chromosomes at metaphase (**Figure 1b**). SAC inactivation has been previously reported after knocking down FA proteins, indicating this is not a unique response to PARP inhibitor but rather a global deficiency in FA cells. Supporting the hypothesis of a SAC defect in BS cells, there was no mitotic arrest observed in response to PJ34. This would mean that the lagging chromosomes observed at metaphase were not triggering the SAC, allowing lagging chromosomes to proceed through anaphase and into the resulting interphase cells as micronuclei.

The arrest of metaphase cells at the SAC can also be monitored using the accumulation of Cyclin B1, a cyclin that accumulates in G2-phase, peaks in metaphase and whose rapid degradation is required for entry into anaphase. In order to confirm the data from the mitotic indexes, a western blot was performed for Cyclin B1 on cells collected every 24 hr during PJ34 treatment (**Figure 2b**). Confirming the results from the mitotic indexes, Cyclin B1 rapidly accumulated in wild-type cells after 24 hr treatment. FA cells had a more minor accumulation of Cyclin B1, and BS cells showed no accumulation, confirming the mitotic index data of marginal and no arrest at the SAC, respectively. In accordance with cells undergoing mitotic arrest in both wild-type and FA cells, but not BS cells, continuous PARP inhibitor treatment eventually exhausted the cultures of mitotic cells as evidenced by depleted Cyclin B1 at 72 hrs. Accordingly, BS cells show no depletion of Cyclin B1 over time confirming a severe SAC defect in these cells. Altogether, these data indicate that PARP inhibition compromises the ability of chromosomes to align along the metaphase plate, inducing lagging chromosomes and SAC arrest in normal cells. However, the SAC is compromised in cells with inherent genomic instability (like BS and FA cells), leading to premature entry into anaphase and accumulating micronuclei in response to PARP inhibitor.

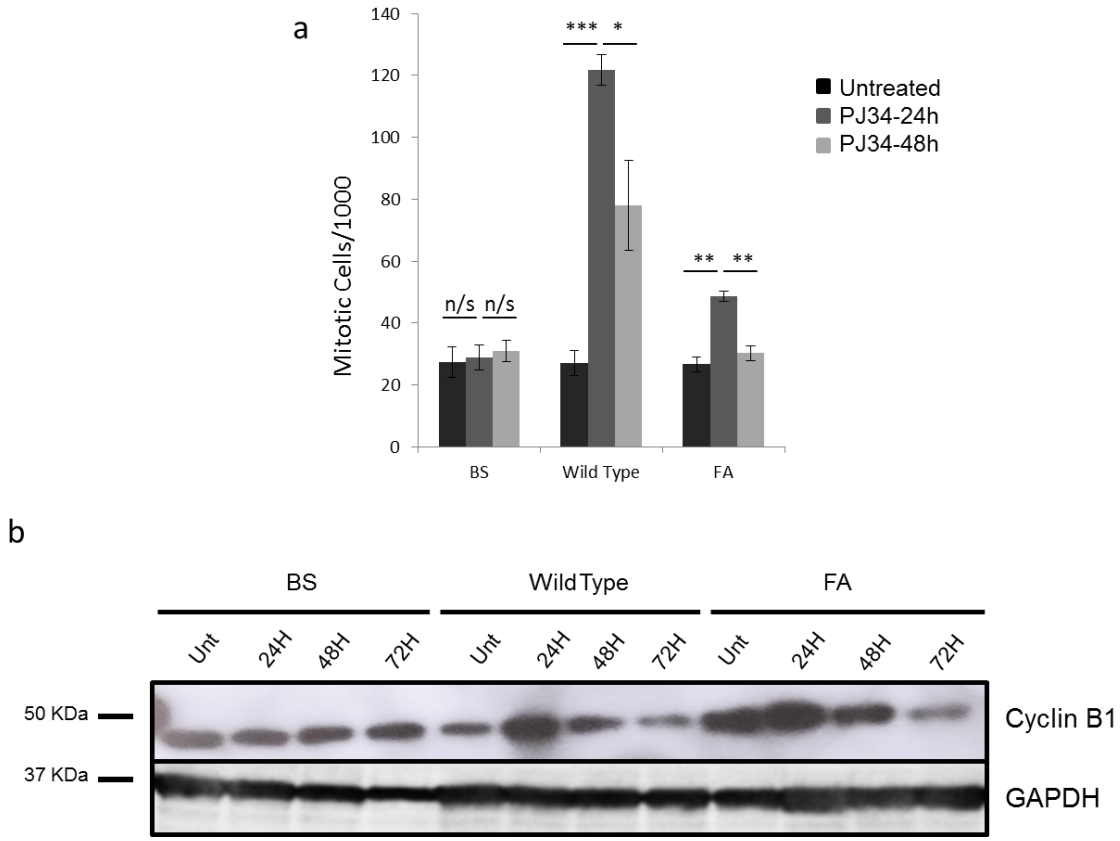

Figure 2: Lagging chromosomes at metaphase trigger the spindle assemble checkpoint, which is blunted in FA and BS cells. (a) Mitotic index over time in response to 16μM PJ34 treatment. For each condition, 1000 cells were analyzed and each experiment was performed in triplicate. (b) Western blot for Cyclin B1 which peaks at metaphase and degrades before anaphase onset. GAPDH is shown as a loading control. Significance was calculated using two-tailed students t-test. * = $p<0.05$, ** = $p<0.01$, *** = $p<0.001$, n/s = not significant.

PJ34 induces supernumerary metaphase plates and multipolar division

Lagging chromosomes and micronucleation indicate PARP inhibition affects global chromosome stability, but cannot explain the previously observed multinucleation. Thus, we wanted to determine if there were gross metaphase or anaphase abnormalities as a result of PJ34 treatment that could produce multinucleated cells. One way of producing multinucleated cells is to undergo multipolar division (MPD) and subsequent cytokinesis failure. MPD is a dysregulated mitotic division that relies on assembling supernumerary metaphase plates leading to anaphase between more than two spindle poles. Cells can then continue with the cell cycle and become highly aneuploid daughter cells, or they can undergo cytokinesis failure and remain as a single large multinucleated cell. The first step in analyzing MPD is to determine whether PJ34 induced additional metaphase plates. Cells with more than one metaphase plate were observed spontaneously, though rarely in untreated wild-type cells (**Figure 3a and S1**). Untreated FA cells had a slight increase in cells with 2 or more metaphase plates, reflecting a possible mechanism for the previously observed multinucleation defect in cells depleted of FA proteins. Close to 20% of BS cells spontaneously had more than one metaphase plate, indicating they possessed an inherent predisposition for MPD. Multinucleation due to the loss of BLM has historically been attributed solely to a defect in cytokinesis, but given the presence of such a high number of spontaneous metaphase plate abnormalities, it is possible that some of the observed multinucleation is due to the presence of supernumerary metaphase plates during mitosis. PJ34

treatment exacerbated this defect, eliciting two or more metaphase plates in 40-50% of cells (**Figure 3a and S1**). Most of the time, the cells contained two plates rather than one, but on occasion there were three metaphase plates. This was most evident in BS cells where despite fewer total cells with induced supernumerary metaphase plates, there was a larger proportion of cells with three metaphase plates rather than two.

Given the induction of supernumerary metaphase plates, it was likely that multipolar division (MPD) would follow. Spontaneous multipolar division is rare in wild-type and FA cells, yet more common in BS cells reflecting a similar pattern seen in the metaphase plate data in Figure 3a (**Figure 3b and 3c**). BS cells are also the only cells to have spontaneous MPD with more than 4 poles, which most likely reflects division in the cells with the most metaphase plates. The MPD induced by PJ34 is primarily tripolar division in wild-type cells after 24 hr, progressing to 4 or more-polar division after treatment for 48 hr. FA and BS cells both have similar numbers of tripolar and 4 or more-polar division at both timepoints, with no worsening over time as observed in the wild-type cells. Once again, PJ34 induced less MPD abnormalities in BS cells despite there being an innate predisposition to supernumerary metaphase plates and MPD. Overall, these data support a role for PARP in maintaining bipolar spindle orientation during mitosis, suggesting PARP inhibition not only interferes with single chromosome stability, but with overall mitotic stability.

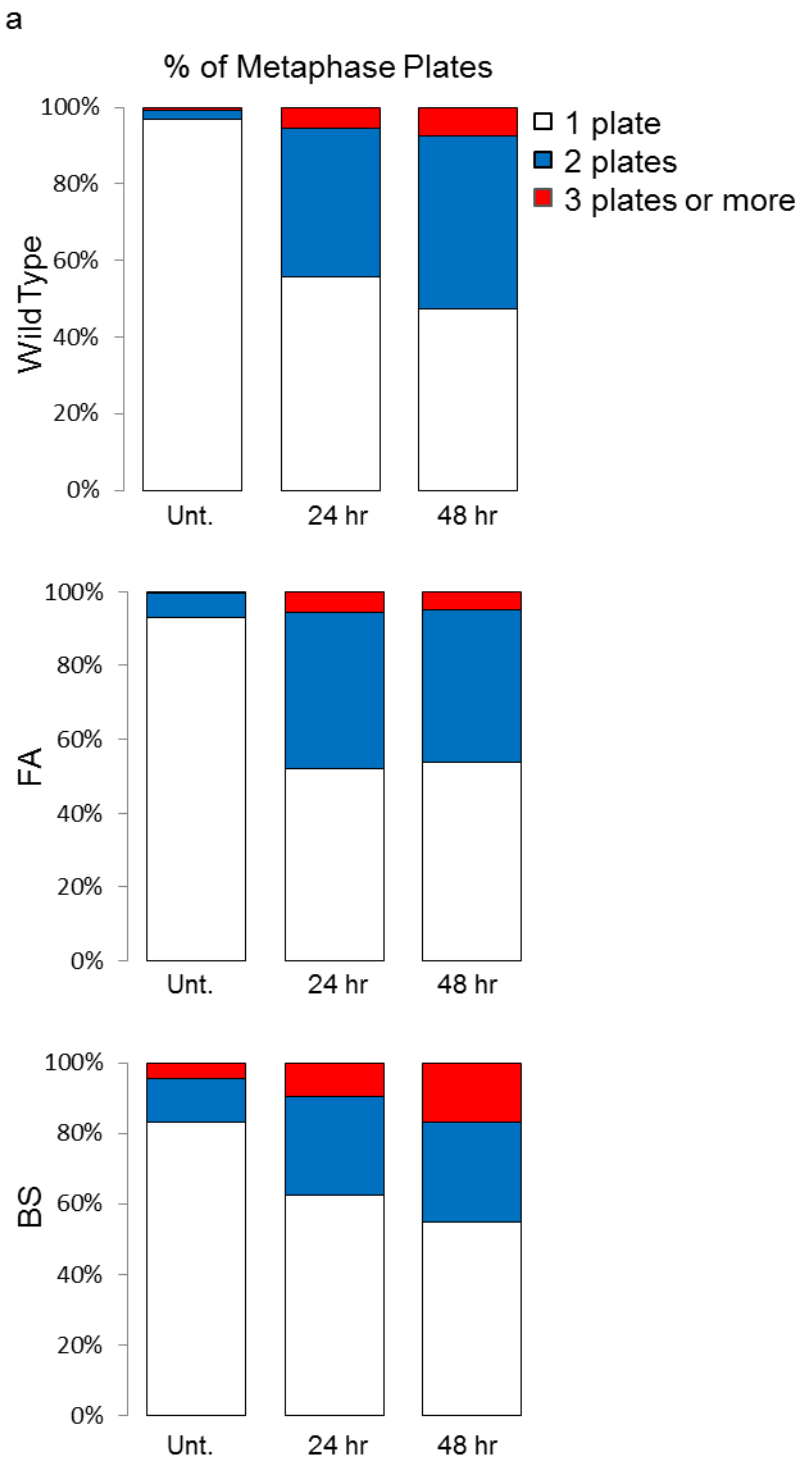

Figure 3: PARP inhibitor induces supernumerary metaphase plates and multipolar division. (a) Supernumerary metaphase plates are described in untreated (Unt), and after 24 or 48 hr of 16 μM PJ34 treatment. For each experiment, 300 cells were scored.

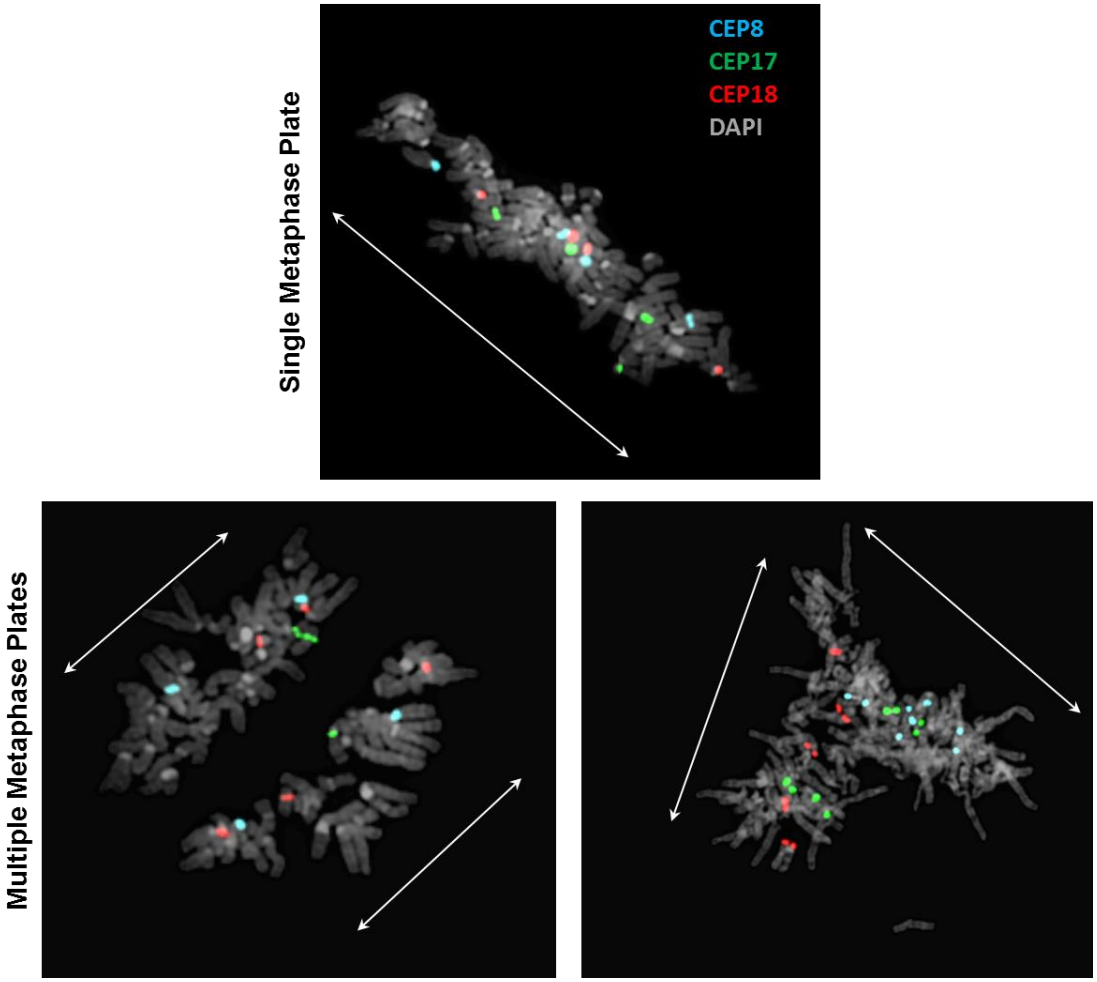

Figure S1: Representative images of single (top) and multiple (bottom) metaphase plates. Multiple metaphase plates can be parallel (left) or perpendicular (right).

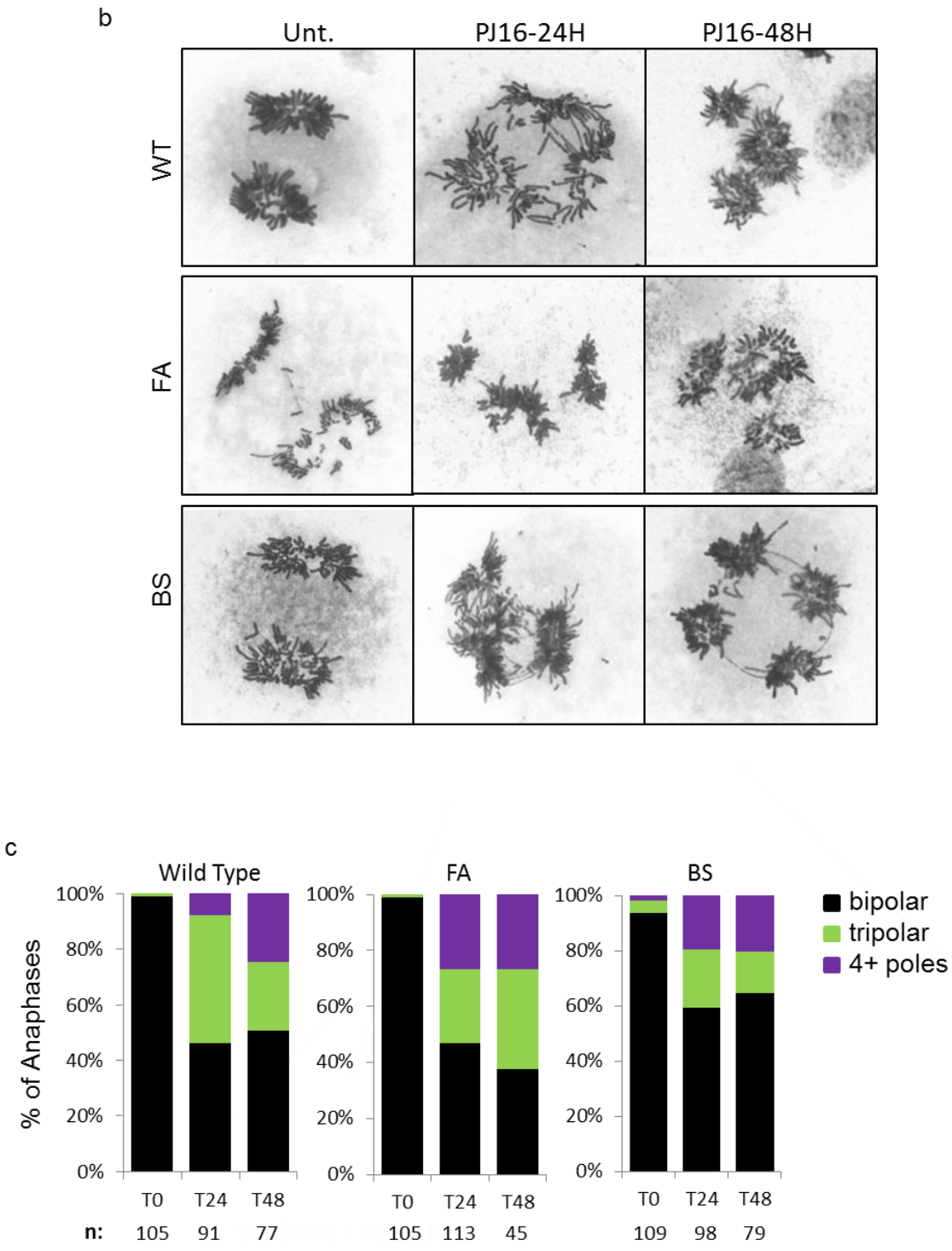

Figure 3: PARP inhibitor induces supernumerary metaphase plates and multipolar division. (b) Representative images of bipolar division in untreated cells and multipolar division in wild-type (WT), FA and BS cells after 16 µM PJ34 treatment. (c) Quantification of the images represented in (b).

PJ-34 induced multipolar division is primarily via loss of centrosome integrity rather than centrosome amplification

The most likely mechanism for generating MPD is to interfere with centrosome integrity or the centrosome duplication process. Centrosomes are the anchors of the spindle poles and the maintenance of exactly two centrosomes composed of a pair of centrioles is essential for maintaining a bipolar spindle. However, there are multiple ways that the centrosomes can be perturbed that can lead to MPD. Dysregulation of the centrosome duplication process can lead to additional centrosomes being generated, each of which is capable of establishing a spindle pole during mitosis. Centriole disengagement is a mechanism of MPD that requires no centrosome amplification, relying on the centriole pair becoming disengaged via a loss of centriole cohesion and traveling apart prior to anaphase. Lastly, fragmentation of the pericentriolar material (PCM) can lead to MPD without centrosome amplification by creating a pseudo-spindle pole capable of nucleating microtubules despite lacking at least one centriole. The induction of MPD and possible connection to centrosome integrity is interesting because PJ34 has been previously shown to have a somewhat opposite mechanism of action—as a centrosome de-clustering agent. It had been shown to exclusively eradicate cancer cells with amplified centrosomes by preventing the centrosome clustering during mitosis that is a recognized survival mechanism.

In order to determine the type of centrosome defect that PJ34 was inducing, via centrosome amplification or via loss of centrosome integrity, we took two different approaches to dissect the chromosome content of multipolar

anaphase cells and identify any centrosome amplification in multinucleated interphase cells. First, we used a fluorescent *in situ* hybridization (FISH) approach to identify any incidences of multipolar division in which centrioles had disengaged. Loss of centrosome integrity defects have a unique chromosome footprint during MPD reflective of one centrosome remaining intact and one centrosome either splitting centriole pairs or fragmenting the PCM. This allows for the use of FISH probes to mark specific chromosomes, with one pole having the full complement of FISH signals, and the other two or more poles all adding up to a single complete set of chromosome signals (**Figure 4a**). Cells were treated with PJ34, collected via mitotic shake off, and stained as in Figure 3 to identify cells undergoing MPD. Then, cells were de-stained and hybridized with FISH probes to Centromere 18 (CEP18; red), Centromere 17 (CEP17; green) and Centromere 8 (CEP8; aqua) (**Figure 4b**). As seen in the left column, bipolar division results in two equivalent daughter cells, each with the same number of red, green and aqua FISH signals. MPD that is characteristic of loss of centrosome integrity, and most likely centriole disengagement, shows the characteristic additivity of two of the spindle poles (left column); while MPD that is not due to centriole disengagement shows a random distribution of chromosomes between the three spindle poles (right column).

In order to confirm these findings, metaphase cells were stained with antibodies to β and γ-tubulin to observe the spindle orientations induced by PJ34 treatment (**Figure S2**). In untreated cells, a single bi-oriented spindle pole between two centrosomes was observed. As shown in the center column, a

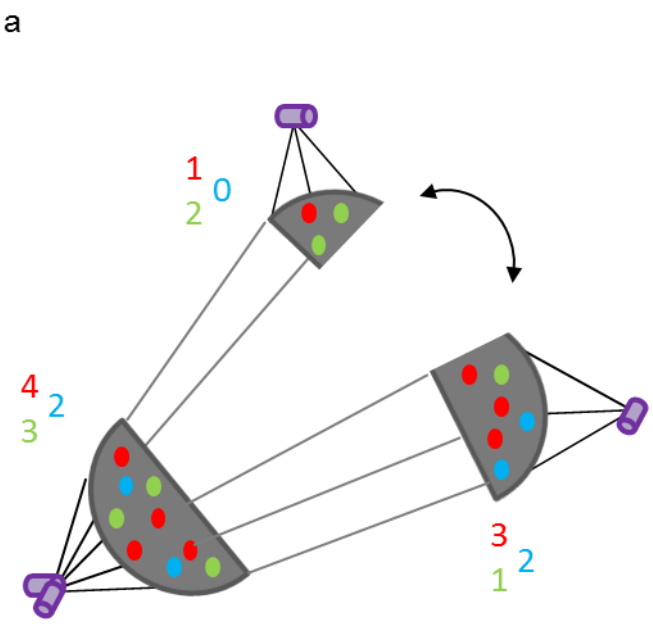

Figure 4: Multipolar division induced by PARP inhibitor is primarily via loss of centrosome integrity. (a) A schematic representation of the FISH probe distribution seen with loss of centrosome integrity.

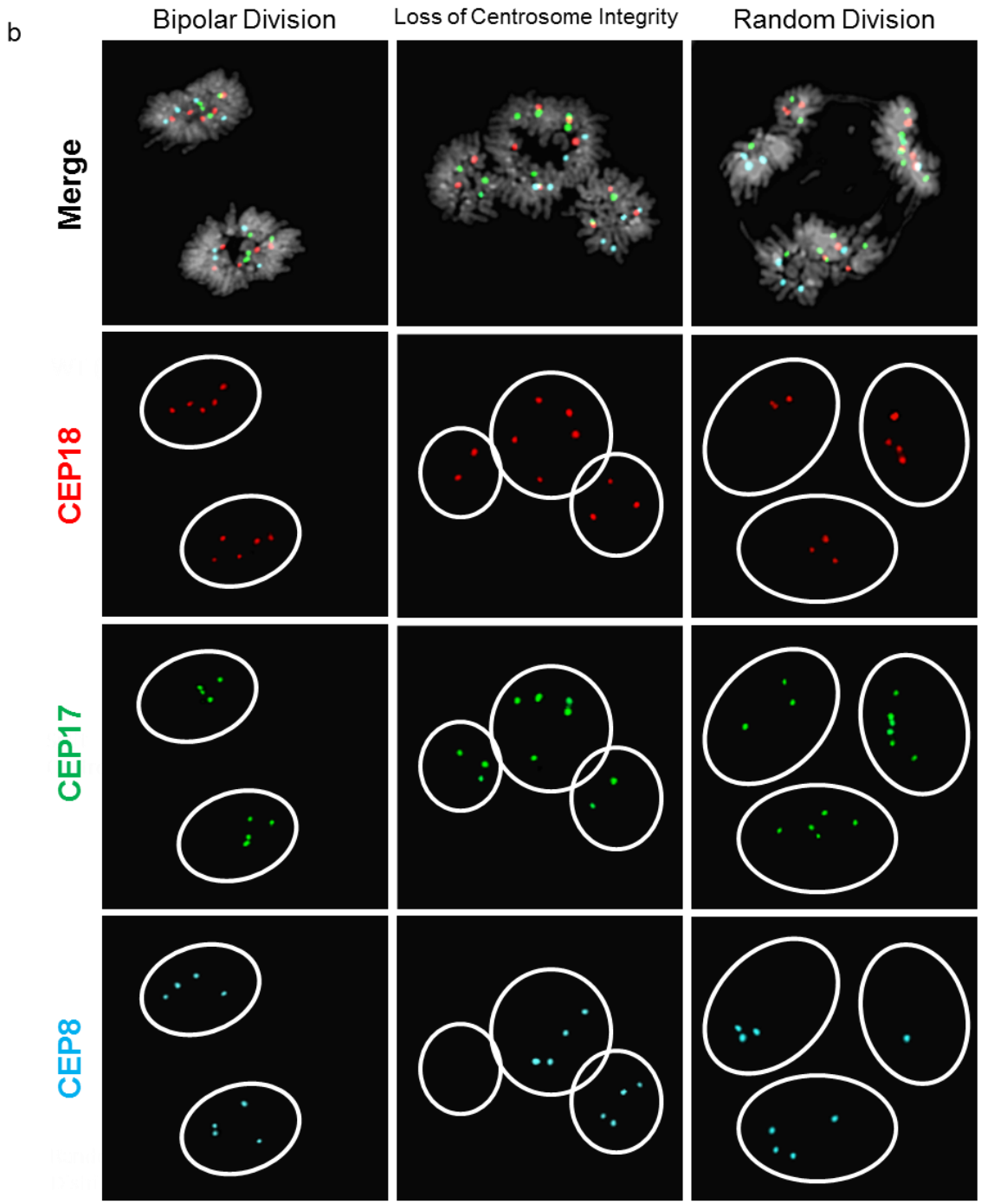

Figure 4: Multipolar division induced by PARP inhibitor is primarily via loss of centrosome integrity. (b) Representative images of FISH on cells undergoing bipolar (left) and multipolar division via loss of centrosome integrity (center) or random division (right) in response to 16 µM PJ34. Each anaphase pole is circled in white to help place FISH signals at the correct location.

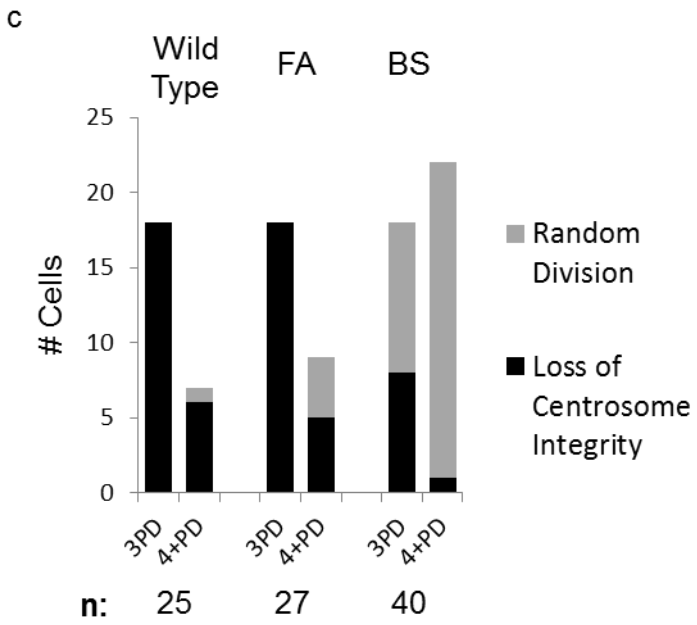

Figure 4: Multipolar division induced by PARP inhibitor is primarily via loss of centrosome integrity. (c) Quantification of the cells represented in (b).

single centrosome has lost integrity and the spindle has fractured. The poles that are due to loss of integrity only form spindle apparatuses back to the intact centrosome and never between each other. The cells undergoing MPD that have random distribution of their chromosomes have microtubule attachments between all the centrosomes resulting in a random collection of chromosomes at each pole during anaphase. Unexpectedly, there were instances of 4-polar division that were additive, with one pole remaining intact and one splitting into more than two poles (**Figure S2**). This phenomenon was observed in both the FISH assay and with microtubule staining. Centriole disengagement cannot explain these since there are not three centrioles in a centrosome capable of disengaging, only two. It is likely, then, that in a small subset of these PJ34-induced MPD events, PCM fragmentation occurs as well. Thus, PARP is essential for gross centrosome integrity and PJ34 treatment manifests as varied centrosome defects.

When specifically looking at the genome instability cells studied here, these different types of MPD are almost exclusive to different cell types. Wild-type and FA cells mainly undergo MPD due to loss of centrosome integrity, while BS cells undergo primarily random MPD (**Figure 4c**). In cases of tripolar division, wild-type and FA cells exclusively go through MPD due to loss of single centrosome cohesion, while half of BS cells do this and half undergo random division. In cases of higher order MPD, the majority of wild-type and FA cells still undergo loss of single centrosome stability. BS cells almost exclusively undergo random division under these conditions. Given these results, it was likely that

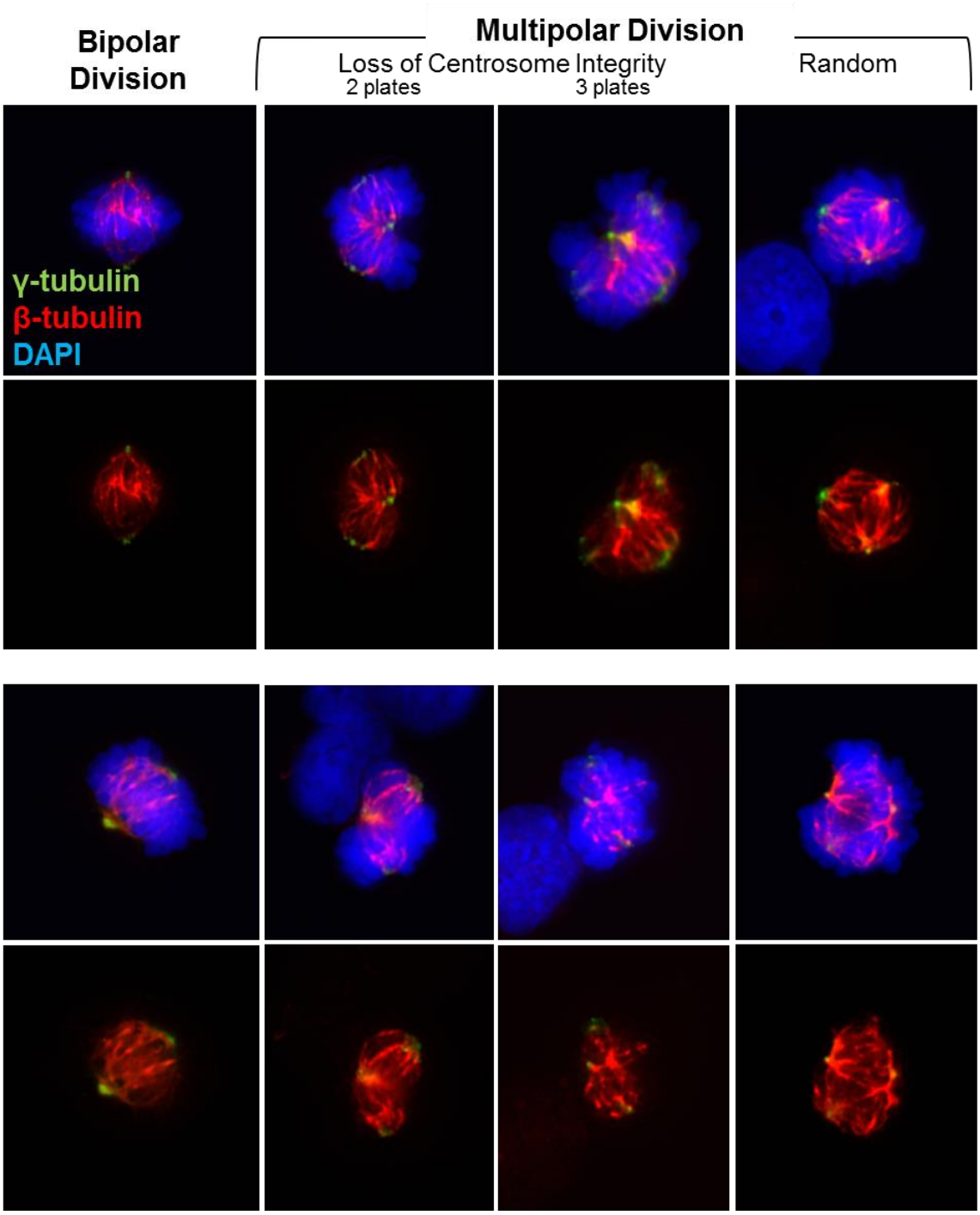

Figure S2: Representative images of bipolar (left), and multipolar spindle apparatuses showing the loss of centrosome integrity (center columns) or complete multipolar attachment that results in random chromosome distribution (right).

PJ34 was affecting the BS cells uniquely in a way that was facilitating multipolar microtubule attachment and random division of chromosomes.

Despite universal MPD, PJ34 induces centrosome amplification only in BS cells only

Given the propensity of BS cells to undergo random division of chromosomes during anaphase, we hypothesized that the MPD phenotype that BS cells display when dividing was due to centrosome amplification exclusively in these cells. The loss of PARP1 has been shown to result in centrosome hyperamplification in $PARP^{-/-}$ mouse embryonic fibroblasts, supporting a model whereby the loss of PARP1, either through inhibition or mutation, is capable of deregulating the centrosome duplication cycle. In order to identify centrosome amplification, cells were treated with PJ34 for 24 hr and stained with γ-tubulin to mark the centrosomes in interphase cells (**Figure 5a**). Both single nucleus and multinucleated cells were analyzed for the number of centrosomes present and the possession of more than two centrosomes was considered amplified. Single nucleus cells rarely had amplified centrosomes, whether untreated or under conditions of PJ34 treatment (**Figure 5b**). Specifically looking at multinucleated cells, centrosome amplification was nonexistent in untreated cultures and PJ34 induced only rare instances of centrosome amplification in wild-type and FA cells. In accordance with our hypothesis, single nucleus cells continued to have normal centrosome numbers, yet a significant portion of spontaneous multinucleated cells and half of the PJ34-induced multinucleated BS cells displayed centrosome amplification. This suggests that BS cells have an innate and unique

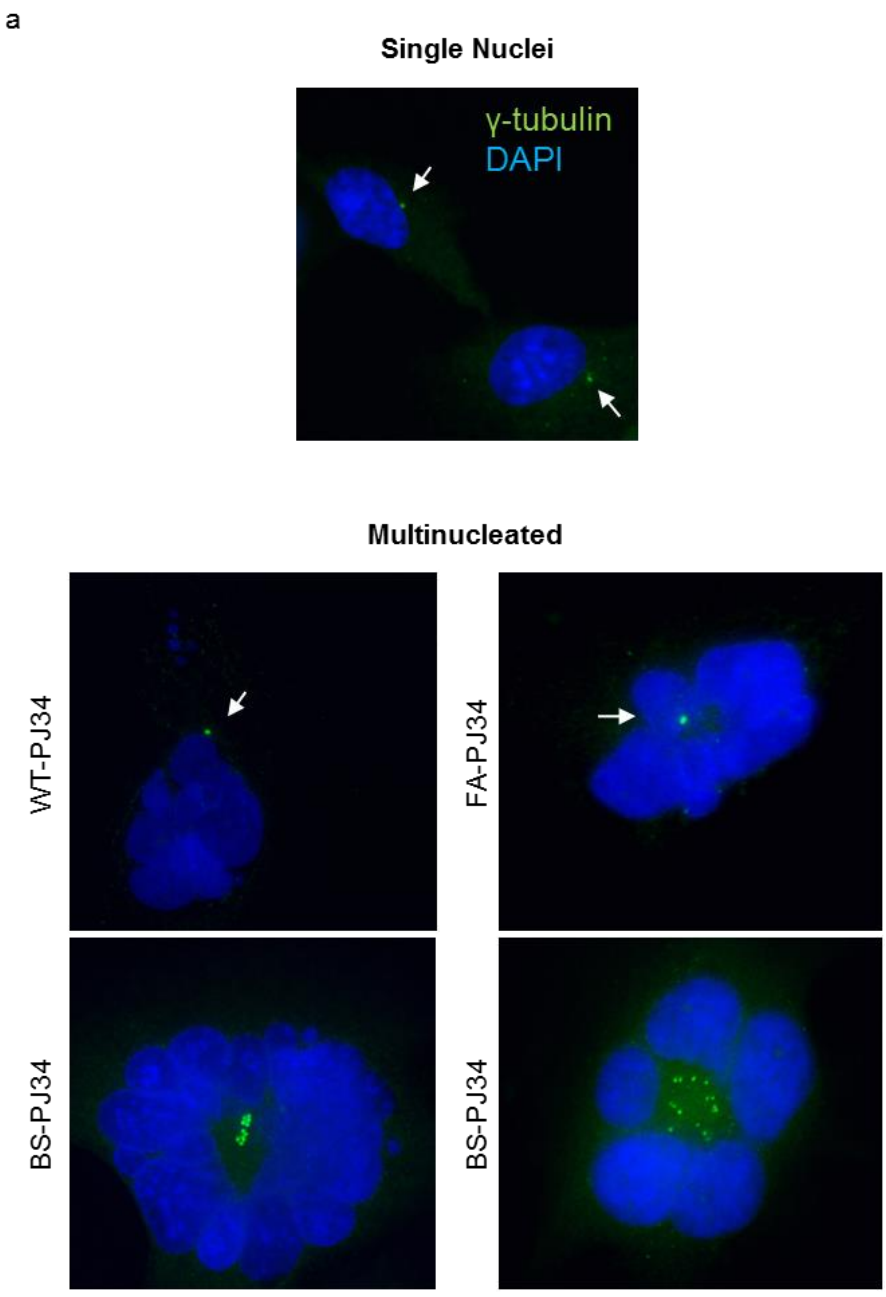

Figure 5: Centrosome amplification is unique to BS cells in response to PARP inhibitor. (a) Representative images of single centrosomes in single nuclei (top), single centrosomes in multinucleated WT and FA cells (middle), and amplified centrosomes in BS cells (bottom). For each condition, at least 300 cells were scored from 3 independent experiments after treatment with 16 μM PJ34. Additional multinucleated cells were scored in PJ34-treated samples to finely gauge the percentage of centrosome amplification. Arrows indicate single centrosomes.

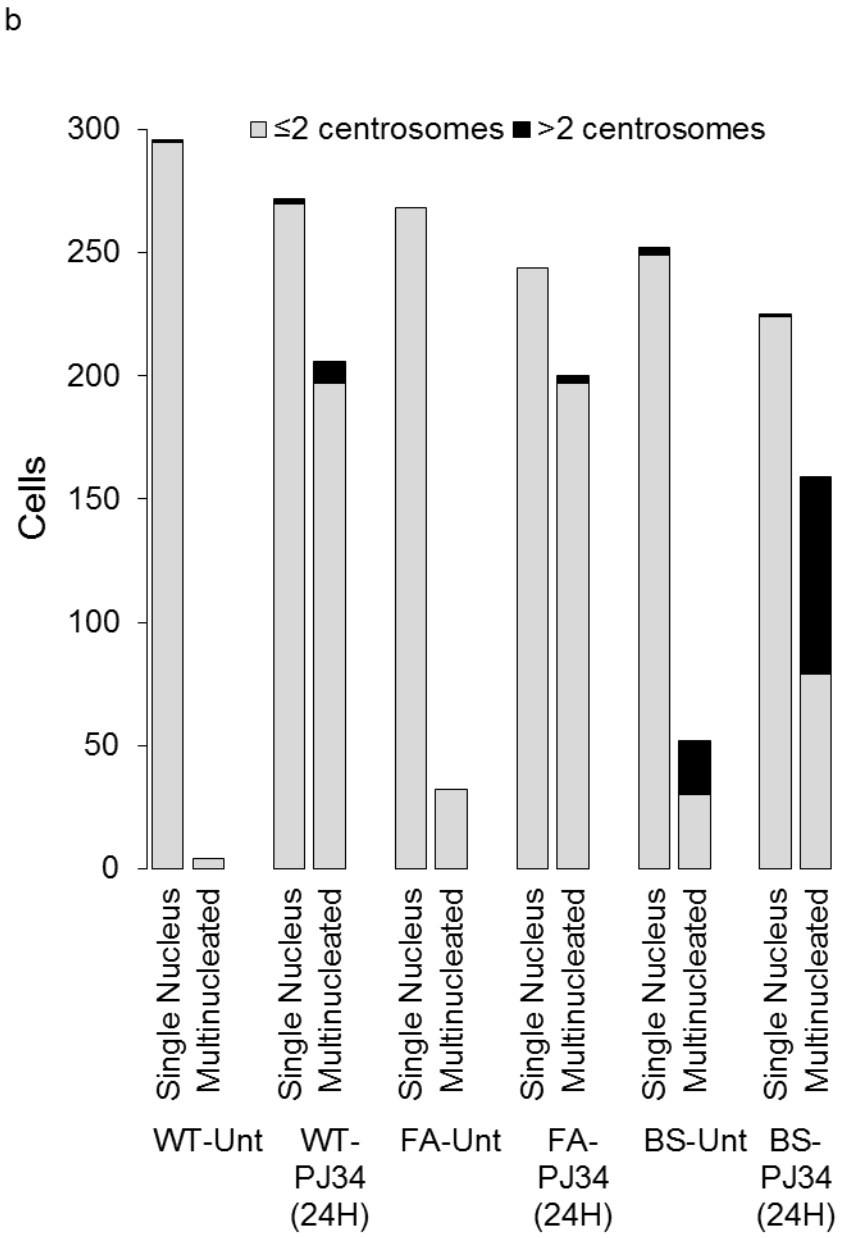

Figure 5: Centrosome amplification is unique to BS cells in response to PARP inhibitor. (b) Quantification of the images represented in (a). 2 or fewer centrosomes were considered normal and more than two were considered amplified.

susceptibility to centrosome amplification that is exacerbated by PARP inhibitor treatment.

Centrosome amplification explains the discrepancy in the types of MPD that PJ34 induces in BS cells versus wild-type or other genome instability-type (FA) cells. Centrosome amplification allows for multipolar spindle formation where all centrosomes are joined, rather than centriole disengagement which is akin to splitting a single bipolar spindle apparatus in two. Thus centrosome amplification can lead to arbitrary chromosome complements at each pole at anaphase, while centriole disengagement has a specific chromosome distribution pattern.

PJ34-induced MPD can result in mitotic catastrophe or completed division with resulting hypoploid cells

Mitotic catastrophe has long been the accepted mechanism of PARP-mediated cell death, but not all cells are equally susceptible. If mitotic catastrophe is a direct result of failed MPD, then one would expect relatively similar levels of MPD and multinucleation. Looking back to Figure 3, FA and wild-type cells had almost identical levels of PJ34-induced MPD, yet there are significantly more multinucleated FA cells as a result (**Figure 6a and S3**). Similarly, BS cells had even less PJ34-induced MPD and yet have significantly more multinucleation than wild-type cells. Mitotic catastrophe is a p53-mediated cell death and in accordance with observed multinucleation, phosphorylated p53 (and total p53) are increasingly elevated after PJ34 treatment in BS and FA cells

(Figure 6b). However, wild-type cells do not show p53 accumulation after 24 hr suggesting, along with the multinucleation data, that wild-type cells undergoing MPD are meeting a different fate.

If MPD is not triggering mitotic catastrophe all of the time, particularly in wild-type cells, then it is possible that some of the cells are completing cytokinesis and forming hypoploid cells rather than remaining as giant multinucleated cells. In order to test this, cells were treated with PJ34 and assessed in interphase for chromosome content using FISH probes on chromosomes 6, 13, and 17. The normal signal pattern is 2 red/3 green/4 aqua signals and under conditions of bipolar division, this signal pattern should persist (**Figure 6c, left**). Under conditions of PARP inhibitor treatment, cells began to accumulate what appeared to be the product cells of completed MPD. These cells were missing >40% of the expected FISH signals, suggesting not a minor aneuploidy problem, but a single catastrophic reduction in chromosome content consistent with completing MPD (**Figure 6c, right**). Analyzing the prevalence of these cells over time suggests that wild-type cells are much more likely to generate these hypoploid cells, particularly after the longer treatment times and in accordance with the resumption of normal levels of p53.

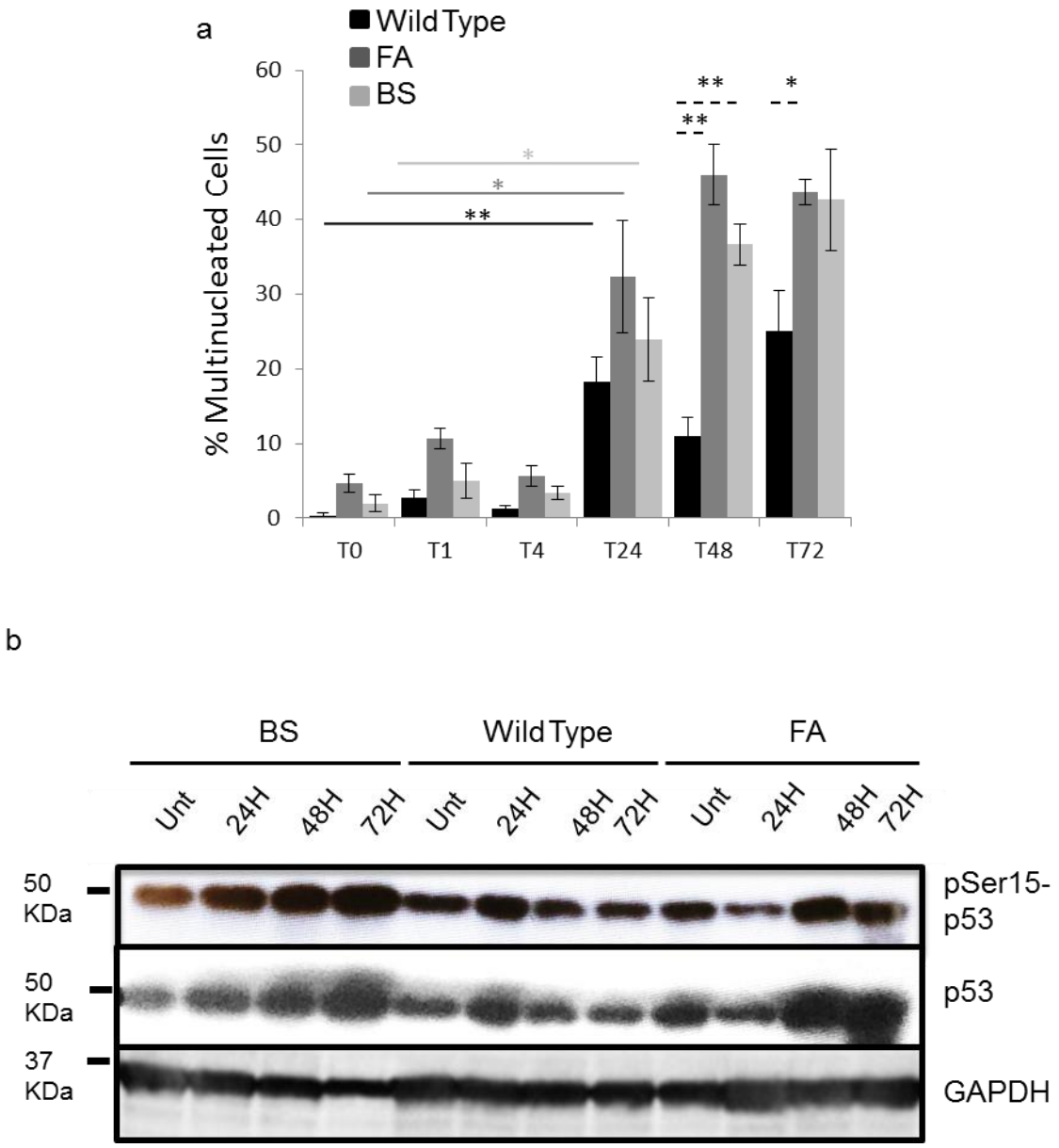

Figure 6: Wild-type cells undergo more completed multipolar division resulting in hypoploid interphase cells while FA and BS cells undergo enhanced mitotic catastrophe (a) The percentage of multinucleated cells over time in response to 16μM PJ34, measuring the endpoint of mitotic catastrophe. For each condition, 300 cells from 3 independent experiments were scored. (b) pSer15-p53 and total p53 levels in response to PJ34 suggesting p53-mediated mitotic catastrophe. GAPDH is shown as a loading control. * = $p<0.05$, ** = $p<0.01$, *** = $p<0.001$.

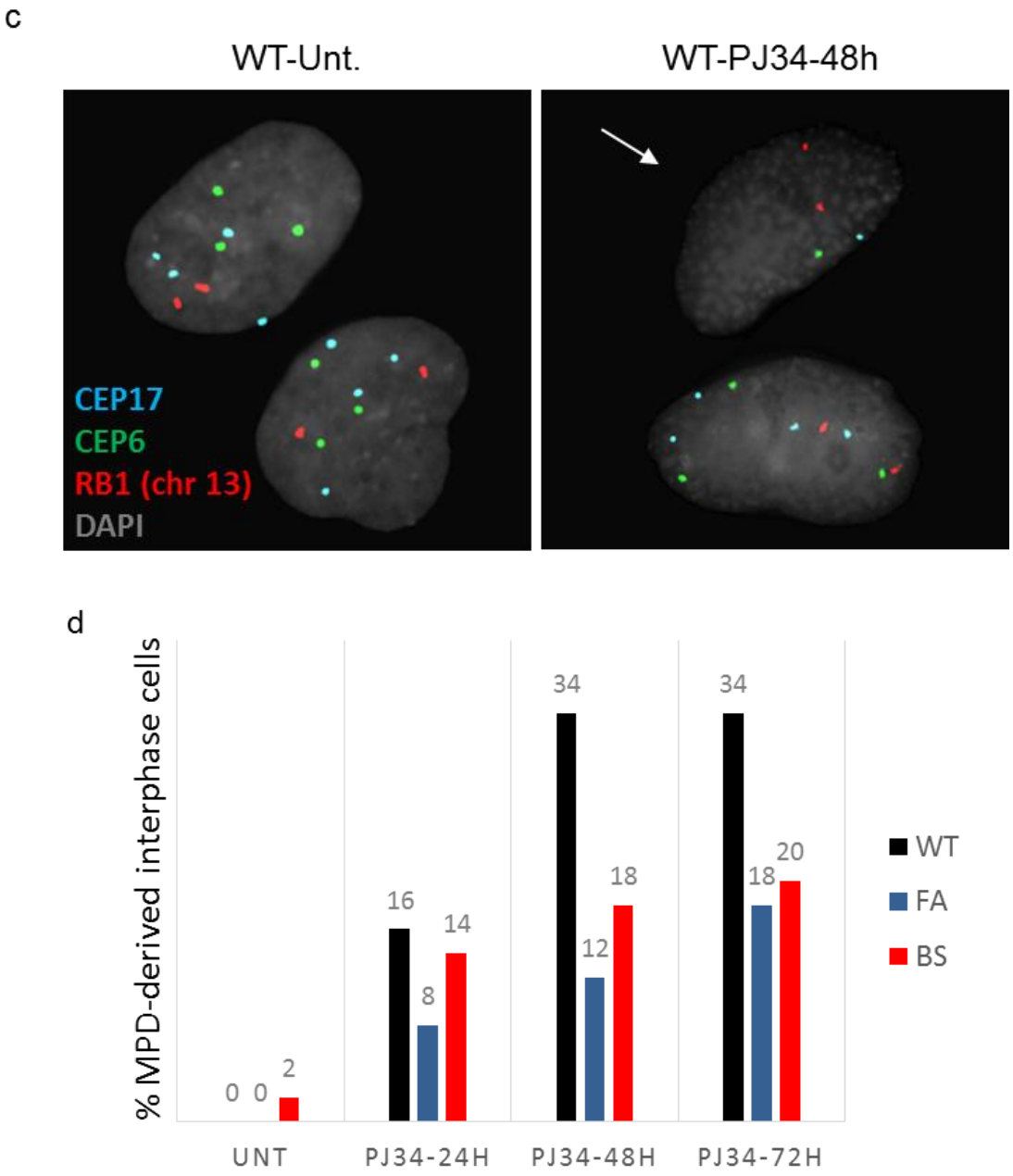

Figure 6: Wild-type cells undergo more completed multipolar division resulting in hypoploid interphase cells while FA and BS cells undergo enhanced mitotic catastrophe. (c) Identification of multipolar division-derived hypoploid cells using FISH probes to CEP6, CEP17, and RB1 on Chromosome 13. 100 cells total were scored for each condition. Arrow indicates a MPD-derived cell. (d) Quantification of the cells represented in (c). Cells were considered MPD-derived if they were missing >40% of the normal complement of FISH signals.

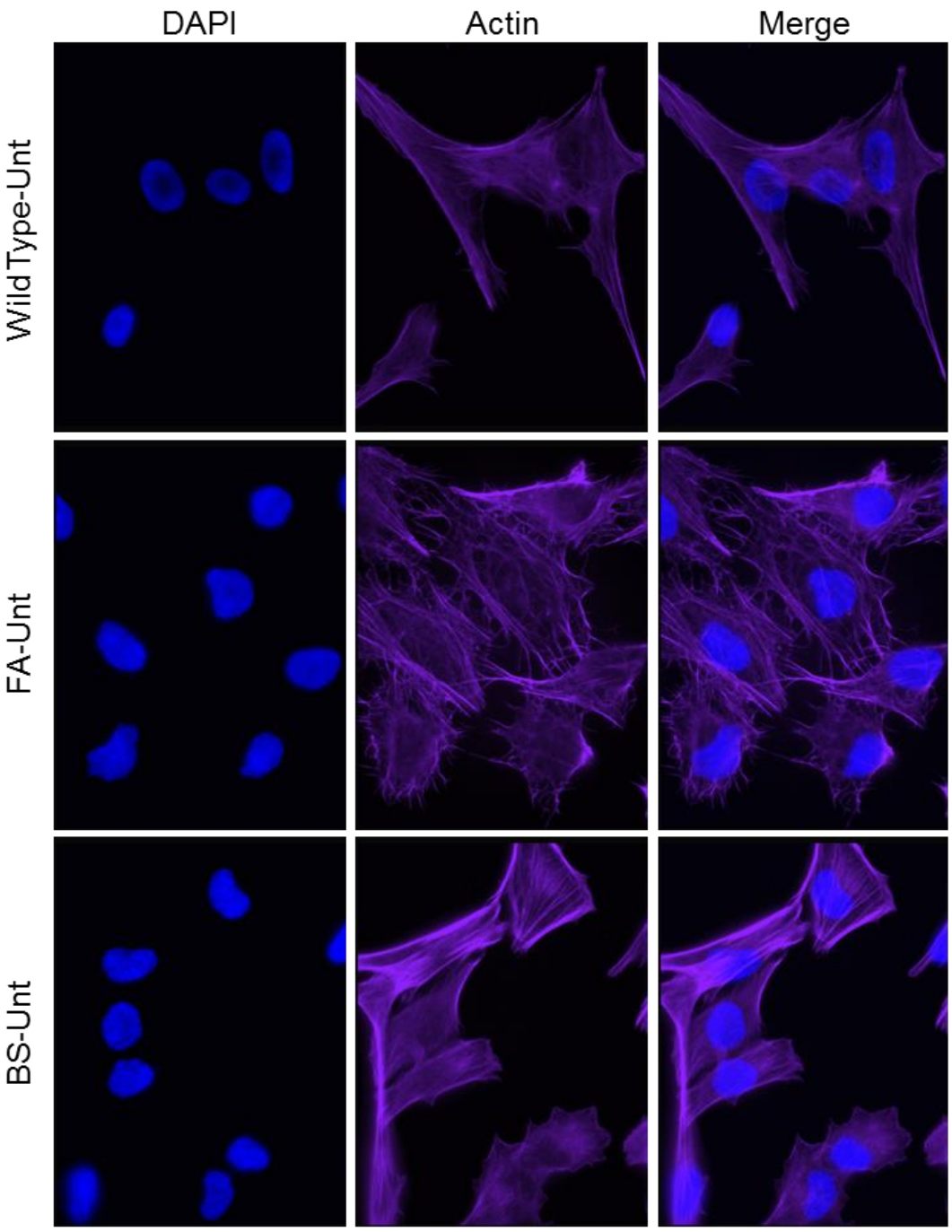

Figure S3: Representative images of multinucleated cells induced by 16 μM PJ34. Actin is used to indicate cell borders. Arrows indicate multinucleated cells.

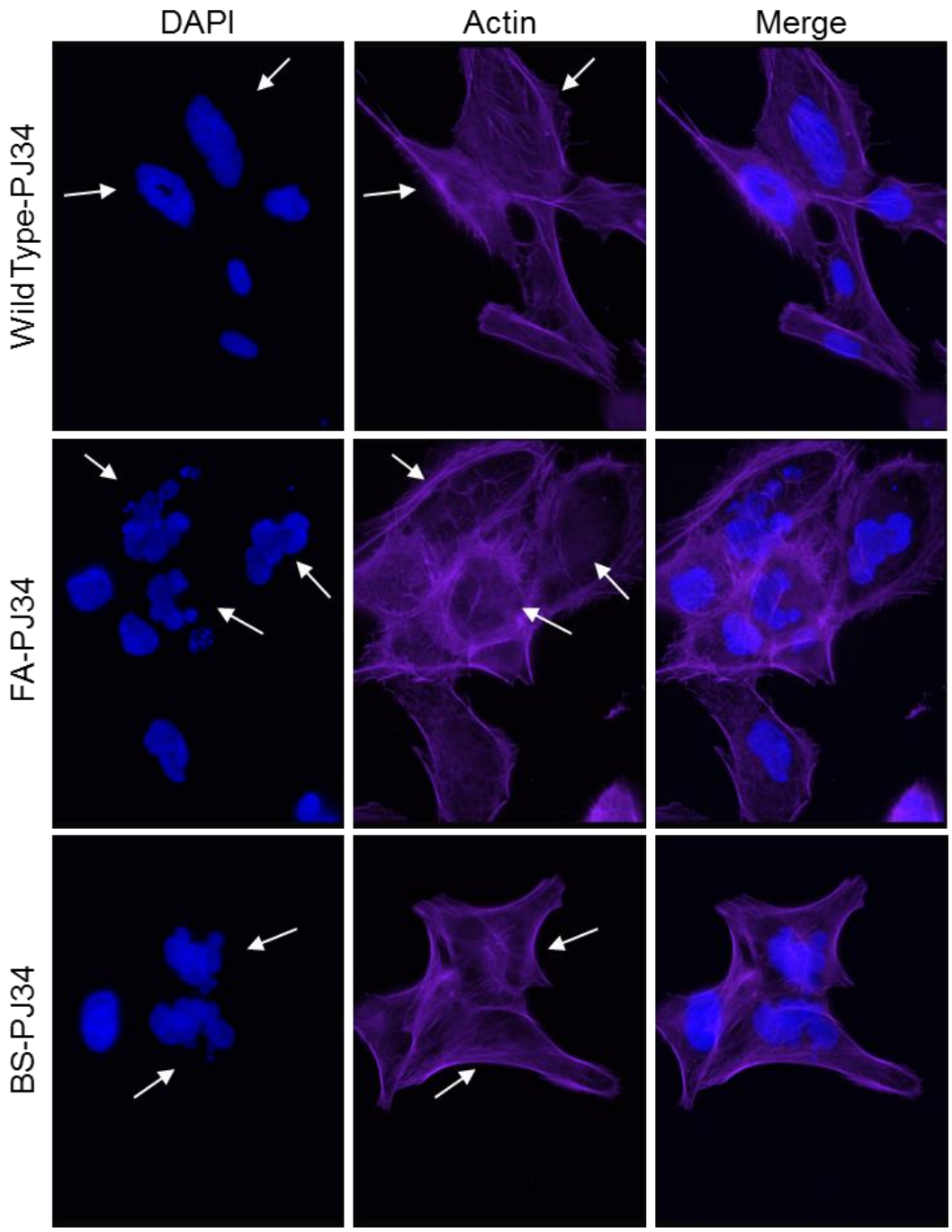

Figure S3 Cont: Representative images of multinucleated cells induced by 16 μM PJ34. Actin is used to indicate cell borders. Arrows indicate multinucleated cells.

Discussion

The emphasis of PARP inhibitor research has long been on the notion of synthetic lethality—the idea that PARP inhibition or HR deficiency alone are not particularly damaging to cancer cells, but together they are exponentially more lethal. This is a universal property of all PARP inhibitors and the reason they were initially brought into the clinic as a promising chemotherapeutic agent. However, recent research suggests that some PARP inhibitors, specifically those that are phenanthrene-derived, have additional mechanisms of action to target cancer cells. Most notably, they have been shown to selectively target cells with amplified centrosomes, a common feature of cancer cells. Mechanistically, they do this by preventing bipolar clustering of supernumerary centrosomes, which is a survival mechanism employed by cancer cells in an effort to avoid continuous and potentially catastrophic multipolar division. Yet other research has identified the poly(ADP)ribosylation activity of PARP1 as an important regulator of centrosome duplication and that loss or inhibition can lead to supernumerary centrosomes. Thus, given the complex nature of the relationship between PARP inhibition and centrosome homeostasis, we took a detailed and comprehensive look at the mitotic instability and centrosome defects induced by PARP inhibition. This analysis was done in the context of both normal cells, and cells associated with the genome instability syndromes Fanconi anemia and Bloom syndrome for two reasons. First, both are deficient in HR and essential HR proteins [47]. Second, FA proteins have been localized to the centrosomes at mitosis where they are essential for maintaining mitotic stability [50]. Third, PARP inhibitors

have been suggested as possible chemotherapeutic options for FA and BS-derived cancers. Thus, we wanted to understand the possible effects of PARP inhibition on non-cancerous cells, particularly in the context of FA and BS patients.

Historically, the model of PARP inhibitor-induced MPD was that MPD was a consequence of either induced centrosome de-clustering in cells with already amplified centrosomes, or by directly induced centrosome amplification. However, the work presented here supports a model whereby PARP inhibition generates MPD without relying on supernumerary centrosomes, and can even generate chromosome instability completely distinct from MPD. In cells that underwent normal bipolar division (without amplified and clustered centrosomes) in the presence of PARP inhibitor, numerous lagging chromosomes and micronuclei were observed indicating chromosome instability was not exclusive to cells undergoing MPD. These lagging chromosomes should trigger the spindle assembly checkpoint (SAC) which ensures bipolar attachment of all chromosomes prior to anaphase onset. Accordingly, wild-type cells had a robust SAC while the SAC in FA cells was blunted. It is likely that the diminished SAC response in FA cells is responsible for the high prevalence of aneuploidy in FA cells, and the PARP inhibitor-induced effect seen here reflects a larger issue with maintaining the SAC, even under non-stressed conditions. BS cells, on the other hand, did not show any evidence of an intact SAC. They had fewer lagging chromosomes in response to PJ34 treatment, but did not accumulate metaphases or Cyclin B1 as a result, leading to premature anaphase and

considerably more micronuclei. This suggests that BS cells have a significantly impaired SAC that, like previously observed in FA cells, is most likely an inherent defect associated with the loss of BLM. HR proteins have previously been implicated in maintaining proper bipolar division and BLM particularly has been identified as essential for proper chromosome segregation at mitosis where it is necessary for the centromere disjunction of sister chromatids. Furthermore, BLM is phosphorylated by MPS1 during mitosis where it, as a member of the BTR complex, is required for maintaining mitotic arrest at the SAC, perhaps providing a mechanism to explain the failure of lagging chromosomes to trigger arrest at the SAC [118,119].

On the surface, the unique types of MPD can appear identical. All present with supernumerary metaphase plates and multiple spindle poles, but mechanistically they are very different. Understanding these differences is essential if MPD and abnormal centrosome biology are to be potential targets for chemotherapeutic agents. Traditionally, MPD in response to PARP inhibition or PARP1 knock down has been associated exclusively with the amplification of centrosomes. However, these data suggests that centrosome amplification only occurs under specific conditions, and the most common form of MPD is actually via loss of centrosome integrity. BS cells are susceptible to spontaneous supernumerary centrosomes and were the only cells to undergo PARP inhibitor-induced amplification, suggesting that amplification-directed MPD may be a result only when cells are specifically predisposed to it. This may extend to cancer cells as well where it is common for somatic mutations that affect

centrosome regulation to amass during the course of neoplastic transformation. Importantly, normal cells, and other genome instability cells studied here, still underwent MPD via the loss of centrosome integrity in response to PJ34. This is in conflict with the long-standing belief that normal cells are refractory to PARP inhibitor treatment, and suggests further studies need to be done to understand the full spectrum of PARP inhibitor effects on vital cellular pathways.

Acknowledgements:

This work was supported by NHLBI grant PO1HL048546 and NIH training grant 5T32HL007781.

Conclusion

Individual manuscripts have detailed discussions about the work presented in each. This is a summation of the work as a whole, weaving the individual chapters together and exploring the significance of my research findings to the field of genome instability.

Despite years of diagnostic use for the identification of FA, the nature and formation of chromosomal radials has remained rather enigmatic. Everything from the initial DNA lesion responsible for their formation to the cellular consequences of radials has been the subject of debate with little consensus or resolution. Complicating the field was the long-held belief that the radials observed in FA cells and the radials observed in BS cells were structurally different and the product of divergent DNA repair defects. The first manuscript focused on characterizing BS radials as structurally identical to FA radials. Specifically, the historical characterization of BS radials as the result of homologous sequence interactions was proven false by the data presented, which indicates that BS radials represent the same chromosome abnormality as FA radials. This finding allows for BS radials to be studied in conjunction with FA radials, rather than independently, and offers further insight into the DNA repair pathway dysregulation that leads to radial formation. BLM is not a member of the FA core complex, nor has it been shown to function downstream of FANCD2 monoubiquitination with the other recruited HR proteins. BLM does form a BRAFT supercomplex with FA core complex proteins, although the function of this complex is not well understood. It should also be noted that despite the

presence of normal *BLM* alleles in FA patients, BLM protein is not fully functional due to the associated lack of important phosphorylation marks which guide the function of BLM. Thus, a focus of further study should be on the repercussions of dysregulated BLM in the context of FA patient cells, with the idea that radial formation in FA cells may be dependent on the loss of BLM function. This is a provocative theory since this paper is the first to even place BLM in the core FA pathway with regards to radial formation, but it warrants further study to be able to truly understand the intricacies of genome instability in these disorders. Additionally, it is interesting that many of the hot bands for radial formation are also known fragile sites and while the data presented in Manuscript I pertaining to this point is correlative, it begs further research on the role of BLM and FA proteins at fragile sites. Once established that FA and BS radials were identical, the remaining experiments were performed with FA cells and BS cells alongside wild-type cells to help determine the commonalities relating to radial formation in the two cell types.

Currently there is an inspired debate, based on decades of research, comprised of three competing opinions, over the DNA lesion responsible for radial formation. First is the classic view that ICLs induced by endogenous and exogenous agents, such as mitomycin C and psoralens, are responsible for radial formation. This is the basis of diagnostic testing and years of research into the exquisite sensitivity of FA cells to ICL-inducing agents. Second is the hypothesis that reactive aldehydes are responsible for radial formation. This hypothesis was born out of seminal work done in the UK that showed the

concomitant loss of aldehyde catabolism in conjunction with FA exponentially worsened the FA phenotype leading to bone marrow failure and sporadic hematologic malignancies. Lastly, the least well-known opinion is that reactive oxygen species are responsible for radials. Thus, a wide spectrum of DNA lesions has been associated with radial formation. Given this, the hypothesis suggested in manuscript II was that all of these aforementioned lesions could lead to radial formation due to the simple fact that while the initial lesions are markedly different, each lesion type has a common processing step—a transient DSB—which is ultimately responsible for radial formation.

DSBs arise during normal DNA repair of complex lesions or can arise at collapsed replication forks when single strand breaks are left unrepaired. Using PARP inhibitor, I exploited the latter using it to limit PARP1-dependent repair of spontaneous single strand breaks and allowing them to be transformed into DSBs. This alone is sufficient to drive radial formation in FA and BS cells, indicating DSBs are the common lesion responsible for radial formation and the means by which the DSB is generated is, for the most part, irrelevant.

PARP inhibitor has been suggested as a potential chemotherapeutic agent for FA and BS-derived tumors as an extension of their efficacy in BRCA2-deficient tumors. There is an immense and immediate need for chemotherapeutic agents that can be tolerated by FA and BS patients since the inherent genome instability precludes these patients from receiving most treatments. However, my data suggest that treating FA or BS patients with PARP inhibitor would not be advisable. In response to both spontaneous and

induced radials, cells trigger a PARP-dependent mitotic cell death that includes hyperfragmentation of chromosomes during mitosis. This ensures that the radial-containing cells die instead of continuing on to become potentially oncogenic cells. Given that radials are mitotically unstable, completed anaphase would likely generate either structural chromosome abnormalities or aneuploidy—both hallmarks of cancer cells. The resulting cell death can eventually be detrimental, suggesting that the bone marrow failure seen in FA and BS may be in part due to cell death due to excessive DNA damage. However, DNA damage-triggered cell death is a protective mechanism that could prevent the development of cancer, and abolishing the mechanism of elimination for these cells may foster the survival of cytogenetically abnormal cells. The discovery of the fate of chromosomal radials opens up a number of questions that need further study to be answered. First, it is shown here that this mechanism of cell death is PARP dependent, but it is unclear what role PARP plays. PARP1 may PAR-ylate other essential spindle assembly checkpoint proteins, or itself be involved in signaling. Additionally, the fact that this mechanism of cell death can be blocked by PARP inhibitor is worrisome as a potential chemotherapeutic for FA or BS patients. PARP inhibitor is able to simultaneously create radials and eliminate the chosen method of cell death to protect against them, fostering an environment of enhanced chromosome instability. Further experiments need to be done to clarify the fate of radials when mitotic cell death is blocked in order to understand the type of instability induced. But the fact that PARP inhibitor can eliminate an

oncoprotective mechanism suggests this would not be an appropriate chemotherapeutic agent for FA or BS patients.

The ever expanding roles of PARP1 in the cell have shifted the focus of possible pathway targets for PARP inhibitor. One aspect that had not been explored well was the role of PARP1 at the centrosome and the ability of PARP inhibitor to induce MPD. Until now, all reports of MPD due to PARP inhibition were as a result of centrosome de-clustering forcing cells that normally undergo pseudo-bipolar division to undergo catastrophic MPD. Thus, PARP inhibitor has been considered for treatment of cancers with supernumerary centrosomes, a relatively common occurrence in tumors. The consensus is, however, that normal cells are refractory to PARP inhibitor treatment due to normal numbers of centrosomes and thus an inability to undergo de-clustering and MPD. The data presented in manuscript III contradicts this finding, and non-oncogenic cells from both wild-type and HR-deficient cells are induced to undergo MPD. Given the accepted mechanism of action, one would presume that PARP inhibition was inducing centrosome amplification in these cells, the centrosomes could not cluster, and the cells were thus undergoing MPD. However, there was no evidence of centrosome amplification despite MPD, and FISH analysis suggested that single centrosomes were losing integrity rather than erroneously duplicating centrosomes. The fact that normal cells were undergoing MPD without specific cellular abnormalities that were being targeted, such as amplified centrosomes, suggests PARP inhibitor may be more toxic to normal cells than is currently realized.

MPD via loss of centrosome integrity and fragmentation of the pericentriolar material has been seen in response to various taxanes, such as paclitaxel. Completion of MPD leads to the production of aneuploid daughter cells. Data suggest that this occurs in response to PARP inhibitor as well, though less in FA and BS cells than in wild-type cells [120-122]. Instead, FA and BS cells undergo more multinucelation and p53 hyperactivation suggestive of elevated mitotic catastrophe, an oncosuppressive mechanism for eliminating cells that would otherwise go on to be aneuploid and potentially oncogenic [116]. Progressively worsening mitotic catastrophe in response to PARP inhibitor has been seen in HR-deficient PTEN-mutated glioblastoma cells, suggesting that susceptibility to mitotic catastrophe may be a common feature of HR deficiency[113]. Considering mitotic catastrophe is morphologically the completion of karyokinesis without the completion of cytokinesis, the specific susceptibility seen in HR-deficient cells may be due to the inherent cytokinesis defects present in FA and BS cells.

These data raise many questions about the mechanisms of action attributed to different PARP inhibitors, and about the efficacy of PARP inhibitor as a general chemotherapeutic agent. First, it would be interesting to understand what is unique about phenanthrene-derived PARP inhibitors that make them able to induce MPD where other PARP inhibitors cannot. The apparent ability to target exclusively cells with supernumerary centrosomes has made phenanthrene-derived PARP inhibitors desirable chemotherapeutic agents for solid tumors in the past and understanding the mechanism of action is crucial.

Second, the data in manuscript III is the first time PARP-mediated MPD has been attributed to the loss of centrosome integrity rather than centrosome amplification. That being said, there are two types of integrity loss and further research should focus on defining specifically whether centriole disengagement or fragmentation of the pericentriolar material is being induced. This would go a long way towards explaining the specific effect of PARP inhibitor on centrosomes, and narrow the targets as far as what protein or structure specifically is being affected. Lastly, these data raise the question of the eventual fate of the cells that successfully undergo MPD. Normal cells that did this would most likely eventually die due to unfavorable aneuploidies, but cancer cells that possess extra chromosomes to begin with may be able to generate cytogenetically diverse clones using this process. Further research should determine whether cancer cells that are forced to undergo MPD give rise to diverse subclones.

Overall, the various cellular effects of PARP inhibitor drive chromosomal instability, which is exacerbated by HR-deficiency, rather than exclusively eliminate cells that have it. The loss of PARP1 leads to prolonged unrepaired DSBs and excessive replication stress due to PARP1's additional role as a necessary protein to restart collapsed replication forks [123,124]. This not only leads to radial formation in FA and BS cells, but the radials are not able to trigger PARP-dependent cell death. Replication stress and unrepaired DNA at mitosis have been tied intimately to the induction of MPD without the need for centrosome amplification [51,52]. While some MPD results in mitotic

catastrophe, there is a significant portion of MPD events that complete cytokinesis and the aneuploid progeny are able to survive for multiple generations, as seen here and in other studies [113]. Thus PARP inhibitor is able to generate both structural and numerical chromosome instability in non-cancer cells which are hallmarks of neoplasia and drive tumorigenesis. This is important since PARP inhibitor is currently used as a chemotherapeutic agent to specifically eliminate cells with multiple centrosomes. The fact that PARP inhibitor, on its own, is able to induce MPD in cells without supernumerary centrosomes suggests it may put an exorbitant amount of stress on normal cells, especially those that are highly proliferative, which is contradictory to the goal of modern chemotherapeutic agents.

References

1. Alter BP, Greene MH, Velazquez I, Rosenberg PS (2003) Cancer in Fanconi anemia. Blood 101: 2072.
2. Arora H, Chacon AH, Choudhary S, McLeod MP, Meshkov L, et al. (2014) Bloom syndrome. Int J Dermatol 53: 798-802.
3. Gari K, Decaillet C, Stasiak AZ, Stasiak A, Constantinou A (2008) The Fanconi anemia protein FANCM can promote branch migration of Holliday junctions and replication forks. Mol Cell 29: 141-148.
4. Walden H, Deans AJ (2014) The Fanconi anemia DNA repair pathway: structural and functional insights into a complex disorder. Annu Rev Biophys 43: 257-278.
5. Longerich S, San Filippo J, Liu D, Sung P (2009) FANCI binds branched DNA and is monoubiquitinated by UBE2T-FANCL. J Biol Chem 284: 23182-23186.
6. Sato K, Toda K, Ishiai M, Takata M, Kurumizaka H (2012) DNA robustly stimulates FANCD2 monoubiquitylation in the complex with FANCI. Nucleic Acids Res 40: 4553-4561.
7. Meetei AR, Yan Z, Wang W (2004) FANCL replaces BRCA1 as the likely ubiquitin ligase responsible for FANCD2 monoubiquitination. Cell Cycle 3: 179-181.
8. Chan KL, North PS, Hickson ID (2007) BLM is required for faithful chromosome segregation and its localization defines a class of ultrafine anaphase bridges. EMBO J 26: 3397-3409.

9. Kumari A, Owen N, Juarez E, McCullough AK (2015) BLM protein mitigates formaldehyde-induced genomic instability. DNA Repair (Amst) 28: 73-82.

10. Bugreev DV, Yu X, Egelman EH, Mazin AV (2007) Novel pro- and anti-recombination activities of the Bloom's syndrome helicase. Genes Dev 21: 3085-3094.

11. Rockmill B, Fung JC, Branda SS, Roeder GS (2003) The Sgs1 helicase regulates chromosome synapsis and meiotic crossing over. Curr Biol 13: 1954-1962.

12. Holloway JK, Morelli MA, Borst PL, Cohen PE (2010) Mammalian BLM helicase is critical for integrating multiple pathways of meiotic recombination. J Cell Biol 188: 779-789.

13. Hanada K, Ukita T, Kohno Y, Saito K, Kato J, et al. (1997) RecQ DNA helicase is a suppressor of illegitimate recombination in Escherichia coli. Proc Natl Acad Sci U S A 94: 3860-3865.

14. Schvarzstein M, Pattabiraman D, Libuda DE, Ramadugu A, Tam A, et al. (2014) DNA Helicase HIM-6/BLM Both Promotes MutSgamma-Dependent Crossovers and Antagonizes MutSgamma-Independent Inter-Homolog Associations During Caenorhabditis elegans Meiosis. Genetics 198: 193-207.

15. Chaganti RS, Schonberg S, German J (1974) A manyfold increase in sister chromatid exchanges in Bloom's syndrome lymphocytes. Proc Natl Acad Sci U S A 71: 4508-4512.

16. Suhasini AN, Brosh RM, Jr. (2012) Fanconi anemia and Bloom's syndrome crosstalk through FANCJ-BLM helicase interaction. Trends Genet 28: 7-13.

17. Deans AJ, West SC (2009) FANCM connects the genome instability disorders Bloom's Syndrome and Fanconi Anemia. Mol Cell 36: 943-953.

18. Meetei AR, Sechi S, Wallisch M, Yang D, Young MK, et al. (2003) A multiprotein nuclear complex connects Fanconi anemia and Bloom syndrome. Mol Cell Biol 23: 3417-3426.

19. Naim V, Rosselli F (2009) The FANC pathway and BLM collaborate during mitosis to prevent micro-nucleation and chromosome abnormalities. Nat Cell Biol 11: 761-768.

20. Pichierri P, Franchitto A, Rosselli F (2004) BLM and the FANC proteins collaborate in a common pathway in response to stalled replication forks. EMBO J 23: 3154-3163.

21. Howlett NG, Taniguchi T, Olson S, Cox B, Waisfisz Q, et al. (2002) Biallelic inactivation of BRCA2 in Fanconi anemia. Science 297: 606-609.

22. Kalb R, Neveling K, Hoehn H, Schneider H, Linka Y, et al. (2007) Hypomorphic mutations in the gene encoding a key Fanconi anemia protein, FANCD2, sustain a significant group of FA-D2 patients with severe phenotype. Am J Hum Genet 80: 895-910.

23. Chester N, Kuo F, Kozak C, O'Hara CD, Leder P (1998) Stage-specific apoptosis, developmental delay, and embryonic lethality in mice

homozygous for a targeted disruption in the murine Bloom's syndrome gene. Genes Dev 12: 3382-3393.

24. German J, Sanz MM, Ciocci S, Ye TZ, Ellis NA (2007) Syndrome-causing mutations of the BLM gene in persons in the Bloom's Syndrome Registry. Hum Mutat 28: 743-753.

25. German J, Crippa LP, Bloom D (1974) Bloom's syndrome. III. Analysis of the chromosome aberration characteristic of this disorder. Chromosoma 48: 361-366.

26. Schroeder TM, German J (1974) Bloom's syndrome and Fanconi's anemia: demonstration of two distinctive patterns of chromosome disruption and rearrangement. Humangenetik 25: 299-306.

27. Kuhn EM (1978) Mitotic chiasmata and other quadriradials in mitomycin C-treated Bloom's syndrome lymphocytes. Chromosoma 66: 287-297.

28. Newell AE, Akkari YM, Torimaru Y, Rosenthal A, Reifsteck CA, et al. (2004) Interstrand crosslink-induced radials form between non-homologous chromosomes, but are absent in sex chromosomes. DNA Repair (Amst) 3: 535-542.

29. Bryant HE, Schultz N, Thomas HD, Parker KM, Flower D, et al. (2005) Specific killing of BRCA2-deficient tumours with inhibitors of poly(ADP-ribose) polymerase. Nature 434: 913-917.

30. Farmer H, McCabe N, Lord CJ, Tutt AN, Johnson DA, et al. (2005) Targeting the DNA repair defect in BRCA mutant cells as a therapeutic strategy. Nature 434: 917-921.

31. Weaver AN, Yang ES (2013) Beyond DNA Repair: Additional Functions of PARP-1 in Cancer. Front Oncol 3: 290.

32. Nowsheen S, Bonner JA, Yang ES (2011) The poly(ADP-Ribose) polymerase inhibitor ABT-888 reduces radiation-induced nuclear EGFR and augments head and neck tumor response to radiotherapy. Radiother Oncol 99: 331-338.

33. Calabrese CR, Almassy R, Barton S, Batey MA, Calvert AH, et al. (2004) Anticancer chemosensitization and radiosensitization by the novel poly(ADP-ribose) polymerase-1 inhibitor AG14361. J Natl Cancer Inst 96: 56-67.

34. McCabe N, Turner NC, Lord CJ, Kluzek K, Bialkowska A, et al. (2006) Deficiency in the repair of DNA damage by homologous recombination and sensitivity to poly(ADP-ribose) polymerase inhibition. Cancer Res 66: 8109-8115.

35. Gaymes TJ, Shall S, Farzaneh F, Mufti GJ (2008) Chromosomal instability syndromes are sensitive to poly ADP-ribose polymerase inhibitors. Haematologica 93: 1886-1889.

36. Lyakhovich A, Surralles J (2006) Disruption of the Fanconi anemia/BRCA pathway in sporadic cancer. Cancer Lett 232: 99-106.

37. Taniguchi T, Tischkowitz M, Ameziane N, Hodgson SV, Mathew CG, et al. (2003) Disruption of the Fanconi anemia-BRCA pathway in cisplatin-sensitive ovarian tumors. Nat Med 9: 568-574.

38. Calin G, Ranzani GN, Amadori D, Herlea V, Matei I, et al. (2001) Somatic frameshift mutations in the Bloom syndrome BLM gene are frequent in sporadic gastric carcinomas with microsatellite mutator phenotype. BMC Genet 2: 14.

39. Arora A, Abdel-Fatah TM, Agarwal D, Doherty R, Moseley PM, et al. (2015) Transcriptomic and Protein Expression Analysis Reveals Clinicopathological Significance of Bloom Syndrome Helicase (BLM) in Breast Cancer. Mol Cancer Ther 14: 1057-1065.

40. Wreesmann VB, Estilo C, Eisele DW, Singh B, Wang SJ (2007) Downregulation of Fanconi anemia genes in sporadic head and neck squamous cell carcinoma. ORL J Otorhinolaryngol Relat Spec 69: 218-225.

41. Murai J, Huang SY, Das BB, Renaud A, Zhang Y, et al. (2012) Trapping of PARP1 and PARP2 by Clinical PARP Inhibitors. Cancer Res 72: 5588-5599.

42. Ogden A, Rida PC, Aneja R (2012) Let's huddle to prevent a muddle: centrosome declustering as an attractive anticancer strategy. Cell Death Differ 19: 1255-1267.

43. Castiel A, Visochek L, Mittelman L, Dantzer F, Izraeli S, et al. (2011) A phenanthrene derived PARP inhibitor is an extra-centrosomes de-clustering agent exclusively eradicating human cancer cells. BMC Cancer 11: 412.

44. Kanai M, Tong WM, Sugihara E, Wang ZQ, Fukasawa K, et al. (2003) Involvement of poly(ADP-Ribose) polymerase 1 and poly(ADP-Ribosyl)ation in regulation of centrosome function. Mol Cell Biol 23: 2451-2462.

45. Castiel A, Visochek L, Mittelman L, Zilberstein Y, Dantzer F, et al. (2013) Cell death associated with abnormal mitosis observed by confocal imaging in live cancer cells. J Vis Exp: e50568.

46. Chevanne M, Zampieri M, Caldini R, Rizzo A, Ciccarone F, et al. (2010) Inhibition of PARP activity by PJ-34 leads to growth impairment and cell death associated with aberrant mitotic pattern and nucleolar actin accumulation in M14 melanoma cell line. J Cell Physiol 222: 401-410.

47. Cappelli E, Townsend S, Griffin C, Thacker J (2011) Homologous recombination proteins are associated with centrosomes and are required for mitotic stability. Exp Cell Res 317: 1203-1213.

48. Griffin CS (2002) Aneuploidy, centrosome activity and chromosome instability in cells deficient in homologous recombination repair. Mutat Res 504: 149-155.

49. Kim S, Hwang SK, Lee M, Kwak H, Son K, et al. (2013) Fanconi anemia complementation group A (FANCA) localizes to centrosomes and functions in the maintenance of centrosome integrity. Int J Biochem Cell Biol 45: 1953-1961.

50. Nalepa G, Enzor R, Sun Z, Marchal C, Park SJ, et al. (2013) Fanconi anemia signaling network regulates the spindle assembly checkpoint. J Clin Invest 123: 3839-3847.

51. Burrell RA, McClelland SE, Endesfelder D, Groth P, Weller MC, et al. (2013) Replication stress links structural and numerical cancer chromosomal instability. Nature 494: 492-496.

52. Hut HM, Lemstra W, Blaauw EH, Van Cappellen GW, Kampinga HH, et al. (2003) Centrosomes split in the presence of impaired DNA integrity during mitosis. Mol Biol Cell 14: 1993-2004.

53. Bachrati CZ, Hickson ID (2008) RecQ helicases: guardian angels of the DNA replication fork. Chromosoma 117: 219-233.

54. Ellis NA, Groden J, Ye TZ, Straughen J, Lennon DJ, et al. (1995) The Bloom's syndrome gene product is homologous to RecQ helicases. Cell 83: 655-666.

55. Levitt NC, Hickson ID (2002) Caretaker tumour suppressor genes that defend genome integrity. Trends Mol Med 8: 179-186.

56. Chu WK, Hickson ID (2009) RecQ helicases: multifunctional genome caretakers. Nat Rev Cancer 9: 644-654.

57. Watt PM, Hickson ID, Borts RH, Louis EJ (1996) SGS1, a homologue of the Bloom's and Werner's syndrome genes, is required for maintenance of genome stability in Saccharomyces cerevisiae. Genetics 144: 935-945.

58. German J (1969) Bloom's syndrome. I. Genetical and clinical observations in the first twenty-seven patients. Am J Hum Genet 21: 196-227.

59. Ray JH, German J (1984) Bloom's syndrome and EM9 cells in BrdU-containing medium exhibit similarly elevated frequencies of sister chromatid exchange but dissimilar amounts of cellular proliferation and chromosome disruption. Chromosoma 90: 383-388.

60. Rosin MP, German J (1985) Evidence for chromosome instability in vivo in Bloom syndrome: increased numbers of micronuclei in exfoliated cells. Hum Genet 71: 187-191.

61. Manthei KA, Keck JL (2013) The BLM dissolvasome in DNA replication and repair. Cell Mol Life Sci 70: 4067-4084.

62. Ip SC, Rass U, Blanco MG, Flynn HR, Skehel JM, et al. (2008) Identification of Holliday junction resolvases from humans and yeast. Nature 456: 357-361.

63. Mankouri HW, Hickson ID (2007) The RecQ helicase-topoisomerase III-Rmi1 complex: a DNA structure-specific 'dissolvasome'? Trends Biochem Sci 32: 538-546.

64. Chan KL, Hickson ID (2011) New insights into the formation and resolution of ultra-fine anaphase bridges. Semin Cell Dev Biol 22: 906-912.

65. Rouzeau S, Cordelieres FP, Buhagiar-Labarchede G, Hurbain I, Onclercq-Delic R, et al. (2012) Bloom's syndrome and PICH helicases cooperate with topoisomerase IIalpha in centromere disjunction before anaphase. PLoS One 7: e33905.

66. Biebricher A, Hirano S, Enzlin JH, Wiechens N, Streicher WW, et al. (2013) PICH: a DNA translocase specially adapted for processing anaphase bridge DNA. Mol Cell 51: 691-701.

67. Hemphill AW, Akkari Y, Newell AH, Schultz RA, Grompe M, et al. (2009) Topo IIIalpha and BLM act within the Fanconi anemia pathway in response to DNA-crosslinking agents. Cytogenet Genome Res 125: 165-175.

68. Kim H, D'Andrea AD (2012) Regulation of DNA cross-link repair by the Fanconi anemia/BRCA pathway. Genes Dev 26: 1393-1408.

69. Kee Y, D'Andrea AD (2012) Molecular pathogenesis and clinical management of Fanconi anemia. J Clin Invest 122: 3799-3806.

70. Wang W (2007) Emergence of a DNA-damage response network consisting of Fanconi anaemia and BRCA proteins. Nat Rev Genet 8: 735-748.

71. Thompson LH, Hinz JM (2009) Cellular and molecular consequences of defective Fanconi anemia proteins in replication-coupled DNA repair: mechanistic insights. Mutat Res 668: 54-72.

72. Davies SL, North PS, Dart A, Lakin ND, Hickson ID (2004) Phosphorylation of the Bloom's syndrome helicase and its role in recovery from S-phase arrest. Mol Cell Biol 24: 1279-1291.

73. Schroeder TM, Anschutz F, Knopp A (1964) [Spontaneous chromosome aberrations in familial panmyelopathy]. Humangenetik 1: 194-196.

74. Hanlon Newell AE, Hemphill A, Akkari YM, Hejna J, Moses RE, et al. (2008) Loss of homologous recombination or non-homologous end-joining leads

to radial formation following DNA interstrand crosslink damage. Cytogenet Genome Res 121: 174-180.

75. Gravells P, Hoh L, Solovieva S, Patil A, Dudziec E, et al. (2013) Reduced FANCD2 influences spontaneous SCE and RAD51 foci formation in uveal melanoma and Fanconi anaemia. Oncogene 32: 5338-5346.
76. Shaffer LG, Slovak, M.L., Campbell, L.J.. (2009) ISCN: An International System for Human Cytogenetic Nomenclature (2009): Basel: Karger.
77. Bruun D, Folias A, Akkari Y, Cox Y, Olson S, et al. (2003) siRNA depletion of BRCA1, but not BRCA2, causes increased genome instability in Fanconi anemia cells. DNA Repair (Amst) 2: 1007-1013.
78. Schwartz M, Zlotorynski E, Kerem B (2006) The molecular basis of common and rare fragile sites. Cancer Lett 232: 13-26.
79. Kumar S, Lipman R, Tomasz M (1992) Recognition of specific DNA sequences by mitomycin C for alkylation. Biochemistry 31: 1399-1407.
80. Chan KL, Palmai-Pallag T, Ying S, Hickson ID (2009) Replication stress induces sister-chromatid bridging at fragile site loci in mitosis. Nat Cell Biol 11: 753-760.
81. Howlett NG, Taniguchi T, Durkin SG, D'Andrea AD, Glover TW (2005) The Fanconi anemia pathway is required for the DNA replication stress response and for the regulation of common fragile site stability. Hum Mol Genet 14: 693-701.
82. Rosenberg PS, Greene MH, Alter BP (2003) Cancer incidence in persons with Fanconi anemia. Blood 101: 822-826.

83. Fujiwara Y, Tatsumi M (1975) Repair of mitomycin C damage to DNA in mammalian cells and its impairment in Fanconi's anemia cells. Biochem Biophys Res Commun 66: 592-598.

84. Hook GJ, Kwok E, Heddle JA (1984) Sensitivity of Bloom syndrome fibroblasts to mitomycin C. Mutat Res 131: 223-230.

85. Huang Y, Li L (2013) DNA crosslinking damage and cancer - a tale of friend and foe. Transl Cancer Res 2: 144-154.

86. Deans AJ, West SC (2011) DNA interstrand crosslink repair and cancer. Nat Rev Cancer 11: 467-480.

87. German J, Archibald R, Bloom D (1965) Chromosomal Breakage in a Rare and Probably Genetically Determined Syndrome of Man. Science 148: 506-507.

88. Owen N, Hejna J, Rennie S, Mitchell A, Hanlon Newell A, et al. (2015) Bloom Syndrome Radials Are Predominantly Non-Homologous and Are Suppressed by Phosphorylated BLM. Cytogenet Genome Res 144: 255-263.

89. Garaycoechea JI, Crossan GP, Langevin F, Daly M, Arends MJ, et al. (2012) Genotoxic consequences of endogenous aldehydes on mouse haematopoietic stem cell function. Nature 489: 571-575.

90. Langevin F, Crossan GP, Rosado IV, Arends MJ, Patel KJ (2011) Fancd2 counteracts the toxic effects of naturally produced aldehydes in mice. Nature 475: 53-58.

91. Ridpath JR, Nakamura A, Tano K, Luke AM, Sonoda E, et al. (2007) Cells deficient in the FANC/BRCA pathway are hypersensitive to plasma levels of formaldehyde. Cancer Res 67: 11117-11122.

92. Marietta C, Thompson LH, Lamerdin JE, Brooks PJ (2009) Acetaldehyde stimulates FANCD2 monoubiquitination, H2AX phosphorylation, and BRCA1 phosphorylation in human cells in vitro: implications for alcohol-related carcinogenesis. Mutat Res 664: 77-83.

93. Sczepanski JT, Wong RS, McKnight JN, Bowman GD, Greenberg MM (2010) Rapid DNA-protein cross-linking and strand scission by an abasic site in a nucleosome core particle. Proc Natl Acad Sci U S A 107: 22475-22480.

94. Ide H, Shoulkamy MI, Nakano T, Miyamoto-Matsubara M, Salem AM (2011) Repair and biochemical effects of DNA-protein crosslinks. Mutat Res 711: 113-122.

95. Nakano T, Katafuchi A, Matsubara M, Terato H, Tsuboi T, et al. (2009) Homologous recombination but not nucleotide excision repair plays a pivotal role in tolerance of DNA-protein cross-links in mammalian cells. J Biol Chem 284: 27065-27076.

96. Long DT, Raschle M, Joukov V, Walter JC (2011) Mechanism of RAD51-dependent DNA interstrand cross-link repair. Science 333: 84-87.

97. Fisher AE, Hochegger H, Takeda S, Caldecott KW (2007) Poly(ADP-ribose) polymerase 1 accelerates single-strand break repair in concert with poly(ADP-ribose) glycohydrolase. Mol Cell Biol 27: 5597-5605.

98. Pascucci B, Russo MT, Crescenzi M, Bignami M, Dogliotti E (2005) The accumulation of MMS-induced single strand breaks in G1 phase is recombinogenic in DNA polymerase beta defective mammalian cells. Nucleic Acids Res 33: 280-288.

99. Vilenchik MM, Knudson AG (2003) Endogenous DNA double-strand breaks: production, fidelity of repair, and induction of cancer. Proc Natl Acad Sci U S A 100: 12871-12876.

100. Akkari YM, Bateman RL, Reifsteck CA, Olson SB, Grompe M (2000) DNA replication is required To elicit cellular responses to psoralen-induced DNA interstrand cross-links. Mol Cell Biol 20: 8283-8289.

101. Leskovac A, Vujic D, Guc-Scekic M, Petrovic S, Joksic I, et al. (2010) Fanconi anemia is characterized by delayed repair kinetics of DNA double-strand breaks. Tohoku J Exp Med 221: 69-76.

102. Ceccaldi R, Parmar K, Mouly E, Delord M, Kim JM, et al. (2012) Bone marrow failure in Fanconi anemia is triggered by an exacerbated p53/p21 DNA damage response that impairs hematopoietic stem and progenitor cells. Cell Stem Cell 11: 36-49.

103. Rouleau M, Patel A, Hendzel MJ, Kaufmann SH, Poirier GG (2010) PARP inhibition: PARP1 and beyond. Nat Rev Cancer 10: 293-301.

104. Yu VP, Koehler M, Steinlein C, Schmid M, Hanakahi LA, et al. (2000) Gross chromosomal rearrangements and genetic exchange between nonhomologous chromosomes following BRCA2 inactivation. Genes Dev 14: 1400-1406.

105. Auerbach AD, Adler B, Chaganti RS (1981) Prenatal and postnatal diagnosis and carrier detection of Fanconi anemia by a cytogenetic method. Pediatrics 67: 128-135.

106. Zhang QS, Eaton L, Snyder ER, Houghtaling S, Mitchell JB, et al. (2008) Tempol protects against oxidative damage and delays epithelial tumor onset in Fanconi anemia mice. Cancer Res 68: 1601-1608.

107. Ceccaldi R, Briot D, Larghero J, Vasquez N, Dubois d'Enghien C, et al. (2011) Spontaneous abrogation of the G(2)DNA damage checkpoint has clinical benefits but promotes leukemogenesis in Fanconi anemia patients. J Clin Invest 121: 184-194.

108. Moubarak RS, Yuste VJ, Artus C, Bouharrour A, Greer PA, et al. (2007) Sequential activation of poly(ADP-ribose) polymerase 1, calpains, and Bax is essential in apoptosis-inducing factor-mediated programmed necrosis. Mol Cell Biol 27: 4844-4862.

109. Akhiani AA, Werlenius O, Aurelius J, Movitz C, Martner A, et al. (2014) Role of the ERK pathway for oxidant-induced parthanatos in human lymphocytes. PLoS One 9: e89646.

110. Kitagawa K, Niikura Y (2008) Caspase-independent mitotic death (CIMD). Cell Cycle 7: 1001-1005.

111. Saxena A, Saffery R, Wong LH, Kalitsis P, Choo KH (2002) Centromere proteins Cenpa, Cenpb, and Bub3 interact with poly(ADP-ribose) polymerase-1 protein and are poly(ADP-ribosyl)ated. J Biol Chem 277: 26921-26926.

112. Majuelos-Melguizo J, Rodriguez MI, Lopez-Jimenez L, Rodriguez-Vargas JM, Martin-Consuegra JM, et al. (2014) PARP targeting counteracts gliomagenesis through induction of mitotic catastrophe and aggravation of deficiency in homologous recombination in PTEN-mutant glioma. Oncotarget 6: 4790-4803.

113. Telentschak S, Soliwoda M, Nohroudi K, Addicks K, Klinz FJ (2015) Cytokinesis failure and successful multipolar mitoses drive aneuploidy in glioblastoma cells. Oncol Rep 33: 2001-2008.

114. Yi Q, Zhao X, Huang Y, Ma T, Zhang Y, et al. (2011) p53 dependent centrosome clustering prevents multipolar mitosis in tetraploid cells. PLoS One 6: e27304.

115. Quintyne NJ, Reing JE, Hoffelder DR, Gollin SM, Saunders WS (2005) Spindle multipolarity is prevented by centrosomal clustering. Science 307: 127-129.

116. Vitale I, Galluzzi L, Castedo M, Kroemer G (2011) Mitotic catastrophe: a mechanism for avoiding genomic instability. Nat Rev Mol Cell Biol 12: 385-392.

117. Imreh G, Norberg HV, Imreh S, Zhivotovsky B (2011) Chromosomal breaks during mitotic catastrophe trigger gammaH2AX-ATM-p53-mediated apoptosis. J Cell Sci 124: 2951-2963.

118. Leng M, Chan DW, Luo H, Zhu C, Qin J, et al. (2006) MPS1-dependent mitotic BLM phosphorylation is important for chromosome stability. Proc Natl Acad Sci U S A 103: 11485-11490.

119. Pradhan A, Singh TR, Ali AM, Wahengbam K, Meetei AR (2013) Monopolar spindle 1 (MPS1) protein-dependent phosphorylation of RecQ-mediated genome instability protein 2 (RMI2) at serine 112 is essential for BLM-Topo III alpha-RMI1-RMI2 (BTR) protein complex function upon spindle assembly checkpoint (SAC) activation during mitosis. J Biol Chem 288: 33500-33508.

120. Sakaushi S, Nishida K, Minamikawa H, Fukada T, Oka S, et al. (2007) Live imaging of spindle pole disorganization in docetaxel-treated multicolor cells. Biochem Biophys Res Commun 357: 655-660.

121. Zhu J, Beattie EC, Yang Y, Wang HJ, Seo JY, et al. (2005) Centrosome impairments and consequent cytokinesis defects are possible mechanisms of taxane drugs. Anticancer Res 25: 1919-1925.

122. Bian M, Fu J, Yan Y, Chen Q, Yang C, et al. (2010) Short exposure to paclitaxel induces multipolar spindle formation and aneuploidy through promotion of acentrosomal pole assembly. Sci China Life Sci 53: 1322-1329.

123. Yang YG, Cortes U, Patnaik S, Jasin M, Wang ZQ (2004) Ablation of PARP-1 does not interfere with the repair of DNA double-strand breaks, but compromises the reactivation of stalled replication forks. Oncogene 23: 3872-3882.

124. Bryant HE, Petermann E, Schultz N, Jemth AS, Loseva O, et al. (2009) PARP is activated at stalled forks to mediate Mre11-dependent replication restart and recombination. EMBO J 28: 2601-2615.